SYNTHESIS AND CHARACTERIZATION OF ELECTROSPUN NANOFIBERS FOR ADVANCED DRUG DELIVERY AND CELL CULTURING

A Dissertation by

Muhammet Ceylan

Master of Science, Wichita State University, 2009

Bachelor of Science, Erzurum Ataturk University, 2006

Submitted to the Department of Mechanical Engineering
and the faculty of the Graduate School of
Wichita State University
In partial fulfillment of
the requirements for the degree of
Doctor of Philosophy

May 2014

© Copyright 2013 by Muhammet Ceylan

All Rights Reserved

Note that dissertation work is protected by copyright, with all rights reserved. Only the author has the legal right to publish, produce, sell, or distribute this work. Author permission is needed for others to directly quote significant amounts of information in their own work or to summarize substantial amounts of information in their own work. Limited amounts of information cited, paraphrased, or summarized from the work may be used with proper citation of where to find the original work.

SYNTHESIS AND CHARACTERIZATION OF ELECTROSPUN NANOFIBERS FOR ADVANCED DRUG DELIVERY AND CELL CULTURING

The following faculty members have examined the final copy of this dissertation for form and content, and recommend that it be accepted in partial fulfillment of the requirement for the degree of Doctor of Philosophy, with a major in Mechanical Engineering.

_____
Ramazan Asmatulu, Committee Chair

_____
Hamid Lankarani, Committee Member

_____
Bin Li, Committee Member

_____
Davood Askari, Committee Member

_____
Shang-You Yang, Outside Committee Member

_____
Li Yao, Co Chair Outside Committee Member

Accepted for the College of Engineering

_____
Royce Bowden, Dean

Accepted for the Graduate School

_____
Abu S. M. Masud, Dean

DEDICATION

To my dearest wife, my daughters, and my parents

ACKNOWLEDGEMENTS

First, I would like to express my sincere gratitude to my advisor, Dr. Ramazan Asmatulu, who supervised the work presented in this dissertation from the beginning, and also guided me toward the successful completion of this dissertation. I appreciate his guidance throughout my graduate study at Wichita State University.

I would also like to acknowledge my dissertation committee, Dr. Hamid Lankarani, Dr. Bin Li, Dr. Davood Askari, Dr. Shang-You Yang, and Dr. Li Yao whose suggestion has been very useful in directing my research.

Special thanks to my wife Saadet Ceylan for her support and encouragement throughout my PhD degree. I would like to thank my daughters Elif Nimet Ceylan and Aysenur Ceylan. I would like to thank great friends that I have at the Research Group under Dr. Asmatulu at Wichita State University for their guidance in my research work and thanks to all my friends who stood by me at all times.

I enlarge my gratitude to my parents, Temel Ceylan and Ayten Ceylan also my brothers Mustafa, Ahmet Serkan and Mahmut Ceylan without their constant support and encouragement this day would not be possible. Whenever I needed guidance and support, they were always there for me. I cannot thank them enough for their immeasurable support and guidance.

ABSTRACT

This work is concerned with synthesis and characterization of electrospun nanofibers for advanced drug delivery and cell culturing. Poly-ε-caprolactone (PCL), composed of different inclusions such as gentamicin, plasmid DNA, and gelatin, is used to fabricate nanofibers using electrospinning for drug delivery and cell culturing. The plasmid DNA enhanced green fluorescent protein (EGFP) with cytomegalovirus (CMV) promoter (PCMVb-GFP) was amplified with *Escherichia coli* (*E. coli*). PCL was chosen because it has been approved by the Food and Drug Administration (FDA) in implantable material applications used in the human body, and it has biocompatible and biodegradable material, which plays a critical role in tissue engineering, wound healing, and drug delivery. The main reason for using electrospun nanofibers in this study is because it has high surface area, porosity, and permeability. Scanning electron microscopy (SEM) images show that the nanoscale fiber structures have a diameter ranging of 50 to 250 nm with some bead formations. The cytotoxicity study revealed that PCL nanofibers are not toxic, and cell viability was above 70%. An energy dispersive x-ray spectroscopy (EDS) was used in order to confirm the ratio of the gelatin component in the fibers. To visually express the inclusion of gentamicin in the fibers a fourier transform infrared (FTIR) spectroscopy was used. Differential scanning calorimetry (DSC) and thermal gravimetric analysis (TGA) techniques were also applied on the prepared sample. Overall, this study showed that PCL is a good candidate for several biomedical applications and may open up new possibilities for particularly DNA, gene, nerve cell myelination and drug delivery purposes.

TABLE OF CONTENTS

Chapter Page

1. INTRODUCTION 1

1.1 Pioneering Studies 8
1.2 Conventional Electrospinning 11
1.2.1 Initial Electrospinning Process 11
1.2.2 Coaxial Electrospinning Process 12
1.2.3 Rotating Disk Electrospinning Process 13
1.2.4 Needleless Electrospinning Process 14
1.3 Non-Conventional Electrospinning 16
1.3.1 Near-Field Electrospinning Process 16
1.3.2 Rotating Drum and Translating Spinneret Electrospinning Process 17
1.3.3 Rotating Electrodes Electrospinning Process 18
1.4 Effects of System and Processing Parameters on Electrospun Fibers 19
1.4.1 System Parameters 19
1.4.2 Surface Tension 19
1.4.3 Molecular Weight and Viscosity 20
1.4.4 Effects of Polymer and Solvent 21
1.4.5 Solution Conductivity 21
1.4.6 Processing Parameters 22
1.4.7 Collector Plate and Needle Diameter 23
1.4.8 Distance between Tip and Collector 23
1.4.9 Temperature, Humidity, and Air Velocity 23
1.5 Functional Materials and Devices 24
1.5.1 Composite Reinforcement 24
1.5.2 Filter 24
1.5.3 Smart Textiles and Protective Clothing 24
1.5.4 Energy and Electronics 25
1.5.5 Battery/Cell and Capacitor 25
1.5.6 Sensor 25
1.5.7 Catalyst 26
1.6 References 27

2. SYNTHESIS AND EVALUATION OF ELECTROSPUN PCL-PLASMID DNA NANOFIBERS FOR BIOMEDICAL APPLICATIONS 33

2.1 Abstract 33
2.2 Introduction 33
2.3 Experimental Procedure 36
2.3.1 Materials 36
2.3.2 Methods 37
2.3.2.1 Isolation of pCMVb-GFP Plasmid DNA 37

TABLE OF CONTENTS (continued)

Chapter Page

2.3.2.2 Electrospinning of Nanofibers 37
2.3.2.3 SEM Analysis of Electrospun Fibers 40
2.3.2.4 Biocompatibility and Cytotoxicity Assay of PCL Nanofibers 40
2.3.2.5 DNA Release Rates 41
2.4 Results and Discussion 41
2.4.1 Biocompatibility and Cytotoxicity Assay of PCL Nanofibers and Applications 41
2.4.2 Biomedical Applications 42
2.4.3 Drug Delivery 42
2.4.4 Tissue Engineering 43
2.4.5 Wound Dressing 43
2.4.6 DNA Release Rates 43
2.5 Conclusions 45
2.6 References 46
2.7 Appendix 51

3. EFFECTS OF GENTAMICIN-LOADED PCL NANOFIBERS ON GROWTH OF GRAM-POSITIVE AND GRAM-NEGATIVE BACTERIA 57

3.1 Abstract 57
3.2 Introduction 58
3.3 Experimental Procedure 59
3.3.1 Materials 59
3.3.2 Methods 60
3.3.2.1 Fabrication of Electrospun Nanofibers 60
3.3.2.2 Antibacterial Tests 60
3.4 Results and Discussion 61
3.5 Conclusions 71
3.6 References 71
3.7 Appendix 74

4. EFFECTS OF GENTAMICIN-LOADED PCL NANOFIBERS ON CELL VIABILITY AND RELEASE RATE OF PLASMID DNA 89

4.1 Abstract 89
4.2 Introduction 89
4.3 Experimental Procedure 91
4.3.1 Materials 91
4.3.2 Methods 92
4.3.2.1 Electrospinning of Nanofibers 92
4.3.2.2 Materials Characterization 93

TABLE OF CONTENTS (continued)

Chapter Page

4.3.2.3 Isolation of pCMVb-GFP Plasmid DNA 94
4.3.2.4 Biocompatibility and Cytotoxicity Assay of PCL Nanofibers 94
4.3.2.5 DNA Release Rates 95
4.4 Results and Discussion 95
4.5 Conclusions 100
4.6 References 101

5. NANOFIBER SUPPORT OF OLIGODENDROCYTE PRECURSOR CELL GROWTH AND FUNCTION AS NEURON-FREE MODEL FOR MYELINATION STUDY 104

5.1 Abstract 104
5.2 Introduction 104
5.3 Materials and Methods 106
5.3.1 Generation of PCL and Gelatin Electrospun Nanofibers 106
5.3.2 Contact Angle of Nanofibers. 107
5.3.3 Isolation and Culture of OPCs on Electrospun Nanofibers 107
5.3.4 Growth of OPCs on Electrospun Nanofibers and Cell Viability Assay . 108
5.3.5 Myelination Study of Oligodendrocytes for Nanofibers 108
5.3.6 Immunocytochemistry 109
5.3.7 Scanning Electron Microscopy for Nanofibers 109
5.3.8 Energy Dispersive X-Ray Spectroscopy for Nanofibers 110
5.3.9 Statistical Analysis 110
5.4 Results 110
5.4.1 Characterization of Electrospun Fibers of PCL and Gelatin Co-Polymer 110
5.4.2 Electrospun Nanofibers Support OPCs Growth and Differentiation 112
5.4.3 Differentiated Oligodendrocyte Ensheathed Nanofibers 114
5.5 Discussion 117
5.6 Conclusion 119
5.7 References 120

6. GENERAL CONCLUSIONS 123

7. FUTURE WORK 126

LIST OF FIGURES

Figure		Page
1.1	Conical spiral looping formation during electrospinning process	7
1.2	Schematic view of conventional electrospinning process	12
1.3	Schematic view of coaxial electrospinning	13
1.4	Schematic of electrospinning with rotating disk	14
1.5	Schematic of needleless electrospinning process.	15
1.6	Schematic of non-conventional electrospinning process	17
1.7	Schematic of electrospinning with rotating drum and translating spinneret	18
1.8	Schematic of electrospinning with rotating string of electrodes.	18
1.9	An image of initial electrospinning process	20
1.10	An image of polymer and solvent molecules	21
1.11	Schematic illustration of charges on the surface of the solution.	22
2.1	A schematic illustration of an electrospinning process	39
2.2	PCL Nanofiber with Plasmid DNA.	40
2.3	Cytotoxicity results for PCL nanofiber	42
2.4	DNA release rates as a function of time.	44
3.1	Schematic view of an electrospinning process	60
3.2	Diagram showing the average fiber diameter of the PCL fibers with different concentrations of gentamicin.	62
3.3	SEM images of PCL nanofibers with different wt% of gentamicin : a) 0wt% , b) 2.5wt% , c) 5wt%, and d) 10wt% gentamicin	64
3.4	FTIR graph for Gentamicin	64
3.5	FTIR graph for PCL nanofibers With different wt% of Gentamicin	65

LIST OF FIGURES (continued)

Figure Page

3.6 TGA graph for PCL nanofibers With different wt% of Gentamicin 65

3.7 DSC graph for PCL nanofibers With different wt% of Gentamicin..... 66

3.8 The antibacterial test results of the PCL fibers with different wt% of gentamincin, a) 0wt%, b) 2.5wt% , c) 5wt%, and d) 10wt%, after the seven days of in vitro tests. Top row samples have one layer, middle row samples two layers, and bottom row samples four layers of the PCL fibers..... 67

3.9 Bacterial (*E. coli*) inhibition zones/areas of PCL nanofibers containing different wt% of gentamicin, a) 2.5wt% , b) 5wt% gentamicin c) 10wt%. 68

3.10 Bacterial (*Salmonella*) inhibition zones/areas of PCL nanofibers containing different wt% of gentamicin, a) 2.5wt% , b) 5wt% gentamicin c) 10wt%. 69

3.11 Bacterial (*S. Epidermidis*) inhibition zones/areas of PCL nanofibers containing different wt% of gentamicin, a) 2.5wt% , b) 5wt% gentamicin c) 10wt%..... 70

4.1 A schematic illustration of an electrospinning process..... 92

4.2 SEM images of PCL nanofiber composed of the following materials:(a) 0%gentamicin and 0% plasmid DNA (b) 0%gentamicin and plasmid DNA, (c) 2.5% gentamicin and plasmid DNA, (d) 5% gentamicin and plasmid DNA, and (e) 10% gentamicin and plasmid DNA 96

4.3 Diagram shows average fiber diameter of PCL nanofibers with different percentage of gentamicin and plasmid DNA..... 97

4.4 DNA release rates as a function of time for different composed of PCL nanofiber..... 98

4.5 Cell viability of B104 neuroblast cells..... 98

4.6 Cell viability of L929 fibroblast cells 99

5.1 Characterization of electrospun fibers. (A) SEM image of electrospun PCL fibers. (B) SEM image of PCL-gelatin fibers. (C) Quantification of fiber diameter. (D) Carbon atomic and carbon weight ratio in nanofibers. Scale bar: 2 μm 111

LIST OF FIGURES (continued)

Figure Page

5.2 Measurement of contact angle of PCL nanofibers, PCL-gelatin nanofibers, and gelatin nanofibers. (A) Droplet profiles and contact angle evaluation on different films of dense PCL nanofibers, PCL-gelatin nanofibers, and gelatin nanofibers. (B) Quantification of contact angle of PCL nanofibers, PCL-gelatin nanofibers, and gelatin nanofibers..... 112

5.3 Growth and differentiation of OPCs on films of dense electrospun nanofibers. Growth of OPCs on tissue culture plate (A, B), PCL nanofibers (D, E), and PCL-gelatin nanofibers (H, I). OPCs differentiated into OL cells on tissue culture plate (C), PCL nanofibers (F), and PCL-gelatin nanofibers (J). OPCs were labeled with anti-PDGFα antibody (D, H) or anti-A2B5 antibody (B, E, I). OL cells are labeled with anti-O4 antibody (C, F, J). Scale bar: 100 μm. Experiment was performed the data collected by Dr. Yongchao and Dr.Yao. 113

5.4 alamarBlue cell viability assay of OPCs growing on the films of dense electrospun PCL nanofibers, PCL-gelatin nanofibers and gelatin nanofibers. Experiment was performed the data collected by Dr. Yongchao, Dr.Yao, and Bikesh Shrestha. 114

5.5 Growth of OPCs on coverslips with electrospun nanofibers. After culturing for 3 days, OPCs developed short processes on coverslips with PCL nanofibers (A) and PCL-gelatin nanofibers (B). OPCs were labeled with anti-PDGFα antibody. Some cells were associated with nanofibers. Scale bar: 100 μm. (C) SEM images of PCL-gelatin nanofibers. Scale bar: 20 μm. (D) Analysis of nanofiber diameter. Experiment was performed the data collected by Dr. Yongchao and Dr.Yao..... 115

5.6 Differentiated OPCs ensheath nanofibers. (A) Differentiated OPCs ensheath PCL fibers. (B) Differentiated OPCs ensheath PCL-gelatin fibers. Scale bar: 100 μm. (C) Magnified image of myelinated PCL-gelatin nanofibers, as indicated by arrow in (B). Cells were labeled with anti-MBP antibody. (D) Analysis of percentage of cells wrapping nanofibers (* indicates significant difference compared with differentiated OPCs myelinate PCL nanofibers, $p < 0.01$). (E) Analysis of percentage of myelinated nanofiber segments (* indicates significant difference compared with myelinated segments of PCL nanofibers, $p < 0.01$). Experiment was performed the data collected by Dr. Yongchao and Dr.Yao. . 116

5.7 SEM images showing differentiated OPC-ensheathed PCL-gelatin nanofibers. (A) Differentiated OPCs extend multiple processes. Scale bar: 10 μm. (B) Magnified image showing myelinated and unmyelinated fiber segments, as indicated by arrow in (A). Scale bar: 2 μm. (C) Magnified image showing myelinated and unmyelinated fiber segments, as indicated by asterisk in (A). Scale bar: 2 μm. (D) Magnified images show end of myelinated fiber segments. Scale bar: 2 μm. Experiment was performed the data collected by Dr. Yongchao and Dr.Yao..... 117

LIST OF ABBREVIATIONS

ATCC	American Type Culture Collection
B-104	Neuroblast Cell
CMV	Cytomegalovirus
CO_2	Carbon Dioxide
DMEM	Dulbecco's Modified Eagle's Medium
DNA	Deoxyribonucleic Acid
DSC	Differential Scanning Calorimetry
E. coli	*Escherichia coli*
ECM	Extracellular Matrix
EDS	Energy-Dispersive X-Ray Spectroscopy
EGFP	Enhanced Green Fluorescent Protein
EPL	ε-poly-L-lysine
FBS	Fetal Bovine Serum
FDA	Food and Drug Administration
FTIR	Fourier Transform Infrared
HCI	Hydrogen Chloride
IACUC	Institutional Animal Care and Use Committee
L-929	Fibroblast Cell
LB	Lysogeny Broth
MBP	Myelin Basic Protein
MRSA	Methicillin-Resistant *Staphylococcus aureus*
MTT assay	Colorimetric assay

NaOH	Sodium Hydroxide
OL	Oligodendrocyte
OPC	Oligodendrocyte Precursor Cell
PBS	Phosphate-Buffered Saline
PCL	Poly-ε-caprolactone
PEG	Polyethylene Glycol
PEI	Polyethylenimine
PLA	Poly(lactic acid)
PLGA	Poly(lactide-co-glycolide)
PS	Polystyrene
PVA	Polyvinyl Alcohol
SCI	Spinal Cord Injury
SDS	Sodium Dodecyl Sulfate
S. Epidermidis	*Staphylococcus epidermidis*
SEM	Scanning Electron Microscopy
TCP	Tricalcium Phosphate
TE Buffer	(10 mM Tris-HCl, 1 mM EDTA, pH 8.0)
TGA	Thermogravimetric Analysis
UV	Ultraviolet

LIST OF SYMBOLS

cm	Centimeter
º	Degree
hr	Hour
KeV	Kilo Electron Volt
kV	Kilovolt
µg	Microgram
µl	Microliter
µm	Micrometer
µ	Micron
mg	Milligram
ml	Milliliter
mm	Millimeters
mM	Millimolar
min	Minute
ng	Nanogram
nm	Nanometer
pg	Picogram
pH	Power of Hydrogen
rpm	Revolutions per Minute

CHAPTER 1

INTRODUCTION

Electrospinning is a physical process that uses electrostatic power to form fibers from a fluid solution or liquid melt. The electrospinning methodology has become extremely popular as a remarkable technique for processing nanofibers in the laboratory. For example, well-established industries use electrospinning to fabricate efficient filters. When investigating the history of any specific technology, it is difficult to sift through the progression of civilization and science. The inventions record starts with current electricity generation and insulation. Electrospinning would not be possible in the absence of these processes [1]. The historical account of the electrospinning development over time is large, and in this dissertation, the most important material related to electrospinning was selected to understand its progression. The research and development of electrospinning have been undertaken by the industrial sector; unfortunately, a large amount of information is hidden because of its commercial sensitivity. It is generally known that the story of electrospinning begins with the considerable contribution of Anton Formals in the 1930s, but the history of this industrial process started 30 years before that with the work of J. F. Cooley and 10 years prior to Cooley with a process description by C.V. Boys.

In the seventeenth century, during the time of Queen Elizabeth I, William Gilbert investigated the electrostatic attraction of fluid; this is the first recorded investigation of this sort. He was president of the Royal College of Physicians and the Queen's personal physician. Gilbert was a supporter of scientific investigation. He discredited the notion that garlic could influence the working of the magnetic compass and that diamonds, when utilized as a rubbing material for a magnet, might inverse its polarity. He proved that electrostatic and magnetic attractions are

different phenomena. Gilbert developed the fluid drop and cone shape, which is the first record of the deformity of a fluid drop, known as the Taylor cone [2]. In 16903, Gilbert died of the Black Death in London. His position in court did not afford him the right to healthy conditions in the city.

In the eighteenth century, a static electricity charge was created by a triboelectrical charge, meaning via the friction of two materials. In the nineteenth century, technology developed along with the generation of high-voltage electricity. This accomplishment was due to the improvement of science during the century. George Mathias Bose, who is probably the Leyden jar co-inventor, defined the application of high electric potentials to drops of fluid turning to aerosols [3]. The Von Guericke triboelectrical static electricity generating machine was developed by Bose, who added a charge collector. He published his results as poems [4].

In the nineteenth century, Louis Schwabe was the inventor of the extrusion spinneret. For the test material, he used glass and spun fibers to make demonstration pieces similar to William and Sowerby's glass damask. In 1840, this damask was displayed at the Manchester Mechanics Institute [5]. George Audemars of Lausanne, Switzerland, patented a procedure for turning collodion, which was removed from mulberry trees. His initial experiment involved dipping a needle into a solution and drawing it out, dragging a long thread of quickly hardening collodion behind it [6], a process which proved to be time-consuming. In 1873, Joseph Antoine Ferdinand Plateau, from the University of Ghent, developed a good understanding of the nature of segments of fluid by characterizing experiments with the separation of sections of molten iron and mercury [7]. John William Strutt, known as Lord Rayleigh, admitted taking the phenomenon from Plateau's work when he published the model of column breakup [8]. The idea that a column of liquid will break up into droplets as soon as the length exceeds its circumference was

demonstrated experimentally by Strutt using a stroboscope [9]. Talented physicist Charles Vernon Boys built a torsion balance to measure the universal gravitational constant and the density of Earth in 1888 [10]. What the torsion balance needed was stable and reliable suspension fiber. Boys used an old, but known, electrical spinning process consisting of a small dish, which was insulated and connected with an electrical machine [11]. He was able to draw fibers from a number of different melts, for instance, from beeswax, shellac, gutta-percha, sealing wax, and collodion. He was also able to control the formation of beaded threads. However, the fibers he produced did not have the mechanical properties required for the torsion balance. Then he selected fused quartz as the proper material. This material was not fit for electrospinning, so he created a method of drawing a fiber, which involved fastening a fragment of fused quartz to a crossbow bolt, heating the fragment, and firing the crossbow. From this process, the fiber was wound onto a wooden former. The achievement here was quite good in that he obtained a fiber 90 feet in length with a thicknesses estimated to be less than 1/100,000 inch, or about 254 nm, which was definitely below the resolution of any available optical microscope.

In the twentieth century, John Francis Cooley, a professional inventor and electrician from Penn Yan, New York, invented a rotary steam engine, or pump progenitor of a rotating cycle, later used in the Wankel engine and a flying machine at Rochester, New York. Cooley's machine came only seven years after the Wright brothers, and it was 80 feet (24 m) long with a 42-foot (12-m) wing span and required a crew of two. The flying machine never left the ground and was finally seized by court order due to an unpaid grocery bill. Cooley filed the first electrospinning patent [12].

Anton Formhals made very important contributions to the development of electrospinning and attained 22 patents. His first development was a machine design based on a saw-toothed rotating fiber emitter [13]. Between 1964 and 1969, Sir Geoffrey Ingram Taylor made an important advance in the theoretical foundation of electrospinning. His work contributed to the fact that mathematical modeling under the influence of an electric field made the shape of the cone formed by the fluid droplet [14], known as the Taylor cone. Reneker popularized the name “electrospinning” for the process and showed that many organic polymers could be electrospun into nanofibers [15].

Electrospinning is a procedure that creates sub-micron and nanosize fibers possessing qualities such as a high surface area and superior physical properties that are mechanical, electrical, and thermal assets in comparison to their bulk-size fibers. Electrospinning can be correlated to the relative principle of spinning solutions in high DC electric fields. Under appropriate conditions, virtually any synthetic and naturally occurring polymer can be attained through electrospinning. During the process, in order to overcome the surface tension exerted by the polymeric solutions a high voltage or electric field is used. Once the threshold intensity is reached, which is a certain limit, the intensity of the electric field is elevated above a point in which the hemispherical surface of the polymer solution at the end of the capillary tube begins to elongate and form into a structural Taylor cone [16]. Electrospun fibers are obtained from plastic stretching of a polymeric solution jet. At the same time as plastic stretching of the polymeric solution, the solvent evaporates and the polymer solidifies at micro- and nanoscales on a grounded surface.

Electrospinning is derived from the term “electrostatic spinning” due to the fact that an electrostatic field is used to fabricate fibers. The use of this word has been increasing since 1994 [17, 18]. The electrospinning process was first patented by Formhals in 1934 [17]. In 1969,

Taylor studied the shape of the polymeric droplet at the end of a capillary tube, which revealed that a jet is ejected from the apex of cone (later termed Taylor cone) [16]. After this discovery, many researchers around the globe began to focus on the fabrication and characterization of electrospun fibers. Compared to other conventional methods such as melt spinning, wet spinning, extrusion spinning, and so on, electrospinning is relatively the easiest and most direct process of fabricating a non-woven mat of polymer fibers. Electrospinning offers the advantage of fibers in the micro to nano range. In addition, electrospinning presents a high surface-to-volume ratio compared to conventional fiber-forming techniques [19].

Electrospinning is not a new discovery or technique for manufacturing submicron-size fibers. It has been used since the 1930s; however, until recently, it was never able to obtain industrial importance because of the low productivity of and lack of interest in resultant products. Today, special needs for biomedical, filtration, sensor, textile, and military applications have rejuvenated interest in this technique [20, 21]. Electrospinning produces a very slim-charged jet by using a high electric field or force on the surface of a polymeric solution. This polymeric solution is then apprehended by surface tension at the end of the capillary tube. The liquid meniscus emerging from the capillary has a stress of γ/r, where γ is the surface tension of the polymeric solution and r is the radius of the meniscus. The stress created as a result of the applied field, also known as Maxwell stress, can be given by

$$\sigma_{ij} = \varepsilon V_i V_j + \frac{1}{\mu_o} B_i B_j - \frac{1}{2}\left(\varepsilon V^2 + \frac{1}{\mu_o} B^2\right)\delta_{ij} \tag{1.1}$$

where ε is the permittivity, V is the applied voltage (spinning voltage), B is the magnetic field, and δ_{ij} is Kronecker's delta. After disregarding the magnetic aspect and dividing by H^2, where H is the distance between the capillary tube and the collector screen, equation (1.1) can be reduced to [22]

$$\sigma = (\varepsilon V^2)/H^2 \tag{1.2}$$

Other forces acting on the polymeric solution that are not taken into account due to their very little effect compared to the high-electrostatic force include inertia, hydrostatic pressure, and viscoelastic forces. Balancing the Maxwell stress and the capillary stress will yield the critical spinning voltage V_c that needs to be overcome in order to initiate electrospinning [22]:

$$V_C = \sqrt{\frac{\gamma H^2}{\varepsilon}} \tag{1.3}$$

Polymeric solutions are generally electrospun at 7–10 kV DC; however, in order to produce fibers at nanoscale, the applied voltage must be higher than 10 kV. When a charge is exerted onto the polymeric solution, the mutual charge repulsion prompts longitudinal stresses, due to the fact that the point charges cannot be sustained in a static equilibrium. This is called Earnshaw's theorem.

Once the intensity of the electrostatic field surpasses the threshold limit, Vc, the hemispherical shape of the droplet emerging from the capillary tube develops into a conical shape known as the Taylor cone [16, 23]. First, the jet extends linearly for a typical distance of 2–3 cm, called the jet length [24, 25], and then instability occurs beyond the relaxation of the jet, in which it bends and follows a conical spiral looping path, as shown in Figure 1.1 [24]. The instability is due to the interaction of charges in the electrified jet. The electrostatic field extends the jet thousands of times, which results in it becoming very slim, typically in the nano range. Lastly, the solvent evaporates and the adequate fibers are accumulated onto a screen placed some distance away from the capillary tube.

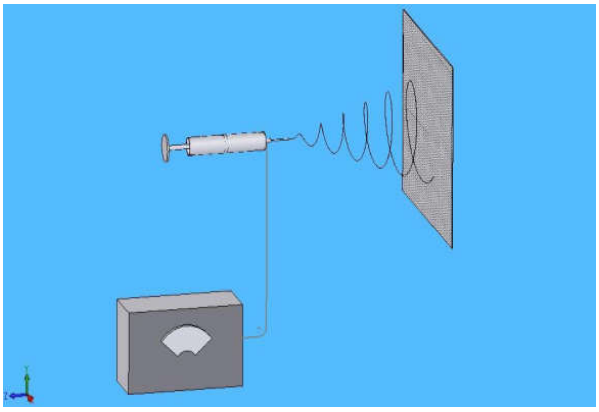


Figure 1.1: Conical spiral looping formation during electrospinning process.

Electrospun nanofibers have a diameter ranging in the range of 3–500 nm. The main advantage of the electrospinning process is its ability to produce nanofibers in a shorter period of time. A vast number of sizes and shapes of fibers can be contrived from numerous polymers. By changing the system and process parameters, the morphology and surface features of electrospun fibers can be controlled. The process of electrospinning process involves many branches of science and technology including mechanical, electrical, polymer, fluid mechanics, rheology, and material science [24].

Polymer nanofibers are used in many applications such as filtration [26, 27], protective clothing [28], and biomedical including wound dressing [29, 30], artificial blood vessels [31, 32], sutures, and drug delivery systems [24]. Aside from these, other applications include solar cells, fuel cells, batteries, super capacitors, light sails, photonic devices, and mirrors [24, 33]. Nanofibers also offer tremendous advantages in applications such as pesticides applied to plants, structural elements in artificial organs, scaffolds for growing cells, and improved food protection [24, 34], and they provide support for enzymes or catalysts that have the potential to promote chemical reactions and reinforcements for composites [24, 35, 36]. The surface of electrospun nanofibers can be coated with various substances in order to modify the nanofiber surface.

Nanofibers may also be used as templates in order to make small tubes. Ceramic or carbon nanofibers derived from polymer precursors extend nanofiber applications involving a high temperature [37, 38]. Ceramic electrospun fibers can be produced by either a sol-gel mixture or a mixture of inorganic and organometallic compounds with a guide polymer. Polymeric electrospun nanofibers can also be coated with a solution of inorganic metallic and organometallics. In all cases, the electrospun nanofibers remove the organic substances in an ambient condition, which is then converted into ceramic electrospun nanofiber [24].

Many substances can be processed through electrospinning in order to fabricate nanocomposite nanofibers. Prior to being electrospun, a few small insoluble particles can be dispersed into a solution. These small particles can be encapsulated within dry nanofibers. The matrix that supports additives/inclusions are provided through the polymer nanofibers and nonwoven mats of nanofibers. Many useful substances can be incorporated into electrospun nanofibers. Simultaneously, different polymers dissolved in the same solvent can be electrospun to form nanofibers with the polymers in separate phases [24].

1.1 Pioneering Studies

Electrospinning is not a new technology and has been around for a long time. It was first pointed out 369 years ago by William Gilbert, after he discovered that a spherical drop of water on a dry surface is drawn into a cone when a piece of electrically charged rubber amber is kept at an acceptable distance above it [16]. This discovery was the start of the electrospinning process. Rayleigh [24, 39, 40] focused his study on the hydrodynamic stability mechanism of a liquid jet in the presence and nonappearance of an applied electrostatic field. In 1882, Raleigh observed the instability mechanism in an electrified liquid jet, expressed as an electrostatic force that disables surface tension, which then acts in the opposite direction throwing out the liquid in the

form of fine jet [24]. In the year of 1960, researcher Taylor [41, 42, 43] observed the disintegration of water drops and discovered that the conical interface between two fluids cannot occur under an electrostatic field while being in an equilibrium state. Taylor observed that the water droplets elongated at the bending of instability at the ends and are then transformed into a conical shape possessing a semi-vertical angle of 49.3°. This discovery of the first development for the Taylor cone was then thoroughly discussed by researchers all over the world [24].

Electrospinning of a polymeric solution has been used sincee the 1930s. Formhals' patents [13, 44] include various experimental setups, the collection of electrospun fibers, and other applications he used during that time. Bumgarten [45] in 1971 and Subbiah et al. [46] in 2005 generated a successful electrospun microfiber when using a polyacylonitrile/ dimethylformamide solution. High voltage was applied to a stainless steel capillary tube containing a suspended polymer solution. These authors discovered that the diameter of a jet approaches a minimum value with an initial increase in the applied voltage and then increases with an increase in the applied field. Larrando and Manley [46] observed the relationship of melt temperature and fiber diameter of ethylene and polypropylene, and discovered that the fiber diameter decreased as the melt temperature increased. In 1987, researcher Hayati [46] established that the effects of an electrostatic field, process conditions and parameters on electrospun fibers. Hayati discovered that the conducting polymeric solution that had a high applied electrostatic field that generated an unsatisfactory and unstable jet, which looped around various directions.

In the years 1994 and 1995, Doshi and Reneker [47, 15] observed the performance of polyethylene oxide when gone through the process of electrospinning. Srinivasan and Reneker [48] electrospun a liquid crystal system poly solution (p-phenyleneterephthalamide) in sulfuric

acid along with an electrically conducting polymer poly (aniline) in sulfuric acid. The first real emergence of the electrospinning process began in 1995 when Reneker and his fellow coworkers started publishing numerous research papers on electrospinning the potential applications in different industries [24]. The electrospinning method was used by Chun [49] and Fong et al. [19], between the years 1995 and 1999 to produce nanofibers from different polymeric solutions, such as amic acid and acrylonitrile.

In 1996 and 1998, Jaeger and co-workers [50, 51] electrospun poly (ethylene oxide) fiber and used a scanning probe microscopy to characterize the electrospun fibers they produced. Around the years of 1997 through 1999, Fang, Reneker [52], and Fong [53] produced nanofibers through the process of electrospinning by using a polymeric solution of Nylon 6 and polyimide. In 1999 and 2007, Kim and Reneker [36] and Xu et al. [35], respectively, researchers observed the reinforcements effect inside a rubber and epoxy matrix in electrospun nanofibers. In the year of 1998, Stenoien used the process of electrospinning to fabricate a silicon polyester composite vascular graft [54]. Zarkoob [55] in 1998 and in Zarkoob and et al. [56] in 2004 used electrospinning to produce silk nanofibers and compared them with naturally occurring silk fibers. In the year 2000, Huang and his peers [57] studied the electrospinning of synthetic elastin-mimetic peptide.

Reneker et al. [33] and Fong et al. [19] established the electrospinning of beaded nanofibers of poly (polyethylene oxide). Gibson et al. [58] researched the transport properties of electrospun fiber mats and discovered that nanofiber layers offer less resistance to moisture vapor diffusional transport. In 2001, Diaz et al. [59] fabricated a conducting electron mat by mixing a conducting material, polyaniline, doped with camphorsulfonic acid and poly (ethylene oxide). Due to the porosity effects of the fiber texture, the conductivity of the electrospun mat

where found to be lower than the cast film. Kim and Lee [60] focused on the thermal characterization of the electrospun polynapthalene terephthalate, polyethylene terephthalate, polyethylene terephalate- co-polynapthalene terephthalate, and polyester. Bognitzki et al. [61, 62] electrospun polylactide-retrieved organic solutions in dichloromethane with the addition of an organosoluable, such as tetraethyl benzylammonium chloride or poly(ethylene oxide). More than 300 research papers were published on electrospinning in 2004.

1.2 Conventional Electrospinning

1.2.1 Initial Electrospinning Process

When the electric field in the electrospinning process reaches a critical value, repulsive forces overcome the surface tension, and an unremitting charged jet of liquid is cast out from the tip of the cone. Repulsive forces are caused by the interaction of the applied electric field and the jet's electrical charge. Ions located in the polymeric solution react and move in response to the electric field and are transfered into a force. The product of the electrostatic field and the movement of the charge carriers is the drift velocity of the charge carriers in a liquid polymeric solution [63]. Charge carriers in a polymeric solution generally have low movement, but in an area where the polymeric solution is active at a high velocity (higher than the drift velocity of charge), they move at the velocity of their surrounding molecules [63]. Rayleigh predicted the maximum amount of charge that a droplet of polymeric solution could take before the electrostatic field exceeds the forces associated with the surface tension [63]. Roth and Kelly explained the dissolving droplet as various small droplets holding approximately 5% of the mass and 25% of the charge [63].

The narrowing of the jet caused by bending instability is linked with the change in electrostatic force per surface area of the fiber. The jet starts to stretch and flog around, creating

a single nanofiber as it travels towards the grounded collector screen. The majority of the solvent evaporates as the jet travels to the screen [23]. The electrospinning technique is closely related to the commercial process of making microscale fibers, except for the fact that electrostatic repulsion is used between surface charges rather than a mechanical or shear force as the drawing force. The flow rate of the polymeric solution can be controlled by a syringe pump. The distance between the grounded collector and the tip of the capillary tip can be alternated. A greater distance (20–30 cm) between the grounded collector and the capillary tip is generally used. Figure 1.2 shows a schematic view of the conventional electrospinning process.

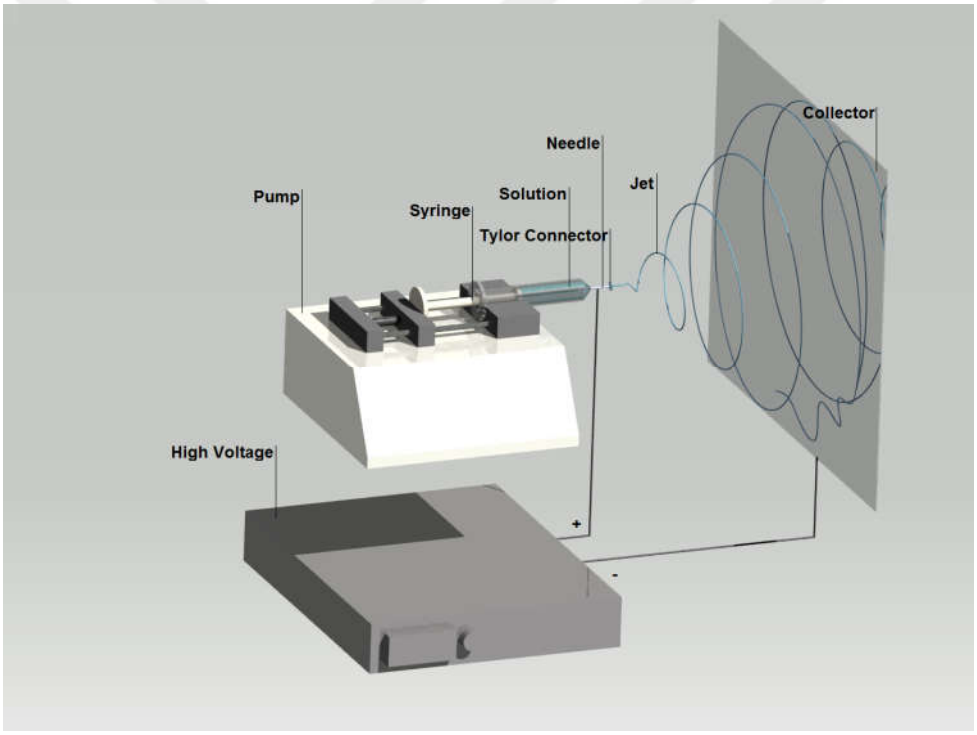


Figure 1.2: Schematic view of conventional electrospinning process.

1.2.2 Coaxial Electrospinning Process

An extended form of electrospinning is known as coaxial electrospinning, which consists of a central tube nozzle with a muzzle on one side. Two polymeric solutions needed for the core and sheath materials are independently fed into the central tube nozzle from which they are

extruded concurrently [63]. A complex droplet comes from the central nozzle, as shown in Figure 1.3.

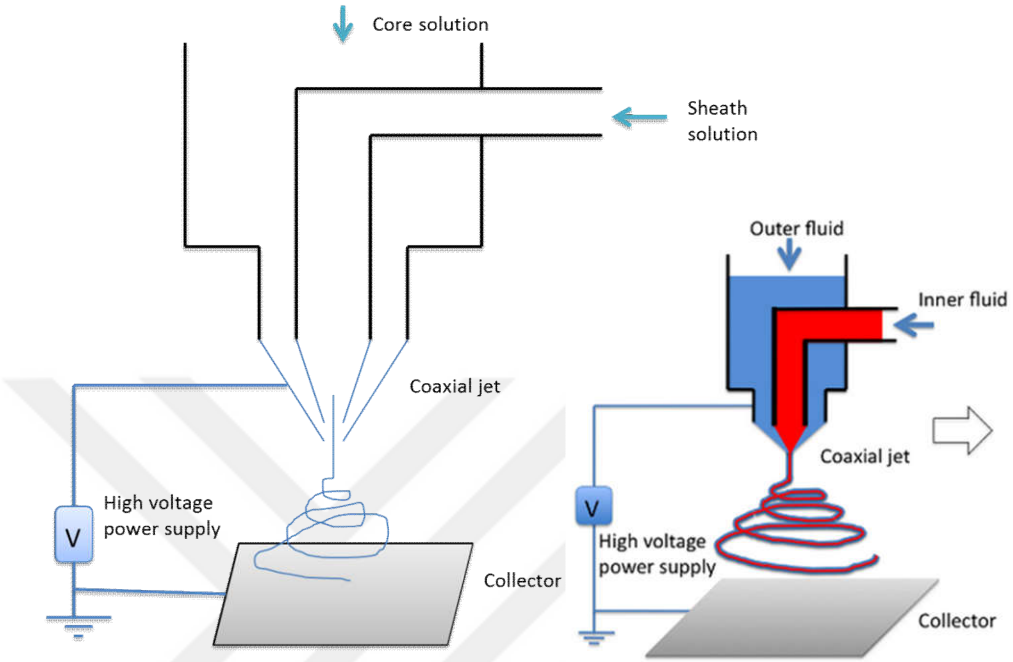


Figure 1.3: Schematic view of coaxial electrospinning.

A compound Taylor cone emerges when a high electrostatic field consisting of core material surrounded by sheath material is applied, and the jet undergoes the same bending instability effect as experienced in traditional electrospinning, followed by evaporation of a jet. The jet is then solidified and collected on a collector screen in the form of one fiber [63].

1.2.3 Rotating Disk Electrospinning Process

Industrial applications call for uniformly situated fibers without beads and pores. The electrospinning process produces and results in uniformly dispersed fibers without a beaded structure. A uniform coat of fibers can be formed by rotating the collector (target), as shown in Figure 1.4. The jet under the influence of an electrostatic field experiences bending instability, due to the interactions of surface charges, as it flows from the tip of the capillary tube to the

rotating disk (drum). It is then assembled together onto the rotating disk, which is moving at a constant velocity. A thick continuous film of nanofibers can be produced using this process.

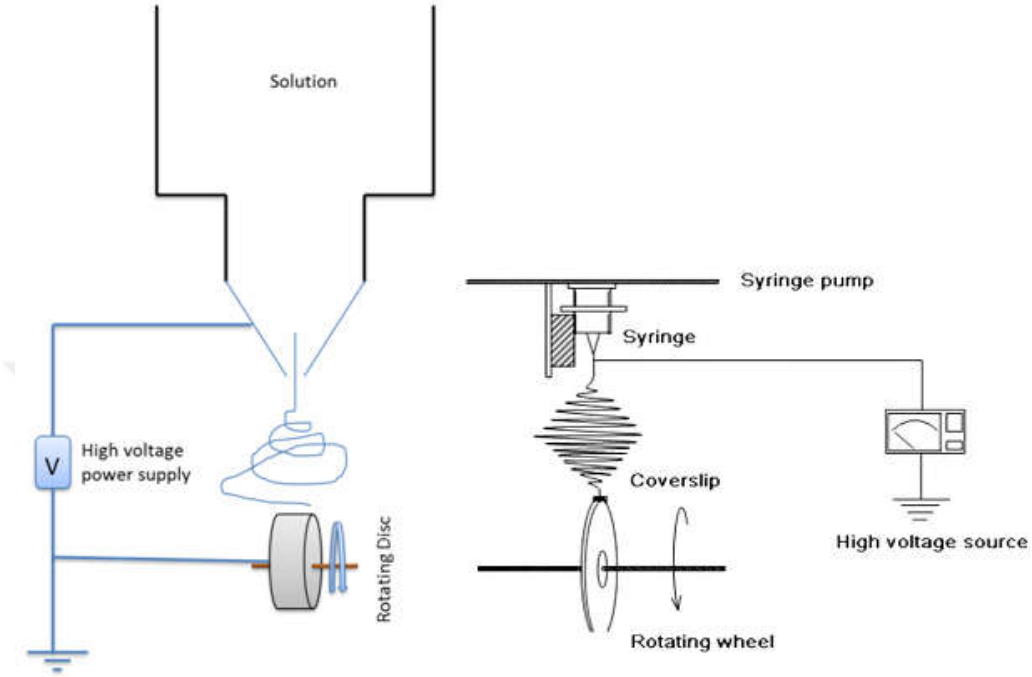


Figure 1.4: Schematic of electrospinning with rotating disk [63].

1.2.4 Needleless Electrospinning Process

Due to the fact that electrospinning is a low-production process, efforts such as increasing the number of needles (multiple needle setup) and using the air jacket to improve the solution's flow rate are being made to further the productivity of electrospinning [63]. Needle-electrospun nanofibers have not been used widely because of the low production rate, i.e., 0.3g/hr, even though they have tremendous industrial applications [63]. Since each nozzle generates only one jet in needle electrospinning, productivity is low. In a multiple-needle setup, a large working area is mandatory so that strong interactions between adjacent jets can be avoided, and materials must be cleaned systematically to stop polymeric solution blockage in nozzles [63].

Needleless electrospinning technology has recently been a substitute for addressing the issues of low production and a large working space. Needleless electrospinning (Figure 1.5) is characterized by direct fibers generated from an open liquid bath. In this process, numerous jets start off simultaneously from the liquid bath without any capillary effect, which is frequently observed and common in needle electrospinning. The jet initiation process in needleless electrospinning is self-organized; therefore, it is difficult to control the spinning process [63]. Fiber morphology, quality, and productivity are determined by spinnerets in needleless electrospinning. Figure 1.5 shows the experimental setup for this process. A copper spiral coil is used as the fiber generator [63]. The coil is rotated at 40 rpm in a liquid bath that is filled with a polymeric solution [63]. The liquid solution becomes charged with the addition of an electrode, and a rotating drum covered with aluminum foil is used to collect the fibers. needleless electrospinning produces finer and uniformly oriented fibers with much higher productivity.

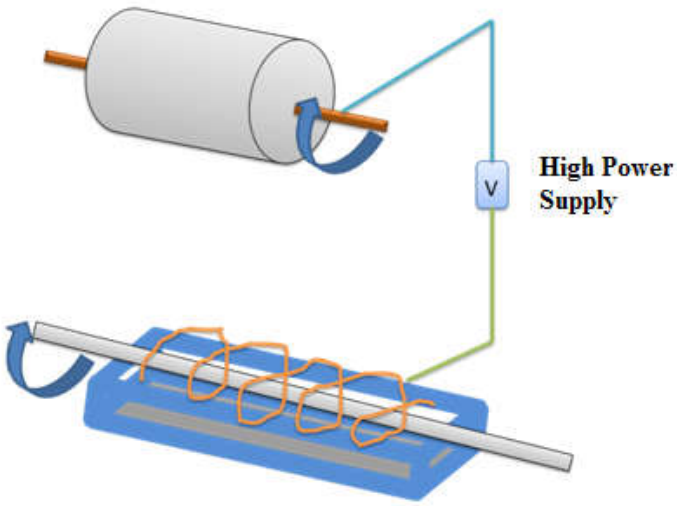


Figure 1.5: Schematic of needleless electrospinning process.

1.3 Non-Conventional Electrospinning

1.3.1 Near-Field Electrospinning Process

Conventional electrospinning manufactures limited materials for industrial applications by producing non-woven randomly oriented fibers. For industrial applications, fibers must form uniformly ordered arrays rather than randomly oriented arrays [63]. Random fiber orientation is mainly important for its bending instability of the electrified jet in the conventional electrospinning process. Near-field electrospinning is an effective process for better fiber alignment and control [63]. Here, a positive charge is added to the polymeric solution, and the collector screen is grounded, similar to conventional electrospinning. The distance between the capillary tip and collector screen is reduced, typically to 0.5–3 mm. In order to introduce a charge to the polymeric solution, a critical voltage of around 1.4 KV is applied [63]. At this low voltage, a droplet of polymeric solution forms at the tip of the capillary tube without initiating the electrospinning process [63]. Following this, an array of sharp tips with diameters of 20 μm is put into this droplet and then quickly removed. This results in numerous jets emerging from the droplet [63]. To ensure effective emanating of the jet from the droplet, the distance between the two adjacent tips should be more than 50 μm. The repulsive forces between adjacent jets keep the fibers from merging together, creating orderly oriented fibers. Figure 1.6 shows a schematic of non-conventional electrospinning.

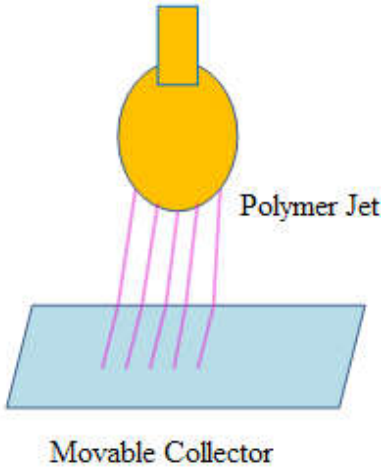


Figure 1.6: Schematic of non-conventional electrospinning process.

1.3.2 Rotating Drum and Translating Spinneret Electrospinning Process

By rotating the collector drum and translating the spinneret, a continuous and uniform film of fiber can be produced. The rotational speed and translating movement of the spinneret are the key parameters in this process. Conventional electrospinning produces a non-uniform film of fibers; however, this process has the advantage of a high production rate, better process control, better alignment, and fiber uniformity. Figure 1.7 shows a schematic of electrospinning with a rotating drum and translating spinneret [63].

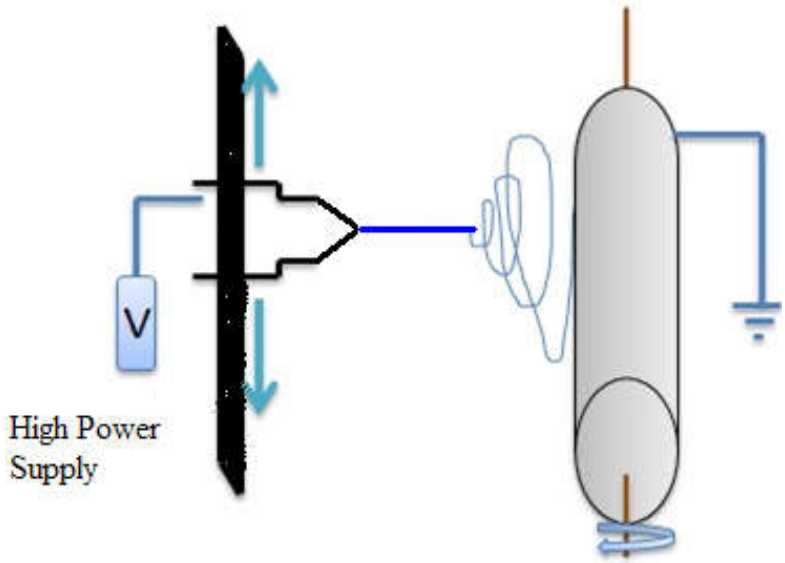


Figure 1.7: Schematic of electrospinning with rotating drum and translating spinneret.

1.3.3 Rotating Electrodes Electrospinning Process

Rotating the strings of electrodes in the bath of polymeric solution and placing a collector screen above this is another way to improve the production rate of electrospun nanofibers. The electrodes are usually connected to the positive terminal of the power supply, and the collector screen is either grounded or connected to the negative terminal of the power supply. This process eliminates the use of multiple spinnerets and replaces them with strings of electrodes, thus providing a better control process and easy fabrication. This process is cost effective and faster than electrospinning with multiple spinnerets. Figure 1.8 shows a schematic of electrospinning with a rotating string of electrodes [63].

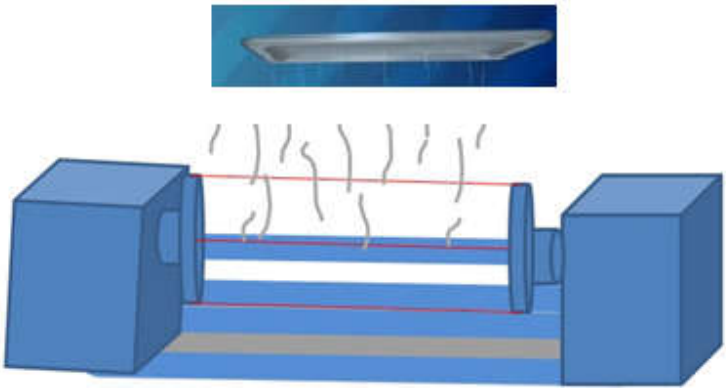


Figure 1.8: Schematic of electrospinning with rotating string of electrodes.

1.4 Effects of System and Processing Parameters on Electrospun Fibers

Processing parameters and system parameters have a big impact on the morphology and diameter of electrospun fibers. Two parameter groups that affect the electrospinning process are as follows [64]:

- System parameters
- Processing parameters

1.4.1 System Parameters

System parameters include the following:

- Surface tension
- Molecular weight
- Viscosity
- Effect of polymer and solvent
- Solution conductivity

1.4.2 Surface Tension

The electrospinning process should begin after the surface tension process. The aim here is to overcome the surface tension of the solution, and to do that, a high charge must be applied to the polymer solution. In this process, stretching takes place as well. When the surface tension of the solution is high, nanofibers with bead or pore formation can be observed. Figure 1.9 shows the initial electrospinning process of a fiber being electrospun from a polyvinyl alcohol (PVA) solution.

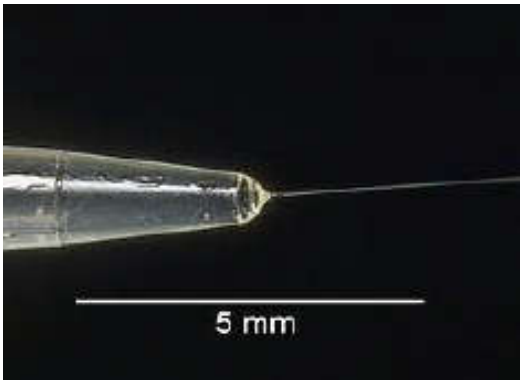


Figure 1.9: Image of initial electrospinning process [64].

1.4.3 Molecular Weight and Viscosity

One of the conditions in the electrospinning process is the polymer. A breakage of the fibers formed indicates that the polymer lacks the appropriate molecular weight and viscosity. If the molecular weight is high, then the length of the polymer chain is also high. Also, viscosity and more entanglements are present, which prevent breakage of the fibers. Viscosity is important because of the direct effect on the diameter of the electrospun fiber. Viscosity can stop the electrospinning process before it starts due to high viscosity. Most of the time, having high viscosity results in a larger fiber diameter, and again, pores and beads are not formed [64]. Figure 1.10 shows polymer and solvent molecules. As can be seen in Figure 1.10 (A), the higher the viscosity, the better the dispersion of the solvent molecules, and in Figure 1.10 (B), agglomerated solvent molecules have lower viscosity.

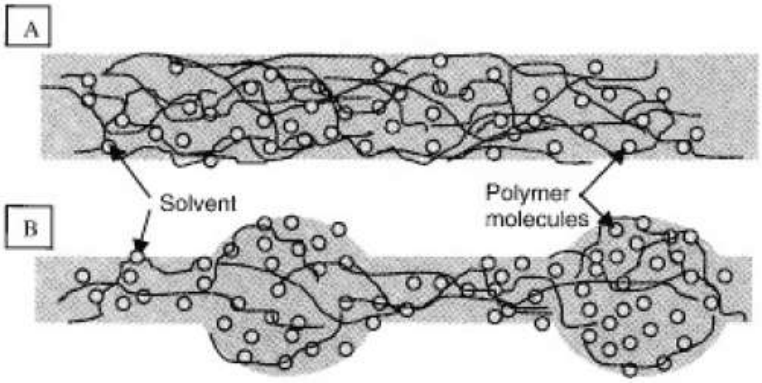


Figure 1.10: Image of polymer and solvent molecules [64].

1.4.4 Effects of Polymer and Solvent

The essential way to choose a solvent is by examining the solubility parameters. To understand whether a solvent is good or not, the interaction between polymer and solvent molecules must be observed. If the interaction is good, then the solvent is good. Good interactions among molecules lead to the dissolution of the polymer. Many polymers are available, and their solvents are not all the same. The main factor to look for when choosing the right solvent is the dissolve parameter—whichever solvent makes the polymer dissolve quickly is the correct solvent for that polymer [64].

1.4.5 Solution Conductivity

Stretching of the solution that occurs in the electrospinning process is due to the surface charge. A solution that has higher conductivity means there is more surface charge and is very easy to stretch. Polymers themselves have less conductivity. The addition of electrolytes and calcium chloride can increase their conductivity by producing ions and hence the voltage required to fabricate smooth fibers. Ions sizes are important as well because smaller-sized ions move very fast in comparison to larger ions. This process is important because the elongation will be greater and the fiber diameter will be reduced. Figure 1.11 shows charges on the surface of the solution.

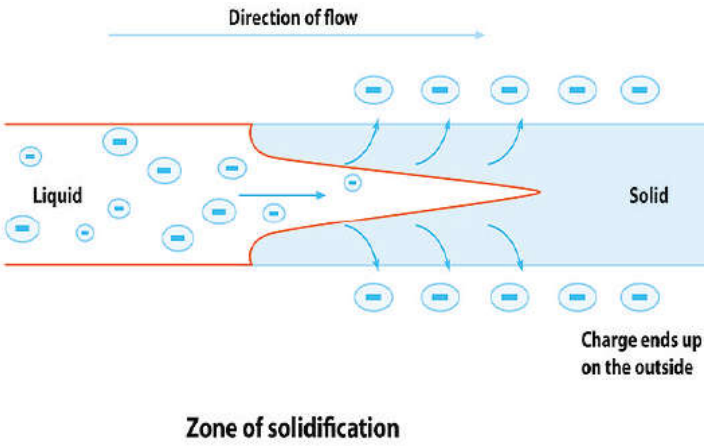


Figure 1.11: Schematic illustration of charges on surface of solution [64].

1.4.6 Processing Parameters

The morphology of fibers depends upon the flow rate of the solution. When resulting fibers with defects such as beads and pores shows that there is an excessive flow rate. A compromise has to be established between the minimum and maximum for the polymer concentration. If the polymer concentration is very high, the beaded structure defect will be formed. As the polymer concentration increases, at the same time the diameter of the electrospun fibers increases. When the polymer concentration increases, the shape of the beaded structure will transform from a spherical to a spindle figure [64]. Some process parameters are given below:

- Electric potential (voltage)
- Feed (flow) rate
- Polymer concentration
- Collector plate
- Diameter of needle
- Distance between tip and collector
- Temperature and humidity

- Air velocity

1.4.7 Collector Plate and Needle Diameter

To start the electrospinning system, there must be an electric field between the tip and the collector. Conductive material is used as the collector in the electrospinning process. Charges will dissipate at the collector, thus permitting fibers to gather on the collector. Compared to a conductive plate, a nonconductive plate may lead to fewer fibers accumulating on the collector. A smaller-diameter needle lessens the possibility of bead formation and decreases the fiber diameter. However, the diameter of the needle should not be too small, or the extrusion cannot be performed.

1.4.8 Distance between Tip and Collector

A short distance between the tip and the collector will lead to a shorter flight time and a higher electrical field. A shorter flight time means that there is not enough time for the solvent to evaporate, possibly leading to bead formation. An increase in the distance between the tip of the syringe and the collection screen will lead to a reduction in fiber diameter.

1.4.9 Temperature, Humidity, and Air Velocity

Most of the time, the electrospinning process occurs at room temperature. Temperature is an important parameter because conducting the electrospinning process above room temperature will reduce the fiber diameter. During the process, increasing humidity also helps to reduce fiber diameter. Having a high air flow will increase the evaporation rate because of the convection and will help reducing fiber diameters [64].

1.5 Functional Materials and Devices

1.5.1 Composite Reinforcement

Composite materials have been receiving keen interest from researchers for the past two decades. Producing composite materials with improved mechanical strength and other performance can be done by using fiber-based reinforcement. Electrospun nanofibers have advantageous mechanical properties compared to traditional microfibers. They also have a higher surface-to-volume ratio compared to conventional fabrics [65]. Furthermore, interaction between the fibers and the matrix may improve considerably by using nanofiber-reinforced composites, which will lead to better reinforcement than conventional fibers. Nanofiber-reinforced composites not only improve mechanical strength but also provide greater transparency [18].

1.5.2 Filter

Filtration is required for most engineering fields and is also necessary in most places such as hospitals, industries, and so on. Filtration is a huge market, estimated to be 700 billion US dollars for the year 2020 [18]. Polymeric nanofibers have been used in filtration applications. Polymeric nanofibers have exceptional properties, for example, high surface area, high porosity, and excellent surface adhesion. Nanofibers can be used as filtering media for separating out particles in the submicron range.

1.5.3 Smart Textiles and Protective Clothing

Nanofibers can be used in protective clothing as well as in other fabrics. Clothing made from electrospun nanofiber membranes are capable of neutralizing chemical agents, without the impedance of air and water vapor permeability. This is due to the high specific surface area, high porosity, and very small pore size of nanofibers. Initial research has shown that electrospun

nanofibers minimally impede moisture vapor diffusion. Also, they are greatly efficient at trapping aerosol particles, compared to conventional textiles [18].

1.5.4 Energy and Electronics

Energy is indispensable for performing any type of work, and the consumption of energy is increasing daily around the world. When the amount of energy reserves in the world is investigated, it can be seen that oil will last as long as 41 years, and natural gas sources will end in 67 years. To overcome the problem of high energy consumption, renewable and sustainable energies are being examined. Rather than oil and natural gas for producing energy, the wind generator, solar power generator, hydrogen battery, and polymer batteries have been used. The wide range of electrospun nanofiber applications used in these types of energy includes supercapacitors, lithium cells, fuel cells, solar cells, and so on. Additionally, using nanofibers in the electrical and electro-optical fields is of great interest. Nanofibers for use in optoelectronic devices and electronic devices can be fabricated.

1.5.5 Battery/Cell and Capacitor

Relative to electrodes, the rate of reactions is proportional to the surface area of the electrode. Membranes made out of electrospun nanofibers are conductive and a great choice for use in porous electrodes when developing high-performance batteries.

1.5.6 Sensor

Sensors play an importance part in human life. Their application range is quite wide, from drinking water to biosensors. Based on sensor interactions, it can be concluded that most sensing methods are as follows:

- Physical adsorption
- Light absorbance

- Chemical reaction between targeted analyte molecules and sensing materials

Moreover, the sensor turns physical, chemical, or optical phenomena into electrical output. Results are converted by the sensor to produce the quantitative measurement of detected molecules by internal or external standards [66]. Because nanofibers have a high surface area and porous membrane structure, they are applicable for sensitive and fast sensing. Nanofibers have shown improved sensitivities over conventional materials. Applications for those conventional materials are as follows [67]:

- Gas sensors
- Chemical sensors
- Optical sensors
- Biosensors

1.5.7 Catalyst

A catalyst is a substance that increases the rate of a chemical reaction. Here, the catalyst acts by attaching onto a substrate that is dependent on its active surface area. Nanofibers can be coated with a catalyst since they have a high surface area, thus increasing the active surface area and leading to improved catalytic activity [68]. Nanofibers posses a large surface area per a unit mass. This feature provides a solid support for enzymes and conventional catalysts, and provides the feasibility for high catalyst loading. Additionally, nanofibrous catalysts have the following advantages:

- Ability to adapt to any geometry
- Low resistance to the flow of liquids and gases

Comparing the catalyst recovery of nanofibrous catalysts versus nanoparticles, nanofibrous catalysts are much better because they can be recycled and reused easily.

The following four chapters, each of which is considered to be a journal paper, will further describe the overall PhD studies.

1.6 References

[1] Filatov, Y., Budyka, A., and Kirichenko, V. (2007). *Electrospinning of micro-and nanofibers: Fundamentals in separation and filtration processes*. Begell House Inc., Redding, CT.

[2] Gilbert, W. (1600). *De magnete magnetcisque corporibus, et de magno magnete tellure (On the Magnet, Magnetick Bodies also, and on the Great Magnet the Earth; a new Physiology, demonstrated by many arguments and Experiments*.The Chiswick Press, London.

[3] Greiner, A., and Wendorff, J. H. (2007). Electrospinning: A fascinating method for the preparation of ultrathin fibers. *Angewandte Chemie International Edition*,*46*(30), 5670-5703.

[4] Bose, G. M. (1744). *Die Electricität nach ihrer Entdeckung und Fortgang mit poetischer Feder entworffen*. Ahlfeld.

[5] Tucker, N., Stanger, J. J., Staiger, M. P., Razzaq, H., and Hofman, K. (2012). The History of the Science and Technology of Electrospinning from 1600 to 1995. *Journal of Engineered Fabrics and Fibers (JEFF)*, *7*(3).

[6] Cook, J. G. (1984). *Handbook of textile fibres: Man-made fibres* v. 2. Woodhead Publishing Limited, Cambridge, England.

[7] Plateau, J. (1873). *Statique Expérimentale et Théorique des Liquides Soumis aux Seules Forces Moléculaires*, vols. 1 and 2 Gauthier-Villars, Paris,France.

[8] Strutt, J. W. (Lord Rayleigh). (1879). On the instability of jets. In *Proc. R. Soc. London A* 10, 4-13.

[9] Strutt, J. W. (Lord Rayleigh). (1879). On the capillary phenomena of jets. *Proceedings of the Royal Society of London*, *29*(196-199), 71-97.

[10] Strutt, J. W. (Lord Rayleigh). (1944). Charles Vernon Boys. 1855-1944. *Obituary Notices of Fellows of the Royal Society*, 771-788.

[11] Boys, C. V. (1887). LVII. On the production, properties, and some suggested uses of the finest threads. *The London, Edinburgh, and Dublin Philosophical Magazine and Journal of Science*, *23*(145), 489-499.

[12] Cooley, J. F. (1900). Improved methods of and apparatus for electrically separating the relatively volatile liquid component from the component of relatively fixed substances of composite fluids. *Patent GB*, *6385*.

[13] Formhals, A. (1934). *U.S. Patent No. 1,975,504*. Washington, DC: U.S. Patent and Trademark Office.

[14] Taylor, G. (1964). Disintegration of water drops in an electric field. *Proceedings of the Royal Society of London. Series A. Mathematical and Physical Sciences*,*280*(1382), 383-397.

[15] Doshi, J., and Reneker, D. H. (1995). Electrospinning process and applications of electrospun fibers. *Journal of Electrostatics*, *35*(2), 151-160.

[16] Taylor, G. (1969). Electrically driven jets. *Proceedings of the Royal Society of London. A. Mathematical and Physical Sciences*, *313*(1515), 453-475.

[17] Bharath R. K. (2006). Ph.D. dissertation, *Miami University*, Oxford, Ohio.

[18] Huang, Z. M., Zhang, Y. Z., Kotaki, M., and Ramakrishna, S. (2003). A review on polymer nanofibers by electrospinning and their applications in nanocomposites. *Composites Science and Technology*, *63*(15), 2223-2253.

[19] Fong, H., Chun, I., and Reneker, D. H. (1999). Beaded nanofibers formed during electrospinning. *Polymer*, *40*(16), 4585-4592.

[20] He, J. H., Wan, Y. Q., and Yu, J. Y. (2004). Application of vibration technology to polymer electrospinning. *International Journal of Nonlinear Sciences and Numerical Simulation*, *5*(3), 253-262.

[21] Wendorff, J. H., Agarwal, S., and Greiner, A. (2012). *Electrospinning: Materials, processing, and applications*. John Wiley and Sons, New York.

[22] Yeo, L. Y., and Friend, J. R. (2006). Electrospinning carbon nanotube polymer composite nanofibers. *Journal of Experimental Nanoscience*, *1*(2), 177-209.

[23] Kalayci, V. E., Patra, P. K., Buer, A., Ugbolue, S. C., Kim, Y. K., and Warner, S. B. (2004). Fundamental investigations on electrospun fibers. *Journal of Advanced Materials*, *36*(4), 43-45.

[24] Kataphinan W.(2004). Ph.D. dissertation, *The University of Akron*, Ohio.

[25] Reneker, D. H., Yarin, A. L., Fong, H., and Koombhongse, S. (2000). Bending instability of electrically charged liquid jets of polymer solutions in electrospinning. *Journal of Applied physics*, *87*(9), 4531-4547.

[26] Kang, Y. K., Park, C. H., Kim, J., and Kang, T. J. (2007). Application of electrospun polyurethane web to breathable water-proof fabrics. *Fibers and Polymers*, *8*(5), 564-570.

[27] Buika, G. (2009). Electrospun PVA nanofibres for gas filtration applications. *Fibres and Textiles In Eastern Europe*, *17*(6), 77.

[28] Gorji, M., Jeddi, A., and Gharehaghaji, A. A. (2012). Fabrication and characterization of polyurethane electrospun nanofiber membranes for protective clothing applications. *Journal of Applied Polymer Science*, *125*(5), 4135-4141.

[29] Chen, J. P., Chang, G. Y., and Chen, J. K. (2008). Electrospun collagen/chitosan nanofibrous membrane as wound dressing. *Colloids and Surfaces A: Physicochemical and Engineering Aspects*, *313*, 183-188.

[30] Thakur, R. A., Florek, C. A., Kohn, J., and Michniak, B. B. (2008). Electrospun nanofibrous polymeric scaffold with targeted drug release profiles for potential application as wound dressing. *International Journal of Pharmaceutics*, *364*(1), 87-93.

[31] Xu, C. Y., Inai, R., Kotaki, M., and Ramakrishna, S. (2004). Aligned biodegradable nanofibrous structure: A potential scaffold for blood vessel engineering. *Biomaterials*, *25*(5), 877-886.

[32] Levy, A. J. (1985). *U.S. Patent No. 4,549,545*. Washington, DC: U.S. Patent and Trademark Office.

[33] Reneker, D. H., Yarin, A. L., Zussman, E., and Xu, H. (2007). Electrospinning of nanofibers from polymer solutions and melts. *Advances in Applied Mechanics*,*41*, 43-346.

[34] Li, W. J., Laurencin, C. T., Caterson, E. J., Tuan, R. S., and Ko, F. K. (2002). Electrospun nanofibrous structure: A novel scaffold for tissue engineering. *Journal of Biomedical Materials Research*, *60*(4), 613-621.

[35] Xu, L. R., Li, L., Lukehart, C. M., and Kuai, H. (2007). Mechanical characterization of nanofiber-reinforced composite adhesives. *Journal of Nanoscience and Nanotechnology*, *7*(7), 2546-2548.

[36] Kim, J. S., and Reneker, D. H. (1999). Polybenzimidazole nanofiber produced by electrospinning. *Polymer Engineering and Science*, *39*(5), 849-854.

[37] Goldstein, P. J. (2004). Master's thesis, *University of Florida*, Florida.

[38] Salem D. R., (2001), *Structure formation in polymeric fibers*, Hanser Publications, Ohio.

[39] Rayleigh, L. (1882). XX. On the equilibrium of liquid conducting masses charged with electricity. *The London, Edinburgh, and Dublin Philosophical Magazine and Journal of Science*, *14*(87), 184-186.

[40] Rayleigh, L. (1879). On the capillary phenomena of jets. *Proceedings of the Royal Society of London*, *29*(196-199), 71-97.

[41] Park, C. H., Kim, C. H., Tijing, L. D., Lee, D. H., Yu, M. H., Pant, H. R., and Kim, C. S. (2012). Preparation and characterization of (polyurethane/nylon-6) nanofiber/(silicone) film composites via electrospinning and dip-coating. *Fibers and Polymers*, *13*(3), 339-345.

[42] Taylor, G. (1964). Disintegration of water drops in an electric field. *Proceedings of the Royal Society of London. Series A. Mathematical and Physical Sciences*,*280*(1382), 383-397.

[43] Taylor, G. (1966). Studies in electrohydrodynamics. I. The circulation produced in a drop by electrical field. *Proceedings of the Royal Society of London. Series A. Mathematical and Physical Sciences*, *291*(1425), 159-166.

[44] Formhals A. (1944). *U.S. Patent No. 2,349,950*. Washington, DC: U.S. Patent and Trademark Office.

[45] Baumgarten, P. K. (1971). Electrostatic spinning of acrylic microfibers. *Journal of Colloid and Interface Science*, *36*(1), 71-79.

[46] Subbiah, T., Bhat, G. S., Tock, R. W., Parameswaran, S., and Ramkumar, S. S. (2005). Electrospinning of nanofibers. *Journal of Applied Polymer Science*,*96*(2), 557-569.

[47] Doshi J. (1994). Ph.D. dissertation, *University of Akron*, Akron, Ohio.

[48] Srinivasan, G., and Reneker, D. H. (1995). Structure and morphology of small diameter electrospun aramid fibers. *Polymer International*, *36*(2), 195-201.

[49] Chun I. (1997). Ph.D. dissertation, *University of Akron*, Akron, Ohio.

[50] Jaeger, R., Bergshoef, M. M., Batlle, C. M. I., Schönherr, H., and Vancso, G. J. (1998). Electrospinning of ultra-thin polymer fibers. In *Macromolecular symposia* 127(1), 141-150.

[51] Jaeger, R., Schönherr, H., and Vancso, G. J. (1996). Chain packing in electro-spun poly (ethylene oxide) visualized by atomic force microscopy. *Macromolecules*, *29*(23), 7634-7636.

[52] Fang, X. D. H. R., and Reneker, D. H. (1997). DNA fibers by electrospinning. *Journal of Macromolecular Science, Part B: Physics*, *36*(2), 169-173.

[53] Fong, H., Liu, W., Wang, C. S., and Vaia, R. A. (2002). Generation of electrospun fibers of nylon 6 and nylon 6-montmorillonite nanocomposite. *Polymer*, *43*(3), 775-780.

[54] Drasler, W. J., Jenson, M. L., Scott, R. J., and Stenoien, M. D. (1998). *U.S. Patent No. 5,840,240*. Washington, DC: U.S. Patent and Trademark Office.

[55] Zarkoob, S. (1998). Ph.D Disertation, *University of Akron*, Ohio.

[56] Zarkoob, S., Eby, R. K., Reneker, D. H., Hudson, S. D., Ertley, D., and Adams, W. W. (2004). Structure and morphology of electrospun silk nanofibers. *Polymer*, *45*(11), 3973-3977.

[57] Huang, L., McMillan, R. A., Apkarian, R. P., Pourdeyhimi, B., Conticello, V. P., and Chaikof, E. L. (2000). Generation of synthetic elastin-mimetic small diameter fibers and fiber networks. *Macromolecules*, *33*(8), 2989-2997.

[58] Gibson, P. W., Schreuder-Gibson, H. L., and Rivin, D. (1999). Electrospun fiber mats: Transport properties. *AIChE Journal*, *45*(1), 190-195.

[59] Díaz-de León, M. J. (2001). Electrospinning nanofibers of polyaniline and polyaniline/(polystyrene and polyethylene oxide) blends. In *Proceeding of The National Conference on Undergraduate Research (NCUR), University of Kentucky* 15-17.

[60] Kim, J. S., and Lee, D. S. (2000). Thermal properties of electrospun polyesters. *Polymer journal*, *32*(7), 616-618.

[61] Bognitzki, M., Frese, T., Wendorff, J. H., and Greiner, A. (2000). Submicrometer Shaped Polyactide Fibers by Electrospinning. *Polymeric materials science and engineering, Washington*, *82*, 115-116.

[62] Bognitzki, M., Czado, W., Frese, T., Schaper, A., Hellwig, M., Steinhart, M., and Wendorff, J. H. (2001). Nanostructured fibers via electrospinning. *Advanced Materials*, *13*(1), 70-72.

[63] Khan, W. S., Asmatulu, R., Ceylan, M., and Jabbarnia, A. (2013). Recent progress on conventional and non-conventional electrospinning processes. *Fibers and Polymers*, *14*(8), 1235-1247.

[64] Srinivasan A., Electrospinning and nanofibers, URL: http://www.nitk.ac.in/static/assets/files/MetMat/Dr.AS/electrospinning.pdf [cited April 13, 2014].

[65] Li, D., and Xia, Y. (2004). Electrospinning of nanofibers: Reinventing the wheel?. *Advanced materials*, *16*(14), 1151-1170.

[66] Fujihara, K., Teo, W. E., Lim, T. C., and Ma, Z. (2005). *An introduction to electrospinning and nanofibers* v.90. World Scientific, Singapore.

[67] Hunley, M. T., and Long, T. E. (2008). Electrospinning functional nanoscale fibers: A perspective for the future. *Polymer International*, *57*(3), 385-389.

[68] Subbiah, T., Bhat, G. S., Tock, R. W., Parameswaran, S., and Ramkumar, S. S. (2005). Electrospinning of nanofibers. *Journal of Applied Polymer Science*, *96*(2), 557-569.

CHAPTER 2

SYNTHESIS AND EVALUATION OF ELECTROSPUN PCL-PLASMID DNA NANOFIBERS FOR BIOMEDICAL APPLICATIONS

2.1 Abstract

In this study, poly-ε-caprolactone (PCL) incorporated with plasmid DNA was electrospun, and the resultant nanofibers were used to observe DNA release from nanofibers. The plasmid DNA enhanced green fluorescent protein (EGFP) with cytomegalovirus (CMV) promoter (PCMVb-GFP) was amplified with *E. coli*. PCL was chosen because it is a biodegradable aliphatic polyester, which plays a critical role in tissue engineering, such as scaffolding, drug, DNA and protein delivery vehicles. The biological character of PCL nanofibers can be detected by different methods. Scanning electron microscopy (SEM) micrographs showed that nanoscaled fiber structures have an average diameter of 102.66 nm. Data showed 1 day, 4 days, and 7 days above 80% of cell viability. These data demonstrated that PCL nanofibers have no cytotoxicity and benign biocompatibility. PCMVb-GFP plasmid-linked electrospun nanofibers continuously released double-stranded DNA for at least seven days. For the first 15 minutes, there was a nanofiber burst release of about 1.8 ng/ml. For the following hours and days, the release was about the same, thus averaging a release of 0.575 ng/ml. Therefore, PCL nanofibers may be an ideal candidate for biomedical applications such as scaffolding, tissue engineering, and protein delivery vehicles.

Keywords: PCL, Plasmid DNA, Electrospun nanofibers, Biomedical application

2.2 Introduction

Electrospinning is a very simple and versatile method to produce nanofibers from a very large number of polymers. Scientists and researchers have shown a keen interest in studying the

the fabrication of nanofibers and also the characterization of electrospun nanofibers. As a result, most electrospun nanofiber parameters, such as diameter, morphology, and patterning, can be controlled. The improvements and developments in electrospun nanofibers are showing potential applications for their use [1]. Currently, applications using electrospun nanofibers have been extended to various fields such as biomedical, functional devices and materials, energy, and electronics [2]. The biomedical applications of electrospun nanofiber include drug delivery [3, 4], wound dressing [2, 5], tissue engineering scaffolds [6, 7], artificial organs [8, 9], and vascular grafts [8–10]. Biomedical applications using electrospun nanofibers are becoming a larger portion of all the possible applications, according to applied patent applications [2]. In this study, an experiment shows that PCL is a good carrier for plasmid DNA. Numerous studies have used different types of polymers and focus on tissue engineering scaffolding and drug delivery [11–15]. The goal is here to build a biocompatible and nontoxic material for drug delivery purposes. For example, this specific material may be used to avoid the recurrence of cancer.

Recently, copolymers such as poly-ε-caprolactone (PCL), poly(lactide-co-glycolide) (PLGA) random copolymer, poly(D,L-lactide)–poly(ethyleneglycol) (PLA–PEG) block copolymer, polycations (ε-poly-L-lysine (EPL), and polyethylenimine (PEI) have been used to deliver genes, drugs, and proteins [11–15]. PCL has been approved by the Food and Drug Administration. It is nontoxic, has low immunogenicity, is well-known as a biomaterial, and is extensively applied in tissue engineering [16–18].

Biocompatible polymers such as PCL, PEI, and PEG are suited for biomedical applications. These have been used for scaffolding [12], tissue engineering [13], wound healing [5], and drug delivery. However, there is untouched area whereby plasmid DNA may be used to avoid the recurrence of cancer. The material prepared in this study is a good candidate for this

application. PCL is biocompatible and a good drug carrier. PCL with a molecular weight of 70,000 was used in this study. PCL is insoluble in water and has a melting temperature of 60ºC, a glass transition temperature of –60ºC, and a decomposition temperature of 200ºC. PCL is a semi-crystalline polymer, and its crystallinity tends to decrease with increasing molecular weight. PCL has a hydrophobic nature, and as a result, drug release can continue for days.

The electrospinning process [19–21] with its wide range of applications has been gaining scientific interest worldwide. The process parameters in electrospinning include viscosity, flow rate of the syringe, applied voltage to the syringe tip, and distance between syringe tip and collector. These parameters can be changed to produce different fibers in the range of nanoscale to microscale. Drug delivery or gene delivery can be conducted using electrospun nanofibers [22]. Some polymers, such as PCL, PEI, and PEG, have been used for this purpose [16–18]. PCL nanofibers possess hydrophobic properties, which can slow the drug-release rate; however, drug delivery takes place continuously for days in the area of interest. Plasmid DNA-enhanced EGFP with CMV promoters have been amplified with *E. coli* and used with PCL electrospun nanofiber to observe the DNA release rate.

The critical point for the electrospinning process is in the application of high voltage, without which it cannot be performed. Following the application of high voltage, the solution is charged and the Taylor cone is shaped. The reasons for using high voltage are described below:

- Reducing fiber diameter.
- Reducing flight time between tip and collector.
- With a proper flight time, increasing crystallinity.

The electrospinning feed rate regulates the amount of solution available for the process. With a given voltage, fibers with a high diameter might show that the flow rate is high too. It also shows that the solvent needs more drying time.

Due to evaporation and also stretching, the diameter of the jet is continuously reduced as it moves toward the target. Evaporation occurs in a way that some of the solvent is gone before reaching the target. Stretching is caused by the jet electrostatic forces. Fiber diameter is related to applied voltage. The diameter decreases with an increase in voltage. When the applied electrical potential increases, the field strength increases, as well, which in turn accelerates changes in the electrified jet and instability region. This will result in producing fibers that are sub-micron size. The drift velocity of the charge carriers is related to mobility of charge carriers by the following equation [23]:

$$u = m_0 V \tag{2.1}$$

where u is the drift velocity, m_o is the mobility of charge carriers, and V is the applied field.

2.3 Experimental Procedure

2.3.1 Materials

Plasmid DNA was produced with PCL purchased from Scientific Polymer Products, Inc., acetonitrile purchased from Sigma-Aldrich, and pCMVb-GFP DNA purchased from Addgene. The plasmid DNA was amplified with *E. coli*. These products were directly used in the electrospinning process without further purification. Fibroblast cells (L-929) were purchased from the American Type Culture Collection (ATCC).

2.3.2 Methods

2.3.2.1 Isolation of pCMVb-GFP Plasmid DNA

Plasmid DNA EGFP with CMV promoter was amplified with *E. coli* and grown on a shaker at 37ºC overnight. Micro-centrifuge tubes were filled with saturated bacterial culture grown in lysogeny broth (LB) containing ampicillin and centrifuged at 4,000 rpm at 4ºC for 3 min, followed by the addition of 0.2 ml of ice-cold solution I (50 mM glucose, 25 mM Tris-Hcl pH 8.0, 10 mM EDTA Ph 8.0), 0.4 ml of solution II (1% sodium dodecyl sulfate(SDS), 0.2 N NaOH), and 0.3 ml of ice-cold solution III (3 M K+ 5 M acetate). Next, the microcentrifuge tubes were put on ice for 10 min and then centrifuged at 12,000 rpm at 4ºC for 5 min. Supernatant was transferred to a fresh micro-centrifuge tube. Isopropanol was added to fill the remainder of the centrifuge tubes, which were then put on ice for 10 min, followed by centrifuging at 12,000 rpm at 4ºC for 5 min. Then, 1 ml of ice-cold 70% ethanol was added to each of the microcentrifuge tubes and centrifuged at a speed of 7,500 rpm at 4ºC for 2 min. Finally, 50 µl of E buffer (10 mM Tris-HCl, 1 mM EDTA, pH 8.0) was added to each tube. Using the Elisa Reader, the concentration of plasmid DNA was detected from the ultraviolet (UV) absorbance at a wavelength of 260 nm (A260).

2.3.2.2 Electrospinning of Nanofibers

The electrospinning process is established on the principle that a polymeric solution has a surface tension weaker than the strong electrical force used to pull a liquid jet from a larger sample. The discharged polymer solution dries or solidifies, leaving a nanoscale polymer fiber on a specified surface. Electrospray and electrospinning processes both involve high voltage [24], which is used to start and accelerate a liquid jet from the tip of a capillary tube. In electrospraying, the liquid jet breaks into very small droplets due to the low viscosity solution

used. On the other hand, in the electrospinning process, a solid fiber is produced as an end product. The syringe contains a charged viscous polymer solution. In the electrospinning process, one conductive rod is placed into the needle to charge the solution, and an electrode is attached onto the grounded surface, which is the collector. Electric voltage is applied to the conductive rod in the syringe that contains the polymeric solution held by its surface tension. Charge repulsion causes tangential forces directly opposite to the surface tension of the polymer, which need to be overcome to form fibers. The semicircular surface of the fluid at the tip of the capillary tube elongates, which is a sign that the intensity of the electric field has increased.

After this elongation process, a conical shape, or Taylor cone, occurs. By increasing the electrical field, a critical value is achieved in order to overcome surface tension of the fluid in the charged jet. The charged fluid goes from tip to cone [25]. The jet of the discharged polymer solution undergoes a drying process in the air where the solvent evaporates and leaves behind a charged polymer fiber. Then it lays itself randomly (non-woven) on a grounded collecting metal screen. The discharged jet totally solidifies in a few hours and is collected on the grounded surface [26–31]. Thus, the resultant product is a nanoporous non-woven nanofiber film, which can be used for various applications because of its high surface area and high aspect ratio [25, 32–37]. Figure 2.1 shows a simplified schematic of the electrospinning process and resulting electrospun polymeric fibers.

An electrospinning setup is quite simple; however, the experimental detail and theoretical analysis show that the process is highly complex. For a better understanding of this complexity, it is necessary to look into different types of instabilities, which are process controlled. Those instabilities are whipping or bending instability, Rayleigh instability, and axisymmetric instability [38]. In bending or whipping instability, the external electric field as well as

electrostatic interactions between the surface charges on the jet create instability. Also, bending instability controls the stretching, acceleration, elongation, and thinning of the electrospun fibers [39]. Other types of instabilities are Rayleigh instability and axisymmetry, which give rise to fluctuations of the jet radius and may also cause droplet formation.

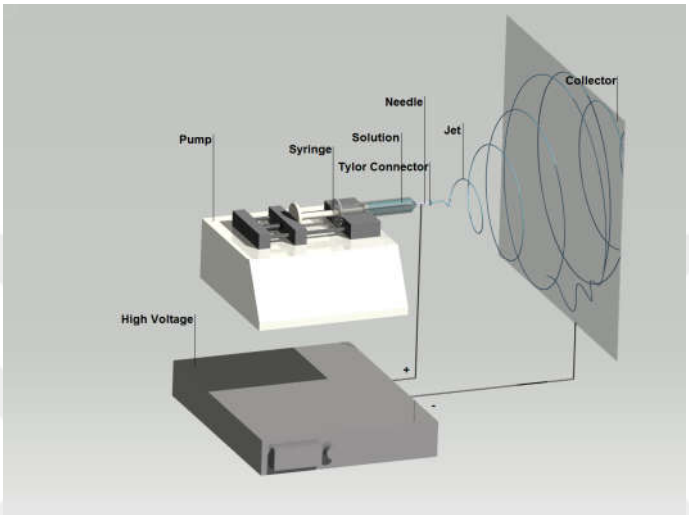


Figure 2.1: Schematic illustration of electrospinning process.

In the current study, the nanofiber was fabricated for the purpose of DNA release by dissolving PCL in acetonitrile and mixing it with pCMVb-GFP plasmid (3.5 mg/ml in TE buffer). The solution was allowed to equilibrate at 50^{o}C for 4 hr with constant stirring to generate 85–15% w/w polymer solution containing 700 µg plasmid DNA in 200 µl TE buffer. The solution was transferred to a 10 ml syringe with a plastic pipette tip and set up in the electrospinning apparatus. The flow of polymer solution from the syringe was controlled by a programmable syringe pump. The nanofiber was electrospun at ~25 KV with a flow rate of 20 µl/min. A collector was fixed at ~25 cm from the needle to gather the nanofiber. After peeling off the nanofiber from the collector, the character of the nanofiber was observed under a scanning electron microscope (Zeiss FESEM Sigma VP).

2.3.2.3 SEM Analysis of Electrospun Fibers

When the filament in the SEM electron gun is sufficiently charged, it emits electrons that are focused onto the sample surface using a series of lenses. The sample surface, when struck with these electrons, emits secondary electrons. When detected by the scanner, the sample topography is reproduced and the SEM image is formed. SEM uses electrons that are emitted from the specimen to reconstruct the image. The operating conditions of the SEM are accelerating voltage of 10 Kev, spot size of 4, and a work distance of 12 mm. Images are taken at various magnifications and across various areas for each sample. Resolution can easily go below 10 nm. Figure 2.2 exhibits an SEM-imaged PCL with plasmid DNA. Appendix A contains additional SEM images.

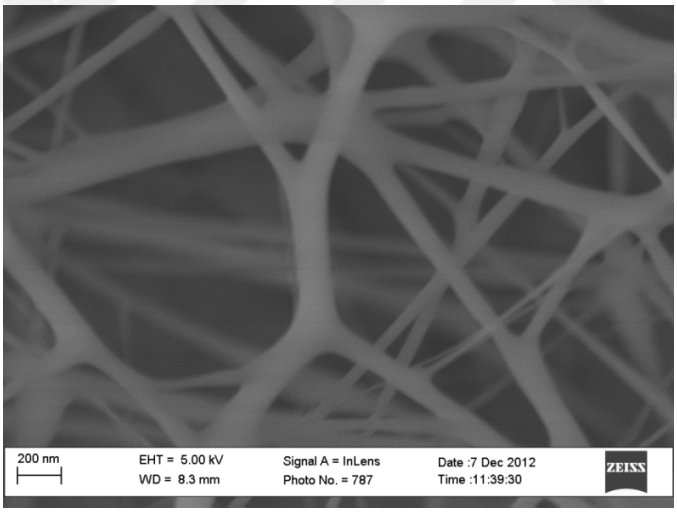


Figure 2.2: PCL nanofiber with plasmid DNA.

2.3.2.4 Biocompatibility and Cytotoxicity Assay of PCL Nanofibers

Sterile nanofibers in a 2 ml Eppendorf tube were submerged with Dulbecco's Modified Eagle's Medium (DMEM) (ATCC, Virginia, USA) containing 5% fetal bovine serum (FBS), 2 mM glutamine, 100 μ/ml penicillin, and 0.1 mg/ml streptomycin. The medium was collection on the first, fourth, and seventh days, and tubes were refilled with fresh medium. Cells were seeded

in a 96-well plate at a density of 5 x 10^4 cells/well and cultured in a standard incubator (37°C, 5% CO_2) for 3 days. Then, 20 µl of 3-(4, 5-dimethylthiazol-2-yl)-2, 5-diphenyltetrazolium bromide (MTT) was added to each well. After six hours, the cells were cracked using a 10% sodium dodecyl sulfonate (SDS) solution, followed by a reading plate at OD 590nm. The Elisa Reader was used for this process.

2.3.2.5 DNA Release Rates

The electrospun nanofiber meshes were cut into 2 x 2 cm sections, and each section was immersed in 1 ml TE buffer in Eppendorf tubes at 37°C. The amount of DNA released into the solution was quantified using PicoGreen assay, according to the manufacture's protocol. Briefly, the elution TE buffers were collected at 15 min, 30 min, 1 hr, 2 hr, 4 hr, 1 day, 3 days, and 7 days and labeled with PicoGreen to detect DNA content. For each time point, there were six samples. A DNA standard solution (100 µg/ml in TE(10 mM Tris-HCl, 1 mM EDTA, pH 7.5) buffer) was diluted in a 2 µg/ml stock solution, at a dilution of 1:2. Based on the concentration of DNA in the standard solution, it is possible to calculate how much double-strand DNA is released into the TE buffer. The PicoGreen reagent was diluted 200 fold in a TE buffer. The elution solutions were measured at 520 nm (with excitation at 480 nm) in a UV microplate reader (CytoFlour Series 4000, Perceptive Biosystems). According to the standard curve, the plasmid DNA concentration in each sample can be calculated.

2.4 Results and Discussion

2.4.1 Biocompatibility and Cytotoxicity Assay of PCL Nanofibers and Applications

L-929 cells were cultured with a normal medium as a nontoxic group, 10% SDS as a toxic group, and nanofiber elution medium as a testing group. The data demonstrate that the number of L-929 cells in the testing group was less than in the nontoxic group and more than in

the toxic group (Figure 2.3). But when diluted by 1:16, SDS significantly facilitated the growth of L-929 cells. The experiment was repeated three times and yielded the same result.

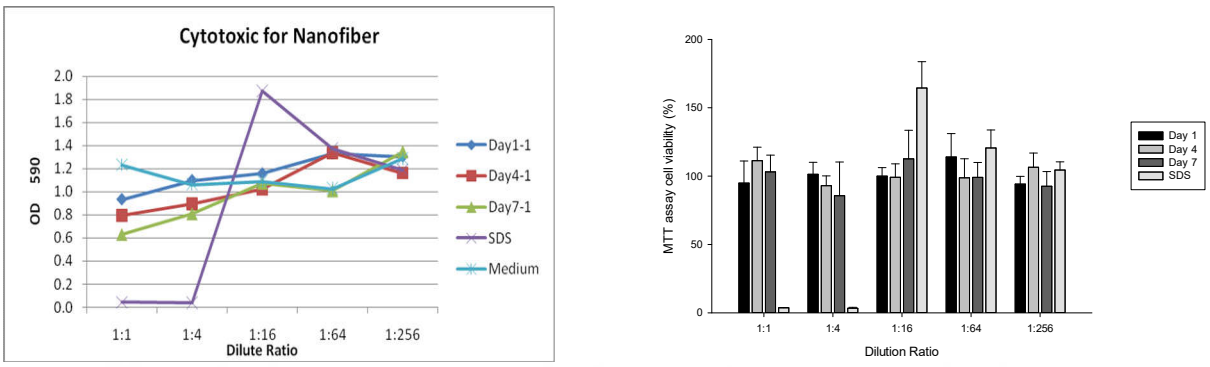


Figure 2.3: Cytotoxicity results for PCL nanofiber

2.4.2 Biomedical Applications

Electrospun nanofibers have broad application areas, one of which is the biomedical field, in such areas as drug delivery, wound dressing, and tissue engineering. Also, electrospun nanofiber can be placed in human organ tissues such as bone, dentin, skin, and cartilage. A current report indicates that in 2015, 180 billion dollars will be spent on nanomaterials in the biomedical as a business field [38].

2.4.3 Drug Delivery

The drug delivery principle states that the drug release rate increases with the increase in surface area. Electrospun nanofibers are used here because of the very large surface-to-volume ratio [2]. Looking at patents who were issued drug delivery using the electrospun method, the first patent was from Belenkaya, in 2003 [40]. Ignatious and Sun demonstrated the stabilization of amorphous drugs using nanofibers [41, 42]. Shalaby worked on the production of biomechanically compatible drug-eluting stents using an electrospun mixture of biodegradable polymers and drugs on the surface of a small metallic stent [43]. Mo et al. prepared electrospun core-shell fibers for coating an endovascular stent [44].

2.4.4 Tissue Engineering

Tissue engineering is a very important, and materials used in this field are required to be ideal in order to mimic the natural extracellular matrix (ECM). This has been provided by non-woven membranes of electrospun fibers [45, 46]. Electrospun nanofibers used for tissue repairing have contained chitosan, as studied by Mo et al. [47]. Mo et al. [47] electrospun natural spider silk and type 1 collagen to produce nanofibers with diameters of 200–260 nm for tissue repair [2]. These electrospun nanofibers showed adequate porosity, great mechanical properties, and biocompatibility, and can be used to repair skin, nerve tissue, and blood vessels.

2.4.5 Wound Dressing

Wound dressing basically involves the treatment of wounds and human skin burns. Due to their high porosity, electrospun nanofibers can be applied over to those areas. High porosity allows gas exchange and the growth of a fibrous structure, thus protecting wounds from infection and dehydration. For wound dressing, pore size is important. For this reason, non-woven electrospun nanofiber membranes generally have pore sizes in the range of 500–1000 nm, which are good enough to prevent bacterial penetration in the wound. The high surface area of electrospun nanofibers makes it very easy for delivery and absorption [48].

2,4.6 DNA Release Rates

PicoGreen is ultra-sensitive to double-stranded DNA, but not to single-stranded DNA and oligonucleotides, which can detect as little as 250 pg/ml of double-strand DNA using a fluorescence microplate. The TE buffer is collected at the predefined point. Data indicate a peak DNA release at 15 min, and after that the number of double-stranded DNA molecules released from nanofiber meshes is basically the same as at all other time points (Figure 2.4). An experiment was run for 7 days; however, it could go longer, after looking at Figure 2.4, because

after the peak, the release was almost steady. Since plasmid DNA is incorporated with PCL, it may release DNA for a longer period of time due to the nature of PCL.

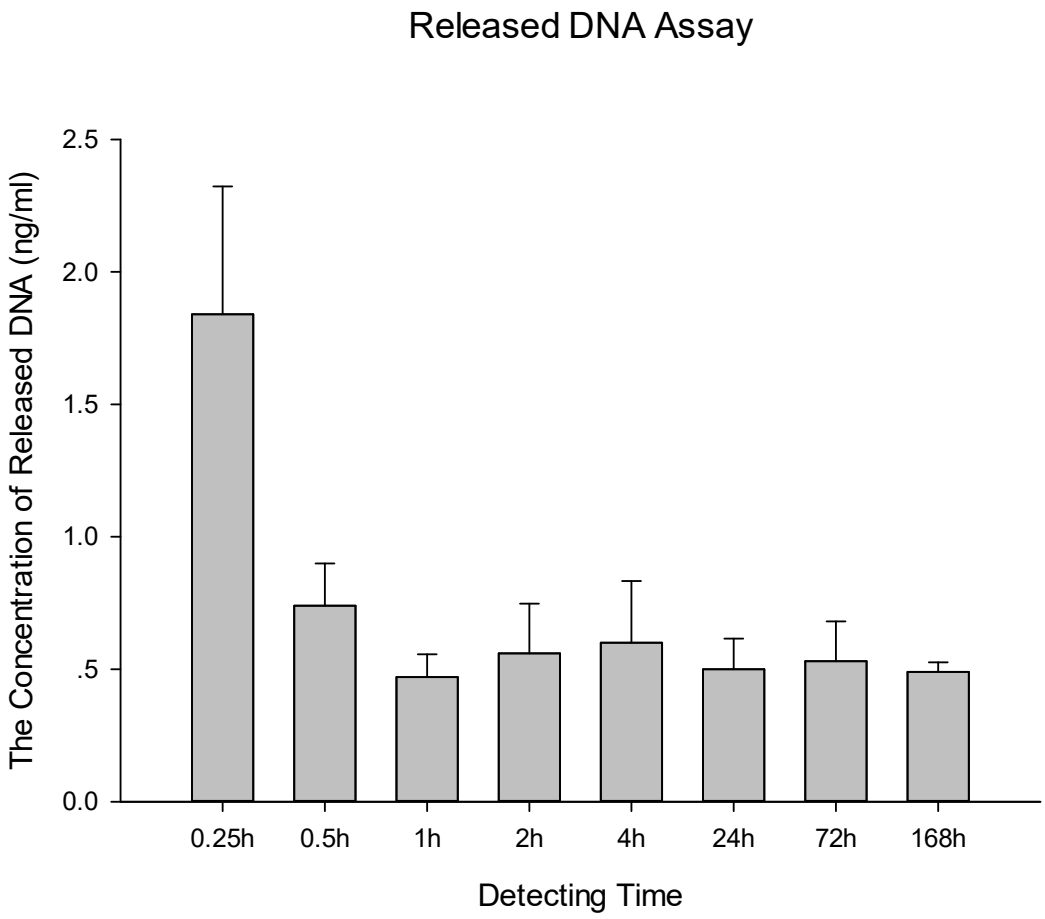


Figure 2.4: DNA release rates as a function of time.

Results show that PCL nanofiber is not toxic and a good carrier for plasmid DNA. This result is comparable to that demonstrated by Yohe et al., although they used PGC-C18 (poly(glycerol monostearate-co-ε-caprolactone)) [14]. Furthermore, a study by Luu et al. [12] involved a DNA delivery scaffold via electrospinning of PLGA (poly(lactide-co-glycolide)) and PLA-PEG (poly(D,L-lactide)–poly(ethylene glycol)) block copolymers. They used DNA for tissue engineering, and their results show that their release test went for more than 20 days. The first two hours exhibited a maximum release. In addition, a study by Lanbeck et al. involved four

antibiotics tests with endothelial cells. The antibiotics used were erythromycin, dicloxacillin, cefuroxime, and benzylpenicillin. Their results show that in a time-related manner, erythromycin and dicloxacillin reduced DNA synthesis in all types of cells; however, cefuroxime and benzylpenicillin did not show any effects [49]. In the study here, antibiotics were not used, unlike in the work of Lanbeck et al. work. Our results show that the PCL nanofiber indicated more than 80% cell viability for 1 day, 4 days, and 7 days. DNA release can go more than 7 days. It has a burst release for the first 15 min and then becomes steady. The release of plasmid DNA depends on various factors, including the nature of the polymer matrix, such as chemical composition, and water solubility. The release also depends upon the fiber diameter, surface area volume of the PCL nanofibers, and permeability of the nanofibers, which are significant factors in the release of plasmid DNA. The work here shows good results and opens new research areas for recurring cancer.

2.5 Conclusions

PCL-electrospun nanofiber mesh has a benign biocompatibility and can be successfully linked with non-viral vectors to serve as a tool for biomedical applications. Data showed 1 day, 4 days, and 7 days above 80% of cell viability, suggesting that the nanofiber mesh can continuously release plasmid DNA with an initial burst release, which may be beneficial for biomedical applications such as drug delivery, gene delivery, tissue engineering, and wound dressing. The initial burst of nanofiber released was about 1.8 ng/ml for the first 15 minutes, and for the following hours and days, the release was about the same, so the average release was 0.575 ng/ml. The advantages of electrospun nanofiber scaffolds include their high surface-to-volume ratio, appropriate porosity and malleability, a wide variety of sizes and shapes, and good biocompatibility, which make it an ideal candidate as a gene delivery tool and therapeutic device.

Acknowledgments

The author thanks Zheng Song, Holly Haynes, Jacqueline Weber, Jimmy Nguyen, and Dr. Paul Wooley for their support during this research.

2.6 References

[1] Fujihara, K., Teo, W. E., Lim, T. C., and Ma, Z. (2005). *An introduction to electrospinning and nanofibers* v.90. Singapore: World Scientific.

[2] Huang, Z. M., Zhang, Y. Z., Kotaki, M., and Ramakrishna, S. (2003). A review on polymer nanofibers by electrospinning and their applications in nanocomposites. *Composites Science and Technology*, *63*(15), 2223-2253.

[3] Wu, X. H., Wang, L. G., and Huang, Y. (2006). Application of electrospun ethyl cellulose fibers in drug release systems. *ACTA Polymerica Sinica*, (2), 264-268.

[4] Katti, D. S., Robinson, K. W., Ko, F. K., and Laurencin, C. T. (2004). Bioresorbable nanofiber-based systems for wound healing and drug delivery: Optimization of fabrication parameters. *Journal of Biomedical Materials Research Part B: Applied Biomaterials*, *70*(2), 286-296.

[5] Ueno, H., Mori, T., and Fujinaga, T. (2001). Topical formulations and wound healing applications of chitosan. *Advanced Drug Delivery Reviews*, *52*(2), 105-115.

[6] Schindler, M., Ahmed, I., and Kamal, J. (2005). A synthetic nanofibrillar matrix promotes in vivo-like organization and morphogenesis for cells in culture. *Biomaterials*, *26*(28), 5624-5631.

[7] Ma, Z., Kotaki, M., Inai, R., and Ramakrishna, S. (2005). Potential of nanofiber matrix as tissue-engineering scaffolds. *Tissue Engineering*, *11*(1-2), 101-109.

[8] Nerem, R. (1999). Tissue Engineering of Vascular Prosthetic Grafts. *Nature Medicine*, *5*(10), 1118-1118.

[9] Miller, D. C., Webster, T. J., and Haberstroh, K. M. (2004). Technological advances in nanoscale biomaterials: The future of synthetic vascular graft design. *Expert Review of Medical Devices*, *1*(2), 259-268.

[10] Stitzel, J., Liu, J., Lee, S. J., Komura, M., Berry, J., Soker, S.,Lim, G., Van Dyke, M., Czerw, R., Yoo, J. J., and Atala, A. (2006). Controlled fabrication of a biological vascular substitute. *Biomaterials*,*27*(7), 1088-1094.

[11] Cohen-Sacks, H., Elazar, V., Gao, J., Golomb, A., Adwan, H., Korchov, N., and Golomb, G. (2004). Delivery and expression of pDNA embedded in collagen matrices. *Journal of Controlled Release*, *95*(2), 309-320.

[12] Luu, Y. K., Kim, K., Hsiao, B. S., Chu, B., and Hadjiargyrou, M. (2003). Development of a nanostructured DNA delivery scaffold via electrospinning of PLGA and PLA–PEG block copolymers. *Journal of Controlled Release*, *89*(2), 341-353.

[13] Kai, D., Prabhakaran, M. P., Stahl, B., Eblenkamp, M., Wintermantel, E., and Ramakrishna, S. (2012). Mechanical properties and in vitro behavior of nanofiber–hydrogel composites for tissue engineering applications. *Nanotechnology*, *23*(9), 095705.

[14] Yohe, S. T., Herrera, V. L., Colson, Y. L., and Grinstaff, M. W. (2012). 3D superhydrophobic electrospun meshes as reinforcement materials for sustained local drug delivery against colorectal cancer cells. *Journal of Controlled Release*, *162*(1), 92-101.

[15] Çapkın, M., Çakmak, S., Kurt, F. Ö., Gümüşderelioğlu, M., Şen, B. H., Türk, B. T., and Deliloğlu-Gürhan, S. İ. (2012). Random/aligned electrospun PCL/PCL-collagen nanofibrous membranes: Comparison of neural differentiation of rat AdMSCs and BMSCs. *Biomedical Materials*, *7*(4), 045013.

[16] Vadalà, G., Mozetic, P., Rainer, A., Centola, M., Loppini, M., Trombetta, M., and Denaro, V. (2012). Bioactive electrospun scaffold for annulus fibrosus repair and regeneration. *European Spine Journal*, *21*(1), 20-26.

[17] Yu, H., VandeVord, P. J., Mao, L., Matthew, H. W., Wooley, P. H., and Yang, S. Y. (2009). Improved tissue-engineered bone regeneration by endothelial cell mediated vascularization. *Biomaterials*, *30*(4), 508-517.

[18] Croisier, F., Duwez, A. S., Jérôme, C., Léonard, A. F., Van der Werf, K. O., Dijkstra, P. J., and Bennink, M. L. (2012). Mechanical testing of electrospun PCL fibers. *Acta Biomaterialia*, *8*(1), 218-224.

[19] Nuraje, N., Asmatulu, R., Cohen, R. E., and Rubner, M. F. (2011). Durable antifog films from layer-by-layer molecularly blended hydrophilic polysaccharides. *Langmuir*, *27*(2), 782-791.

[20] Nuraje, N., Khan, W. S., Lei, Y., Ceylan, M., and Asmatulu, R. (2013). Superhydrophobic electrospun nanofibers. *Journal of Materials Chemistry A*,*1*(6), 1929-1946.

[21] Asmatulu, R., Ceylan, M., and Nuraje, N. (2011). Study of superhydrophobic electrospun nanocomposite fibers for energy systems. *Langmuir*, *27*(2), 504-507.

[22] Agarwal, S., Wendorff, J. H., and Greiner, A. (2008). Use of electrospinning technique for biomedical applications. *Polymer*, *49*(26), 5603-5621.

[23] Kalayci, V. E., Patra, P. K., Buer, A., Ugbolue, S. C., Kim, Y. K., and Warner, S. B. (2004). Fundamental investigations on electrospun fibers. *Journal of Advanced Materials*, *36*(4), 43-45.

[24] Fenn, J. B., Mann, M., Meng, C. K., Wong, S. F., and Whitehouse, C. M. (1989). Electrospray ionization for mass spectrometry of large biomolecules. *Science*,*246*(4926), 64-71.

[25] Marginean, I., Nemes, P., Parvin, L., and Vertes, A. (2006). How much charge is there on a pulsating Taylor cone?. *Applied Physics Letters*, *89*(6), 064104.

[26] Gupta, P., Asmatulu, R., Claus, R., and Wilkes, G. (2006). Superparamagnetic flexible substrates based on submicron electrospun Estane® fibers containing MnZnFe-Ni nanoparticles. *Journal of Applied Polymer Science*, *100*(6), 4935-4942.

[27] Zufan, R., and Megaridis, C. (2005). Electrospinning of Nanofibers. *Report–Laboratory for Droplet and Particle Technology*.

[28] Filatov, Y., Budyka, A., and Kirichenko, V. (2007). *Electrospinning of micro-and nanofibers: Fundamentals in separation and filtration processes*. Begell House Inc., Redding, CT.

[29] Sill, T. J., and von Recum, H. A. (2008). Electrospinning: Applications in drug delivery and tissue engineering. *Biomaterials*, *29*(13), 1989-2006.

[30] Pinto, N. J., Johnson Jr, A. T., MacDiarmid, A. G., Mueller, C. H., Theofylaktos, N., Robinson, D. C., and Miranda, F. A. (2003). Electrospun polyaniline/polyethylene oxide nanofiber field-effect transistor. *Applied Physics Letters*, *83*(20), 4244-4246.

[31] Srinivasan, G., and Reneker, D. H. (1995). Structure and morphology of small diameter electrospun aramid fibers. *Polymer International*, *36*(2), 195-201.

[32] Asmatulu, R., Khan, W., and Yildirim, M. B. (2009). Acoustical properties of electrospun nanofibers for aircraft interior noise reduction. In *ASME 2009 International Mechanical Engineering Congress and Exposition*, Lake Buena Vista, Florida, p.223-227.

[33] Khan, W. S., Asmatulu, R., Ahmed, I., and Ravigururajan, T. S. (2013). Thermal conductivities of electrospun PAN and PVP nanocomposite fibers incorporated with MWCNTs and NiZn ferrite nanoparticles. *International Journal of Thermal Sciences*, *71*, 74-79.

[34] Asmatulu, R., Davluri, S., and Khan, W. (2009). Fabrications of CNT based nanocomposite fibers from the recycled plastics. In *ASME 2009 International Mechanical Engineering Congress and Exposition*, Lake Buena Vista, Florida, p.859-864.

[35] Ceylan, M., Asmatulu, R., Khan, W. and Nuraje, N. (2009). Superhydrophobic behavior of electrospun micro and nanofibers. In *SAMPE Fall Technical Conference, Wichita* p.1-8.

[36] Asmatulu, R., Dandin, V., and Khan, W. (2009). Properties of recycled PVC and PS nanocomposite fibers at various NiZn ferrite loadings. In *SAMPE Fall Technical Conference, Wichita* p. 1-10.

[37] Khan, W., Asmatulu, R., El-Tabey, M. M., Ho, J., and Hamdeh, H. (2009). Electrical properties of nanocomposite fibers under various loads and temperatures. In *ASME 2009 International Mechanical Engineering Congress and Exposition*, Lake Buena Vista, Florida, p. 865-872.

[38] Dersch, R., Steinhart, M., Boudriot, U., Greiner, A., and Wendorff, J. H. (2005). Nanoprocessing of polymers: Applications in medicine, sensors, catalysis, photonics. *Polymers for Advanced Technologies*, *16*(2-3), 276-282.

[39] Hohman, M. M., Shin, M., Rutledge, G., and Brenner, M. P. (2001). Electrospinning and electrically forced jets. I. Stability theory. *Physics of Fluids*, 13(8), 2201-2220.

[40] Belenkaya, B., Polevov, V., and Sakharova, V. (2010). *U.S. Patent No. 7,858,837*. Washington, DC: U.S. Patent and Trademark Office.

[41] Kumbar, S. G., Nukavarapu, S. P., James, R., Hogan, M. V., and Laurencin, C. T. (2008). Recent patents on electrospun biomedical nanostructures: An overview. *Recent Patents on Biomedical Engineering*, *1*(1), 68-78.

[42] Ignatious, F., Sun, L., Craig, A., Crowe, D., Ho, T., and Millan, M. (2005). *U.S. Patent Application 11/064,890*.

[43] Shalaby, S. W. (2008). *U.S. Patent No. 7,416,559*. Washington, DC: U.S. Patent and Trademark Office.

[44] Mo, X., Chen, F., He, C., Wang, H. (2008). *Patent Application CN101156968*.

[45] Ramachandran K, Gouma P-I. “Electrospinning for bone tissue engineering. ” Recent Patent on Nanotechnology 2008; 2(1): 1-7.

[46] Mo, X., Chen, F., He, C. (2007). *Patent Application CN1919352*.

[47] Mo, X., Zhang, L., Xue, Y., He, C. (2008). *Patent Application CN101181648*.

[48] Gravett, D. M., Takacs-cox, A., Toleikis, P. M., Maiti, A., and Embree, L. (2004).*U.S. Patent No. 20,040,219,214*. Washington, DC: U.S. Patent and Trademark Office.

[49] Lanbeck, P., and Paulsen, O. (2001). Short-Term Effects of Four Antibiotics on DNA Synthesis in Endothelial Cells. *Pharmacology and Toxicology*, *88*(4), 204-208.

2.7 Appendix

A tensile test of PCL nanofibers was conducted using the various apparatuses shown in Figures 2.5 and 2.6. Figure 2.7 shows the stress strain curve plotted using the PASCO apparatus.

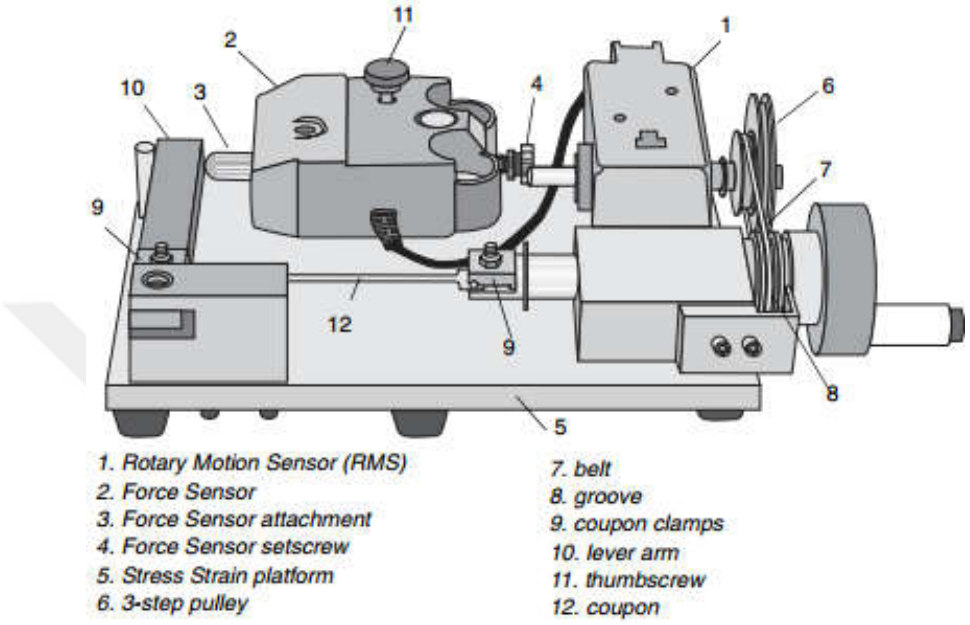


Figure 2.5: Schematic drawing of apparatus from PASCO used for tensile test.

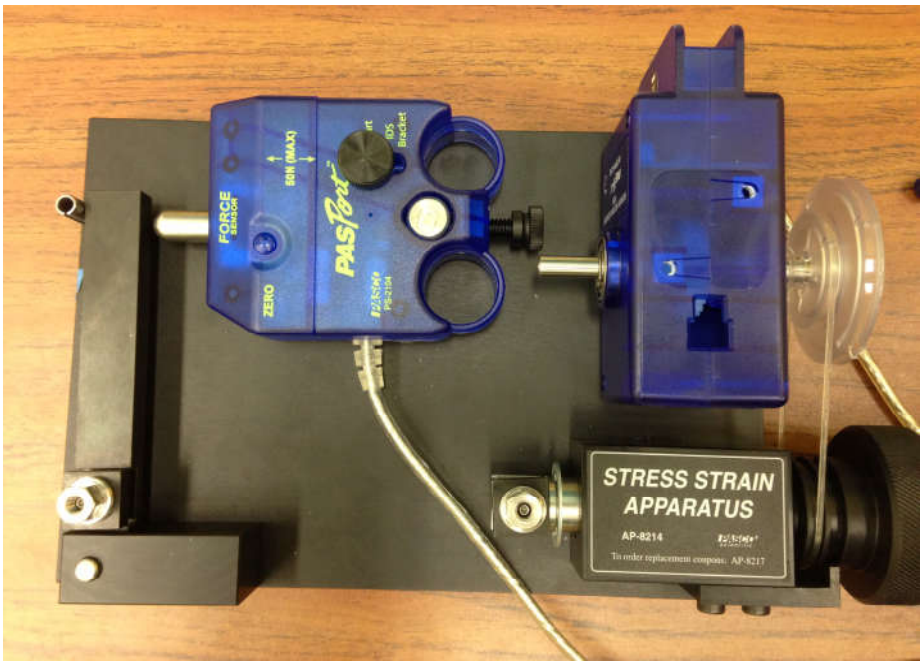


Figure 2.6: Stress strain apparatus model (AP-8214).

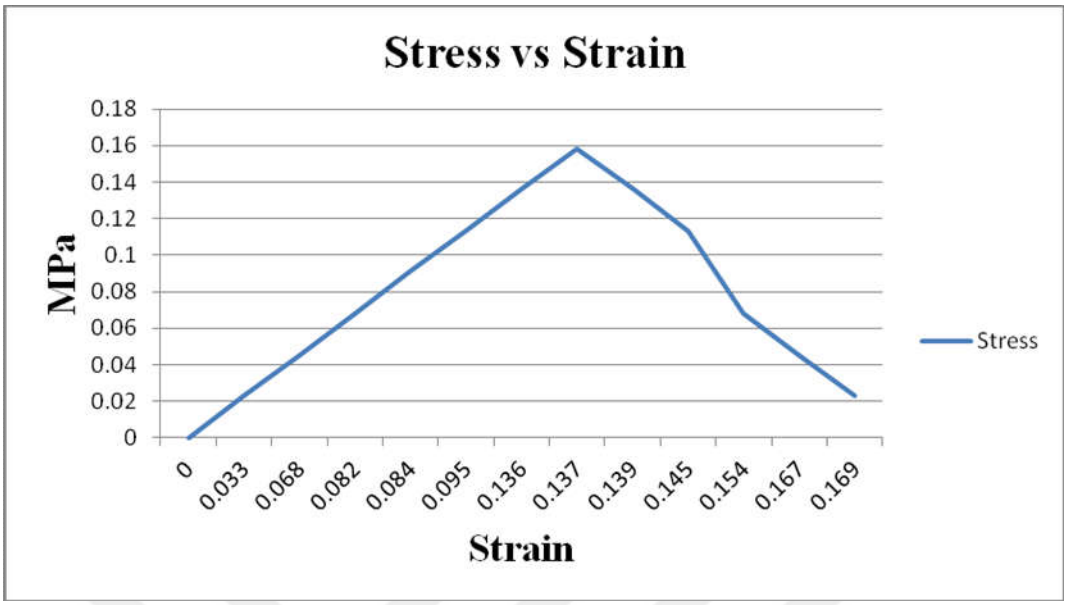


Figure 2.7: Stress strain curve plotted using PASCO apparatus.

Figures 2.8 to 2.16 show SEM images of PCL nanofibers composed with plasmid DNA.

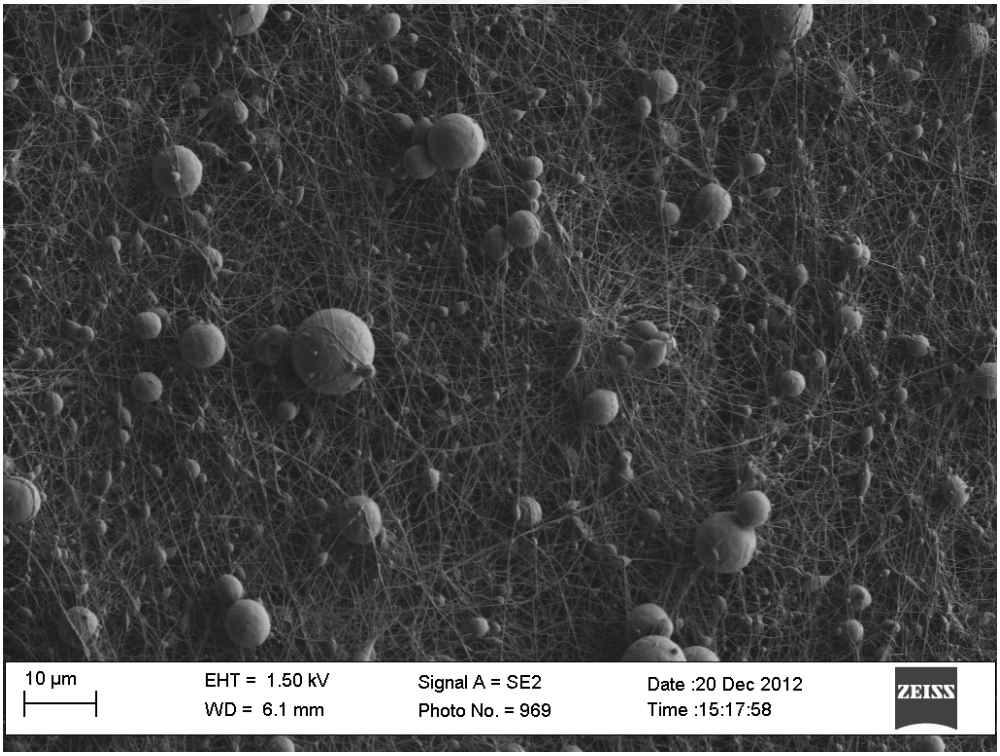


Figure 2.8: PCL nanofiber composed with plasmid DNA.

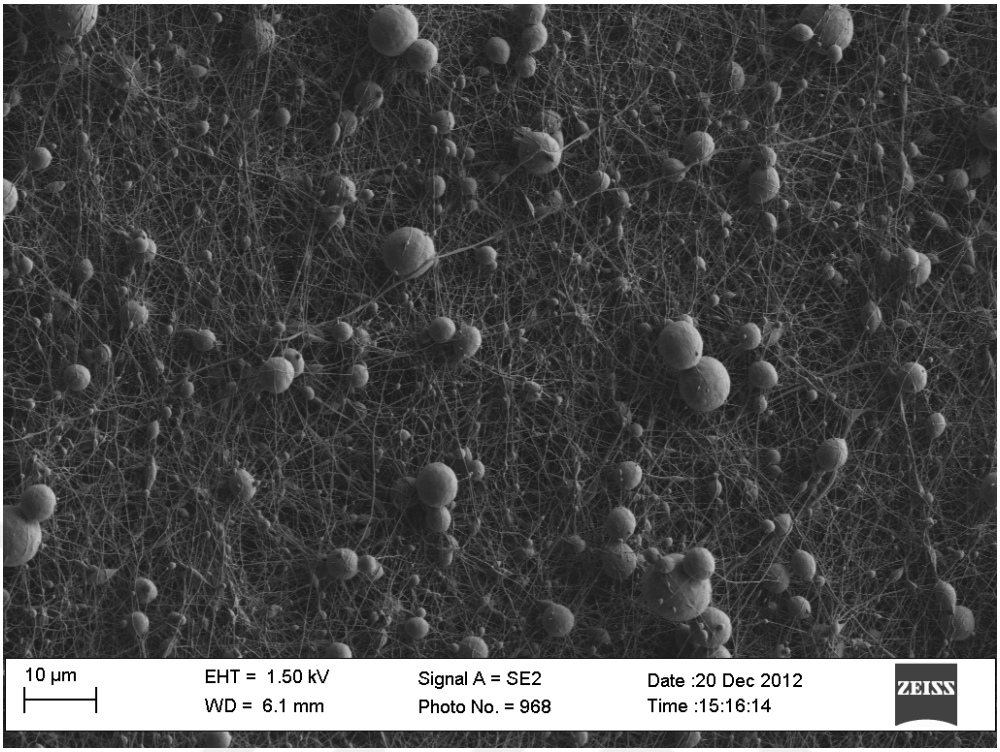


Figure 2.9: PCL nanofiber composed with plasmid DNA.

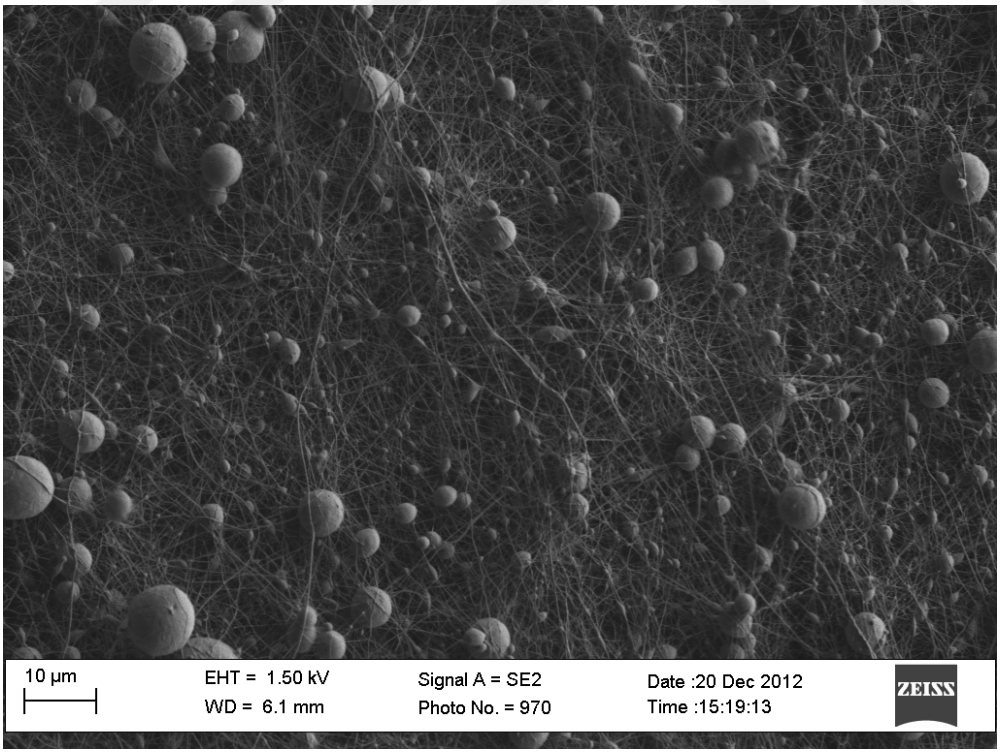


Figure 2.10: PCL nanofiber composed with plasmid DNA.

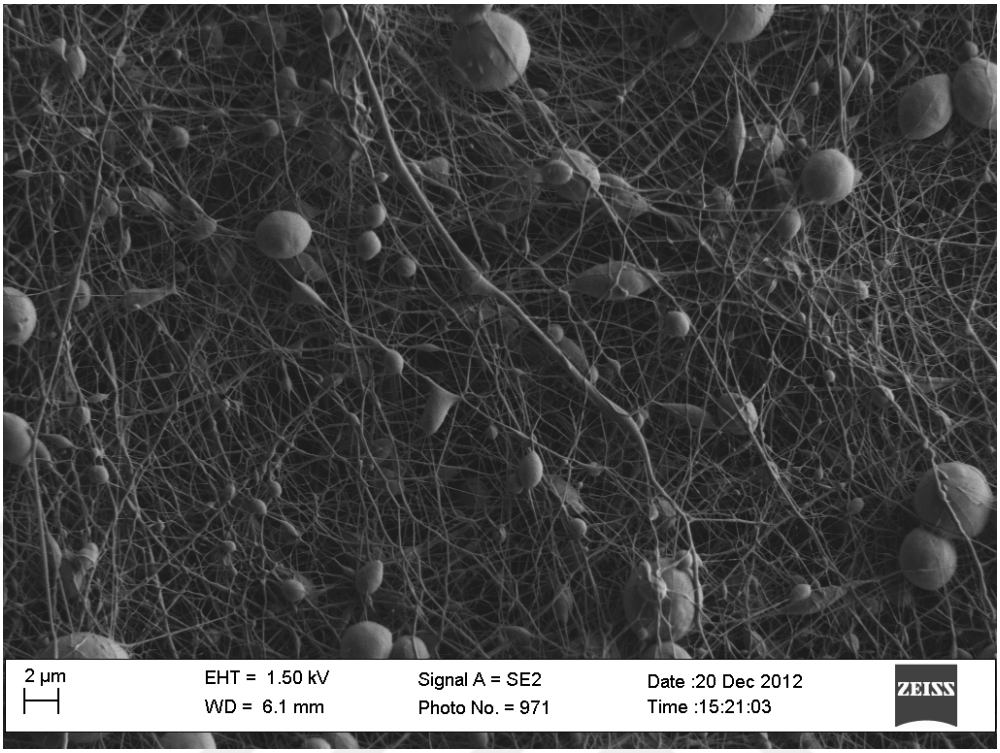


Figure 2.11: PCL nanofiber composed with plasmid DNA.

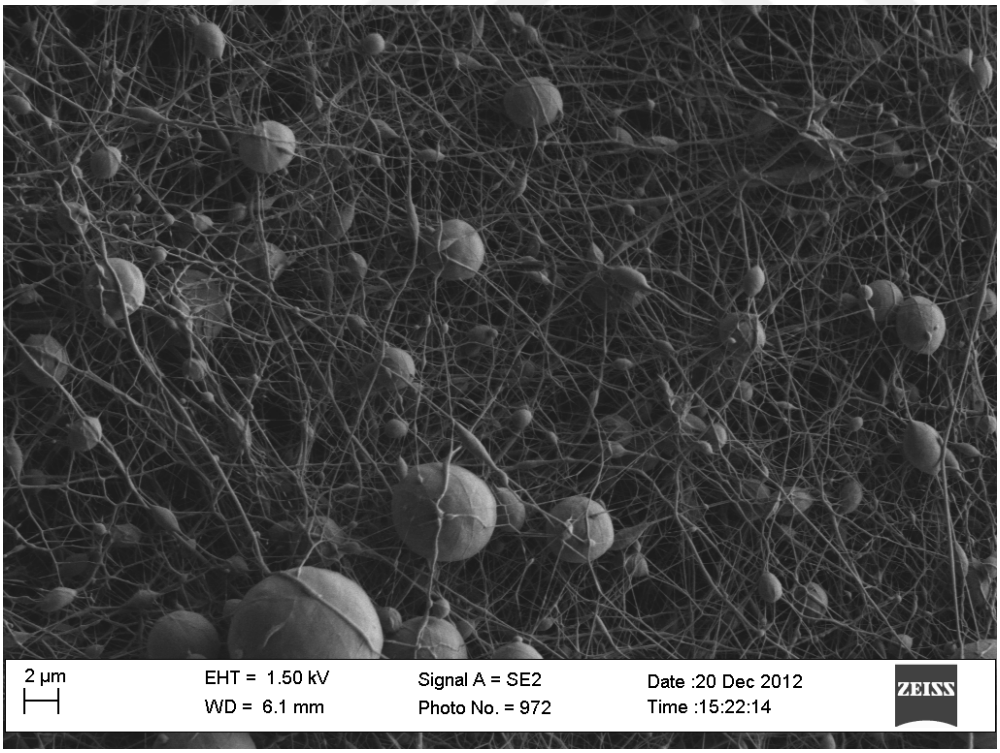


Figure 2.12: PCL nanofiber composed with plasmid DNA.

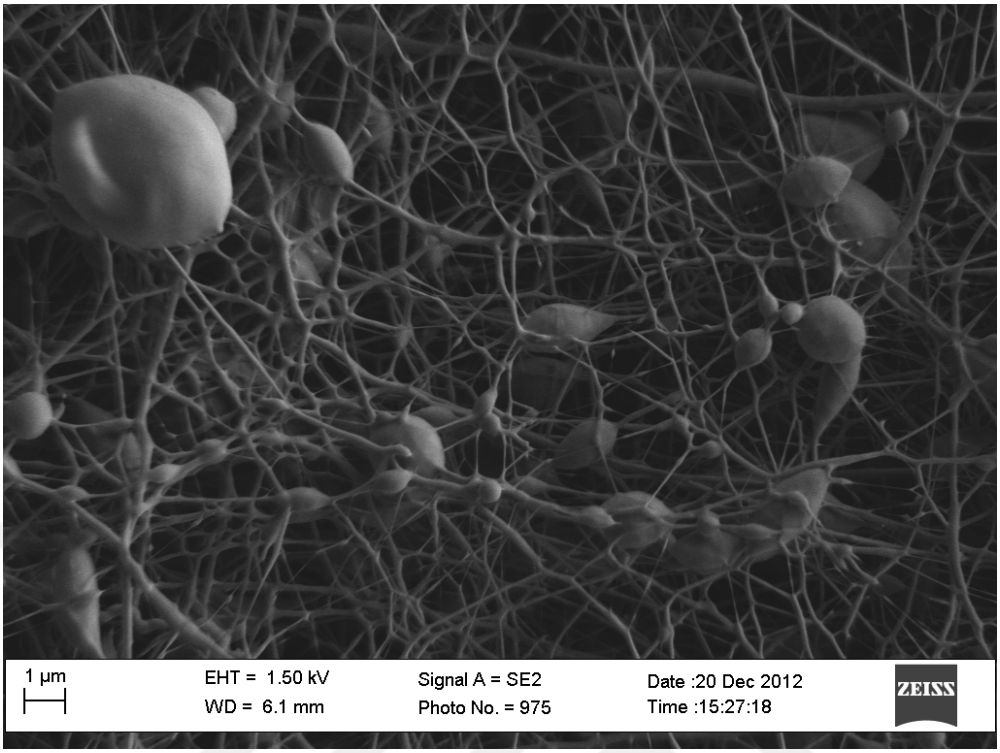


Figure 2.13: PCL nanofiber composed with plasmid DNA.

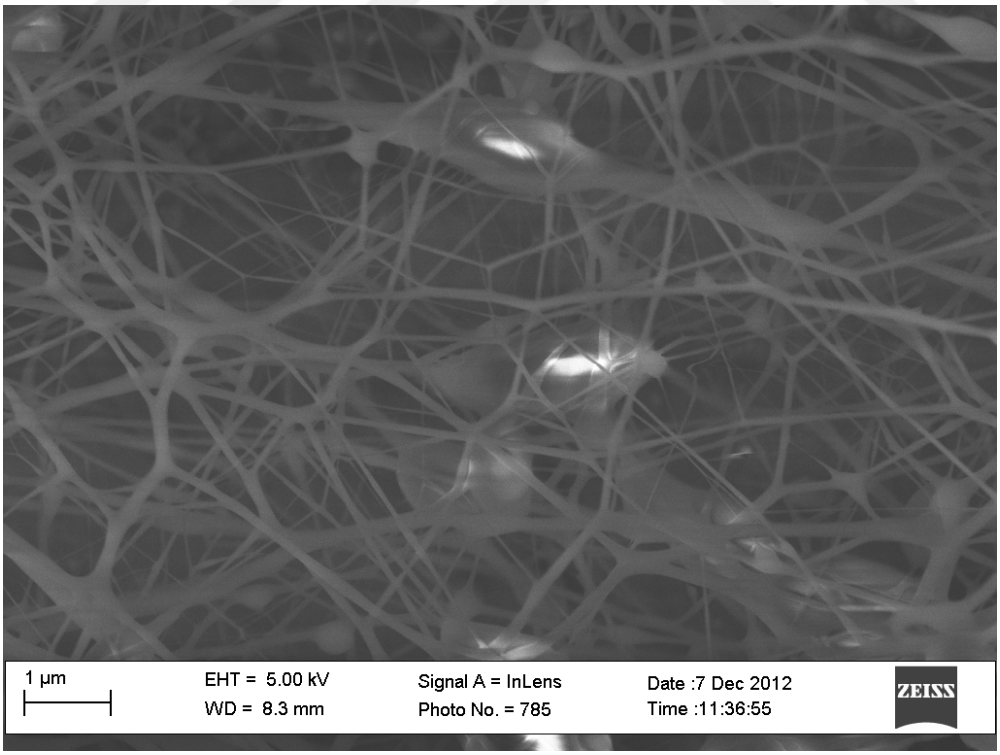


Figure 2.14: PCL nanofiber composed with plasmid DNA.

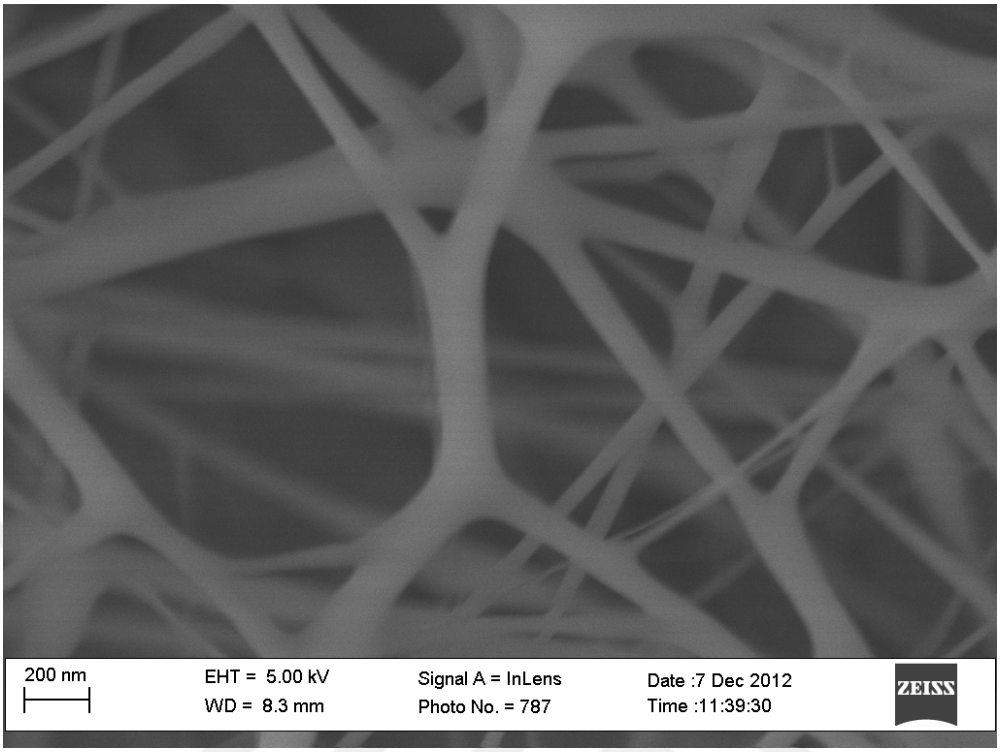


Figure 2.15: PCL nanofiber composed with plasmid DNA.

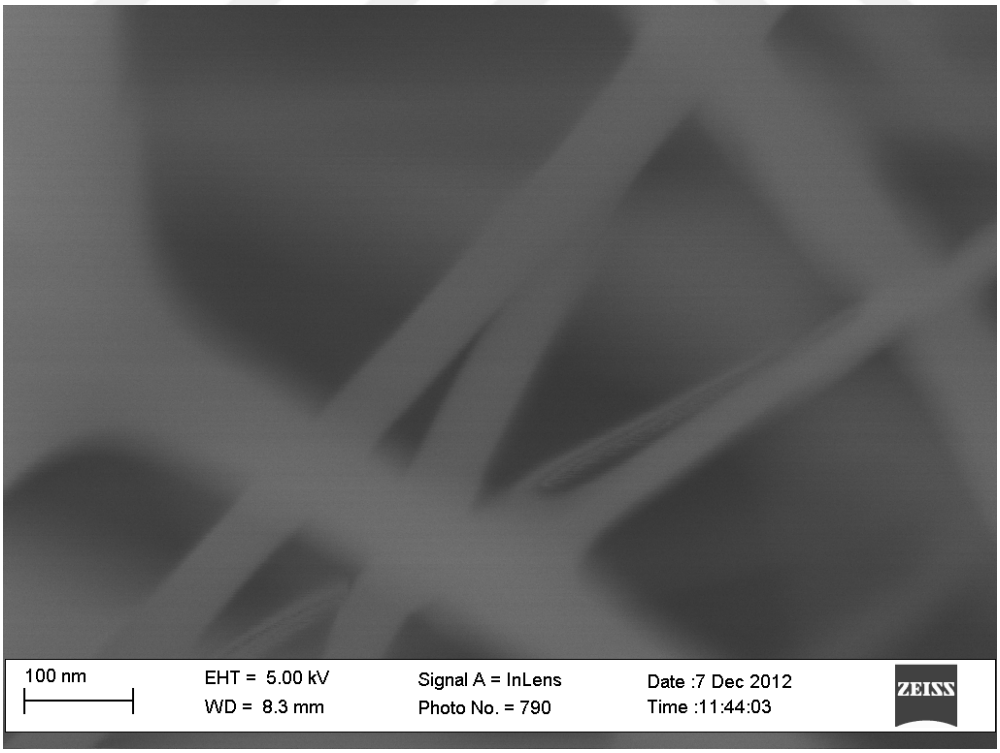


Figure 2.16: PCL nanofiber composed with plasmid DNA.

CHAPTER 3

EFFECTS OF GENTAMICIN-LOADED PCL NANOFIBERS ON GROWTH OF GRAM-POSITIVE AND GRAM-NEGATIVE BACTERIA

3.1 Abstract

Poly-ε-caprolactones (PCLs) incorporated with gentamicin of different concentrations (0, 2.5, 5, and 10 wt%) were electrospun under various conditions, and the resultant nanofibers of different thicknesses (1, 2, and 4 layers) were used against the growth of gram-negative and gram-positive bacteria, such as *E. coli*, *Salmonella*, and *Staphylococcus Epidermidis*. PCL polymer was selected mainly because it is biodegradable aliphatic polyester and plays a critical role in tissue engineering and pharmaceuticals. In future studies, DNA and other therapeutic agents will be loaded onto the same PCL fibers and their efficacies tested as a model treatment for skin cancer. Scanning electron microscopy (SEM) images showed that the resultant fibers were in the range of 50 to 200 nm with an average diameter of 100 nm. Bacterial test results revealed that the gentamicin molecules in the nanofibers were gradually released from the PCL nanofibers during the in vitro tests and prevented bacterial growth at different inhibition zones and kinetics. Overall, this work provides a detailed explanation of how to improve the antibacterial properties of new drug delivery systems for many biomedical fields, such as scaffolding; drug, DNA, and protein delivery; and wound healing.

Keywords: Gentamicin, PCL, Electrospinning, Nanofibers, Antibacterial

3.2 Introduction

Electrospinning has been gaining much attention worldwide because of the size, shape, flexibility, integrity, and cost of the resultant products in various scientific and technological applications, compared to other techniques and their products. Electrospinning allows scientists to produce fibers in the range of micro to nano size and in the forms of beaded and non-beaded. Using different type of polymers helps researchers/scientists to fabricate hydrophobic or hydrophilic fibers of various kinds, which may be useful for many industrial applications [1–3].

Essentially, nanofibers are fabricated by an electrostatically driven jet of a polymer solution. The polymer jet undergoes bending instability due to the interaction of charged particles with the electrostatic field before it is collected on a grounded collector, placed some distance from the capillary tube. The solvent is evaporated during this process. Depending on the type of collector, either solidified fiber in an alignment or non-woven fiber forms are obtain from this process [4–5]. Electrospinning technology opens up unique opportunities for the generation of fiber-based biocide materials, including antimicrobial biopolymers. Electrospun nanofibers have been used for many applications, for instance, tissue engineering, wound dressing, drug delivery [5], sensors [6], and filters [7–8].

Polycaprolactone is an FDA-approved synthetic polymer for use in drug-delivery devices and demonstrated biocompatibility [9]. It is commonly used for medical purposes because PCL has both biocompatibility and slow biodegradability [10]. By combining PCL's fundamental hydrophobic property with the great characteristics of a nanofiber structure, a promising material can be obtained for biomedical use [11]. Nanofiber structures show a nanoscale diameter, high surface-to-volume ratio, small pore size, high porosity, and unique physical properties, which make them appropriate for an extensive range of medical applications [12–13]. Numerous

studies have been done on the electrospinning of PCL. However, it is difficult to generate bead-free fibers via electrospinning [14]. PCL has a hydrophobic property, which slows down drug delivery. At the same time, beaded formation helps to slow down drug delivery [15]. Hydrophobic materials will release drugs over a longer period of time.

This study investigated PCL-based electrospun fibers and developed antibiotic-loaded nanofiber structures displaying modified release characteristics in functional dressings for wound-healing applications. To design the PCL-based nanofiber system, gentamicin was chosen as the incorporated drug because of its well-known antibiotic function of inhibiting or killing bacteria that are common in most typical post-surgical infections. Gentamicin has been used to treat osteomyelitis caused by methicillin-resistant *Staphylococcus aureus* (MRSA) [16–17]. Antibacterial effectiveness against *E. coli*, *Salmonella*, and *S. epidermidis* have also been tested to establish the appropriateness of these applied electrospun fibers for decreasing frequency and severity of post-surgery infections.

3.3 Experimental Procedure

3.3.1 Materials

PCL pellets with a molecular weight of 70,000 were purchased from Scientific Polymer Products, Inc., acetonitrile was purchased from Acros, and gentamicin sulfate powder was provided by National Fish Pharmaceuticals. These materials were used in the present study without any further purifications or modifications. Three different bacteria (*E. coli*, *Salmonella* and *S. Epidermidis*) were reproduced in the Department of Biological Sciences at Wichita State University and used in the present study.

3.3.2 Methods

3.3.2.1 Fabrication of Electrospun Nanofibers

Electrospinning was used to fabricate PCL nanofibers [2–3]. First, PCL (15 wt%) was dissolved in acetonitrile and then different concentrations of gentamicin (2.5, 5, and 10 wt%) were added to the PCL solution. The solutions were mechanically stirred at 700 rpm and 55ºC for 24 hrs. Each prepared polymeric solution was transferred to a 10 ml plastic syringe and electrospun at various conditions to produce nanofibers. Figure 3.1 shows the schematics of an electrospinning process. Scanning electron microscopy (SEM) (ZEISS SIGMA VP) was used to characterize the morphology of the PCL electrospun fibers.

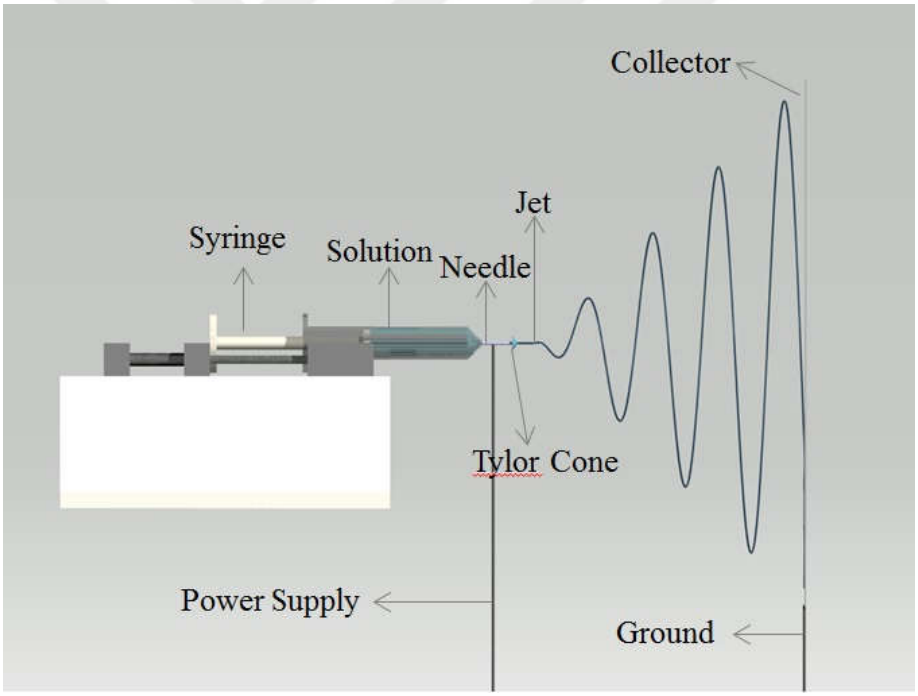


Figure 3.1: Schematic view of electrospinning process.

3.3.2.2 Antibacterial Tests

The bacteria inhibition assay was conducted based on evaluating clear zones of inhibition of *E. coli*, *Salmonella,* and *S. epidermidis* growth around PCL nanofibers loaded with

gentamicin. These tests were adapted from the Kirby-Bauer disk-diffusion method. Agar and lysogeny broth (LB) were mixed with distilled water in an Erlenmeyer flask and autoclaved. After autoclaving, the solution was placed into petri dishes, 8.5 cm in diameter, to allow the agar to harden. *E. coli, Salmonella*, and *S. epidermidis* were cultured, and 200 μL of the bacteria was diluted with 4,000 μL of the LB solution. An amount of 200 μL of the diluted bacterial solution was spread evenly in each prepared petri dish. Nanofibers were cut to approximately 0.8 cm in diameter and placed in each petri dish forming a three-by-three ply pattern of fibers. The first row had one layer of nanofibers, the second row had two layers of nanofibers, and the third row had four layers of nanofibers. Petri dishes were incubated for 37°C to encourage bacteria growth. Photographs were taken for up to seven days. The antibacterial activity of the gentamicin-loaded PCL nanofibers was assessed by measuring the mean diameter of the zone of inhibition to the nearest millimeter. All tests were repeated three times.

3.4 Results and Discussion

Gentamicin-loaded PCL nanofibers were successfully fabricated. Figure 3.2 shows the average diameter of the PCL-gentamicin nanofibers. From the SEM images and also from Figure 3.2, it can be seen that the diameter of the fibers was around 108 nm ± 43.10 nm. There are four different—PCL only, 2.5 wt% gentamicin, 5 wt% gentamicin, and 10 wt% gentamicin loaded. Three images used for each nanofiber set provided 15 measurements from each SEM images to generate Figure 3.2. The 5 wt% gentamicin-loaded PCL fibers exhibited the narrowest distribution and smallest mean fiber diameter. However, there was no significant diameter change by adding gentamicin into the PCL (Figure 3.2).

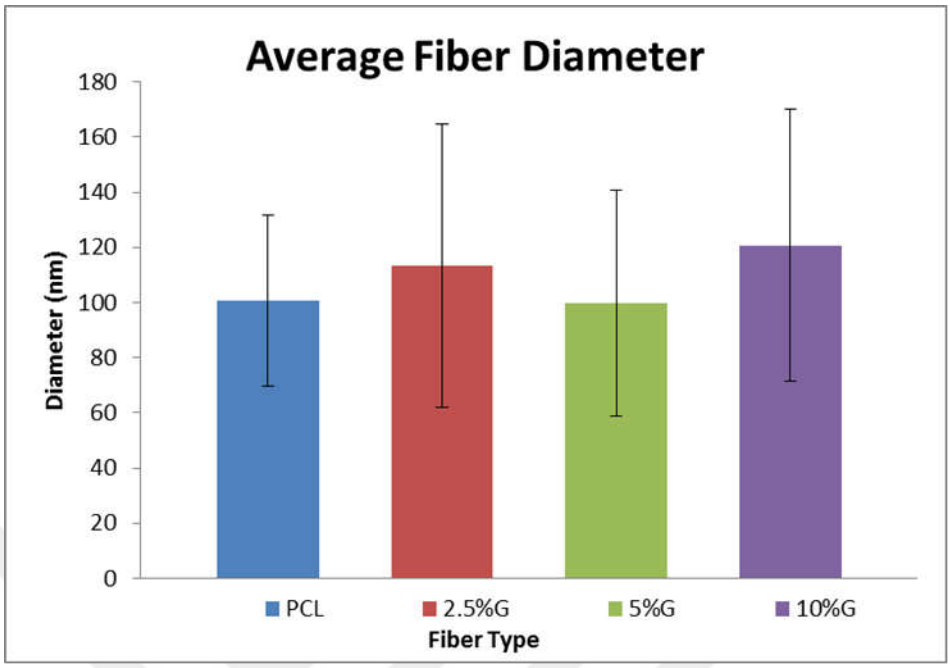


Figure 3.2: Average fiber diameter of PCL fibers with different concentrations of gentamicin.

Results show that *Salmonella* is more susceptible to gentamicin than *E. coli* and *S. epidermidis*. This result is comparable to that demonstrated by Ruckh et al. [18], although they prepared encapsulated rifampicin-PCL nanofiber scaffolds using the electrospinning method. They observed that the release of rifampicin from the PCL nanofiber scaffold towards to *Pseudomonas aeruginosa* and *S. epidermidis.* Furthermore, a study by Liu et al. [19] involved PCL nanofiber yarns containing ampicillin sodium salt. They notice that ampicillin sodium salt affects more *S. aureus* than *Klebsiella pneumoniae.* Moreover, Francis et al. [20] prepared poly(3-hydroxybutyrate) gentamicin-encapsulated microspheres to investigate the release of gentamicin and saw that it was bimodal—an initial burst release followed by a diffusion-mediated sustained release. Sirc et al. [21] fabricated polyvinyl alcohol and polyurethane nanofibers with the addition of gentamicin by using needleless technology. They used *S. aureus* and *P. aeruginosa* and observed the gentamicin release and also the zone of inhibition area. Shawki et al. [22] produced dextran nanofibers with the addition of moxifloxacin by using

electrospinning. Using *E. coli* and *S. aureus*, they observes a zone of inhibition for both cases. Hasirci et al. [23] prepared PCL as the main matrix material, and gentamicin-loaded microspheres composed of β-tricalcium phosphate (β-TCP) and gelatin. Their aim was to use this material as a support for bone tissue. They also examined the material with *E. coli* and *S. aureus*. Their microsphere material exhibited a zone of inhibition for both bacteria. The results in this dissertation study showed that the PCL nanofibers without antibiotic did not show any antibacterial activity. As a result, any antibacterial activity of PCL nanofibers can only be applicable to the gentamicin incorporated within the fibers. These results confirm that PCL-gentamicin nanofibers are potential candidates for biomedical application. These findings further encourage future work in both classical and nontraditional electrospinning fibers, as well as their morphology, mechanical properties, and porosity.

Figure 3.3 shows SEM images of PCL fibers with different wt% of gentamicin. As can be seen, the morphology of fibers consists of pores and beaded structure. Appendix B shows additional SEM images, as well as Fourier transform infrared (FTIR) spectroscopy, thermogravimetric analysis (TGA), and differential scanning calorimetry (DSC) results. These PCL nanofibers were investigated with FTIR spectroscopy. Figures 3.4 and 3.5 show the spectra of gentamicin, PCL, and PCL nanofibers with the addition of 2.5, 5, and 10 wt% gentamicin. The PCL and 2.5, 5, and 10 wt% gentamicin additions indicate a strong sharp peak around 1717 cm^{-1}, which is due to C = O vibrations [24]. C-H peaks are present around 2,942 cm^{-1} [25]. Gentamicin is absorbed around 1,616 cm^{-1}. The different additions of gentamicin to PCL nanofibers show similar peaks in the FTIR spectroscopy.

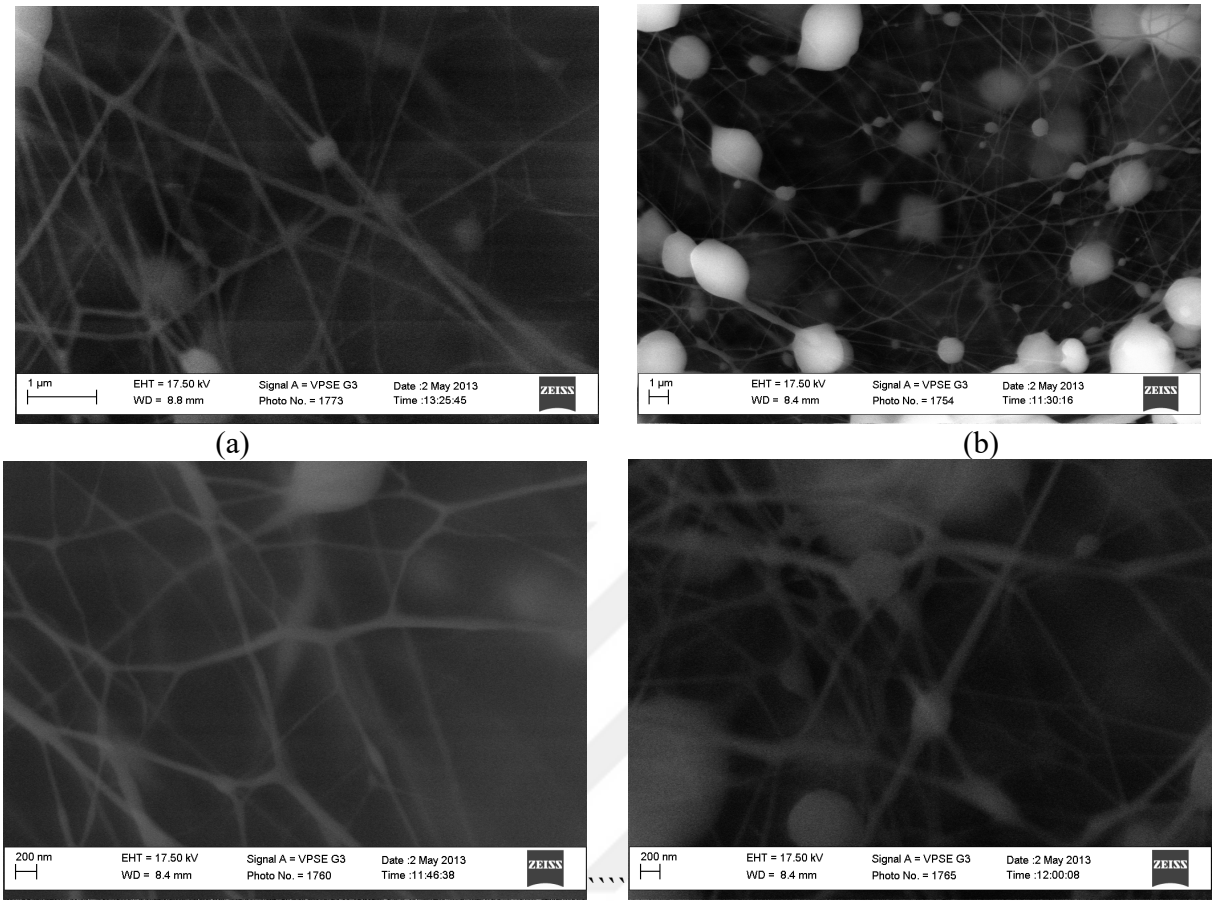


Figure 3.3: SEM images of PCL nanofibers with different concentrations of gentamicin: (a) 0 wt%, (b) 2.5 wt%, (c) 5 wt%, and (d) 10 wt%.

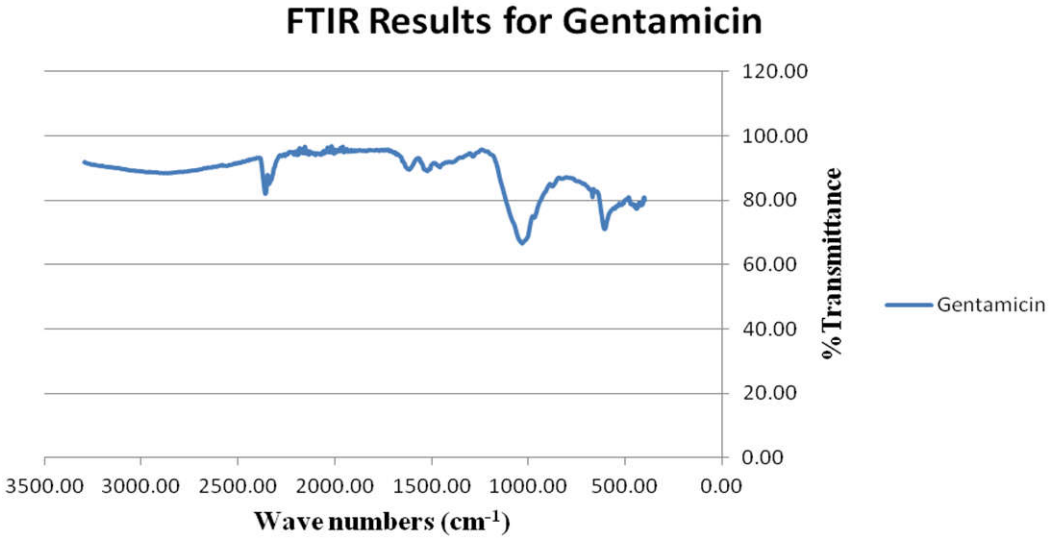


Figure 3.4: FTIR spectroscopy graph for gentamicin.

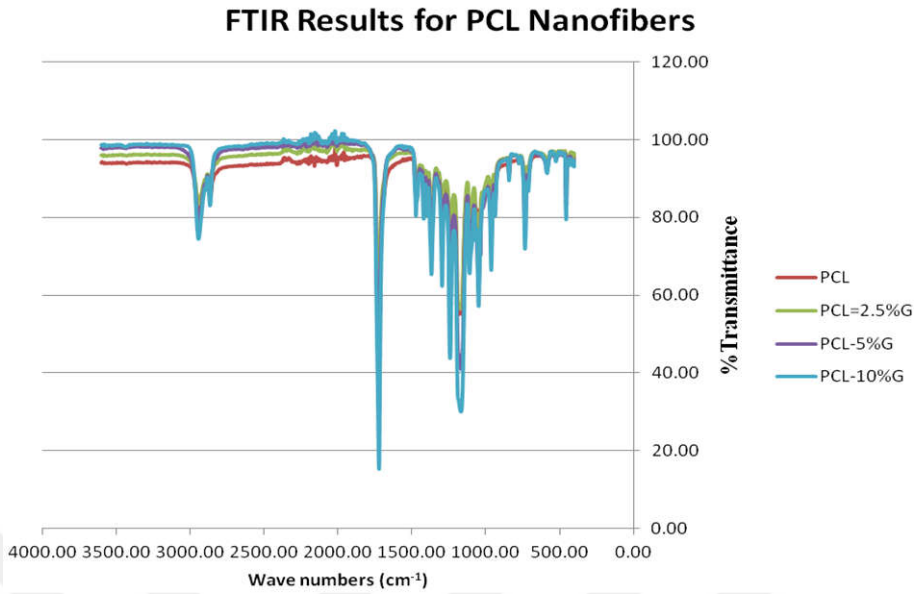


Figure 3.5: FTIR spectroscopy graph for PCL nanofibers with different wt% concentrations of gentamicin.

Figure 3.6 shows the results of TGA of an electrospun nanofiber with the inclusion of gentamicin. These results demonstrated a similar behavior, even though different weight percentages of gentamicin were addition to the PCL nanofibers—there was no major weight loss around 380ºC [24].

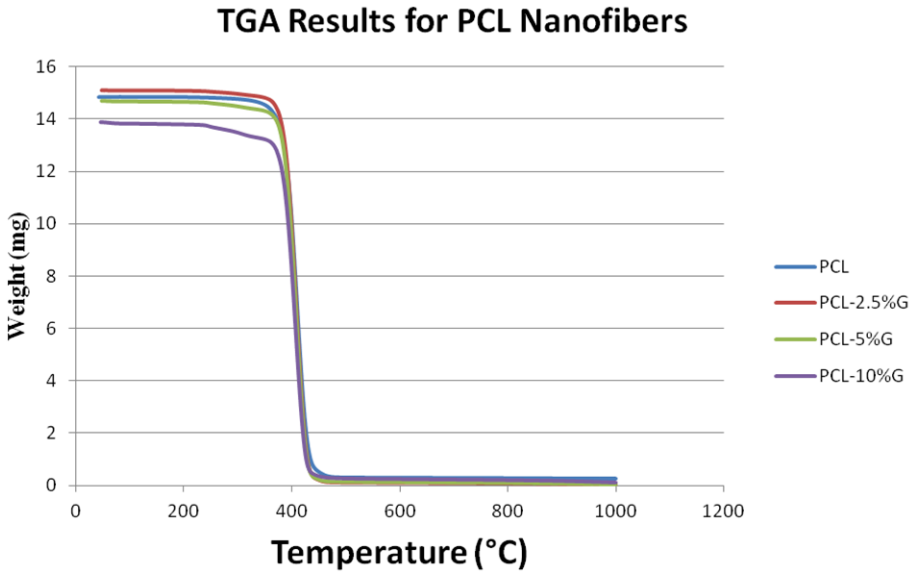


Figure 3.6: TGA graph for PCL nanofibers with different wt% concentrations of gentamicin.

Figure 3.7 shows DSC results of PCL electrospun nanofibers with different percentages of gentamicin. As can be seen, the peaks around 60°C correspond to the melting point of PCL.

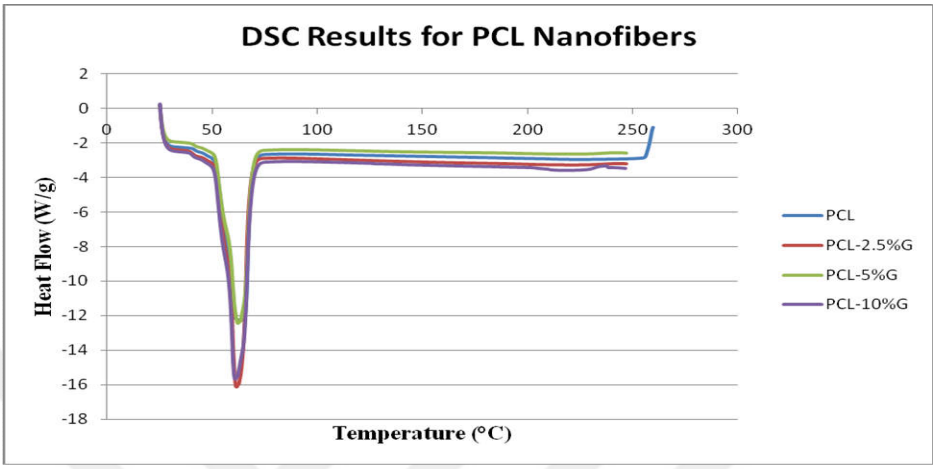


Figure 3.7: DSC graph for PCL nanofibers with different wt% concentrations of gentamicin

Antibacterial properties were evaluated by taking pictures of electrospun nanofibers [2–4] at 1, 3, 5, and 7 days after the initial culture of *E. coli*, *Salmonella*, and S. *epidermidis*. PCL electrospun nanofibers did not show any significant antibacterial function. These PCL nanofibers did not contain any gentamicin so bacteria grew all around the petri dish. Since PCL-only nanofibers did not show any zone of inhibition, it can be stated that gentamicin addition forms a zone of inhibition.

With the increase of gentamicin concentrations and increasing number of layers of fibers, it was found that antibacterial properties of the nanofibers were improved. Figure 3.8 show PCL fibers having 0 wt%, 2.5 wt% , 5 wt%, and 10 wt% gentamicin after seven days. As can be seen, 0% gentamicin does not show a zone of inhibition—bacteria can be seen all over the petri dish. However, 2.5, 5, and 10 wt% gentamicin clearly show zones of inhibition, and by increasing the number of layers of fibers, the inhibition zone was higher. When the gentamicin concentration was increased to 10 wt%, as shown in Figure 3.8(d), the zone of inhibition was increased. Images

were taken after the bacterial study started at 3 hr, 6 hr, 12 hr, day 1, day 2, day 3, day 4, day 5, day 6, and day 7.

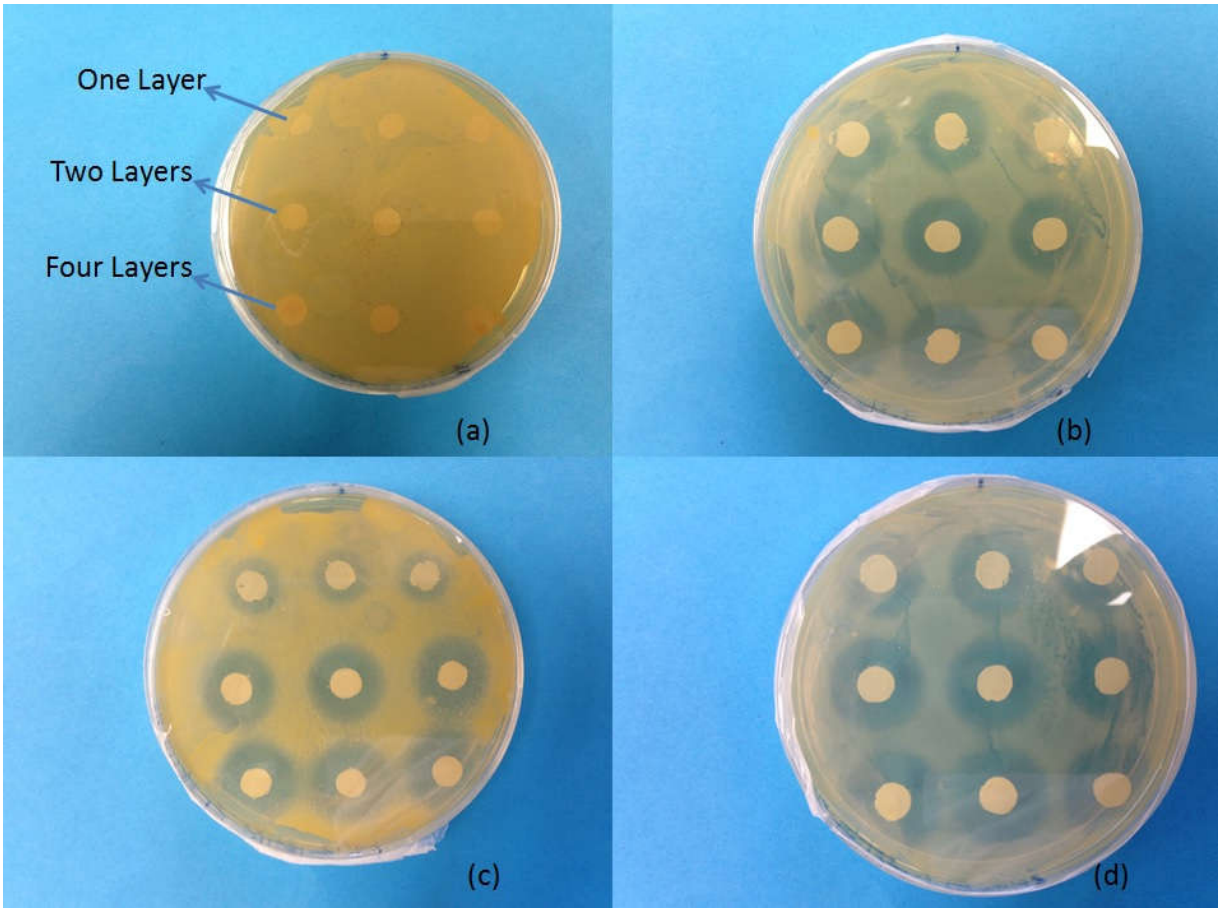


Figure 3.8: Antibacterial test results of PCL fibers with different concentrations of gentamicin: (a) 0 wt%, (b) 2.5 wt%, (c) 5 wt%, and (d) 10 wt%, after the seven days of in vitro tests. Top row samples have one layer, middle row samples have two layers, and bottom row samples have four layers of PCL fibers.

Figure 3.9 shows the *E. coli* bacterial inhibition area of nanofibers containing 2.5, 5, and 10 wt% gentamicin. Zones of inhibitions can be seen due to the fact that all samples contain gentamicin. The 10 wt% gentamicin sample shows a larger inhibition zone compared to the 2.5 wt% and 5 wt % gentamicin samples. The 2.5 wt% sample shows a larger inhibition zone than the 5 wt% sample, which could be attributed to non-uniformity in thickness of the fiber layer.

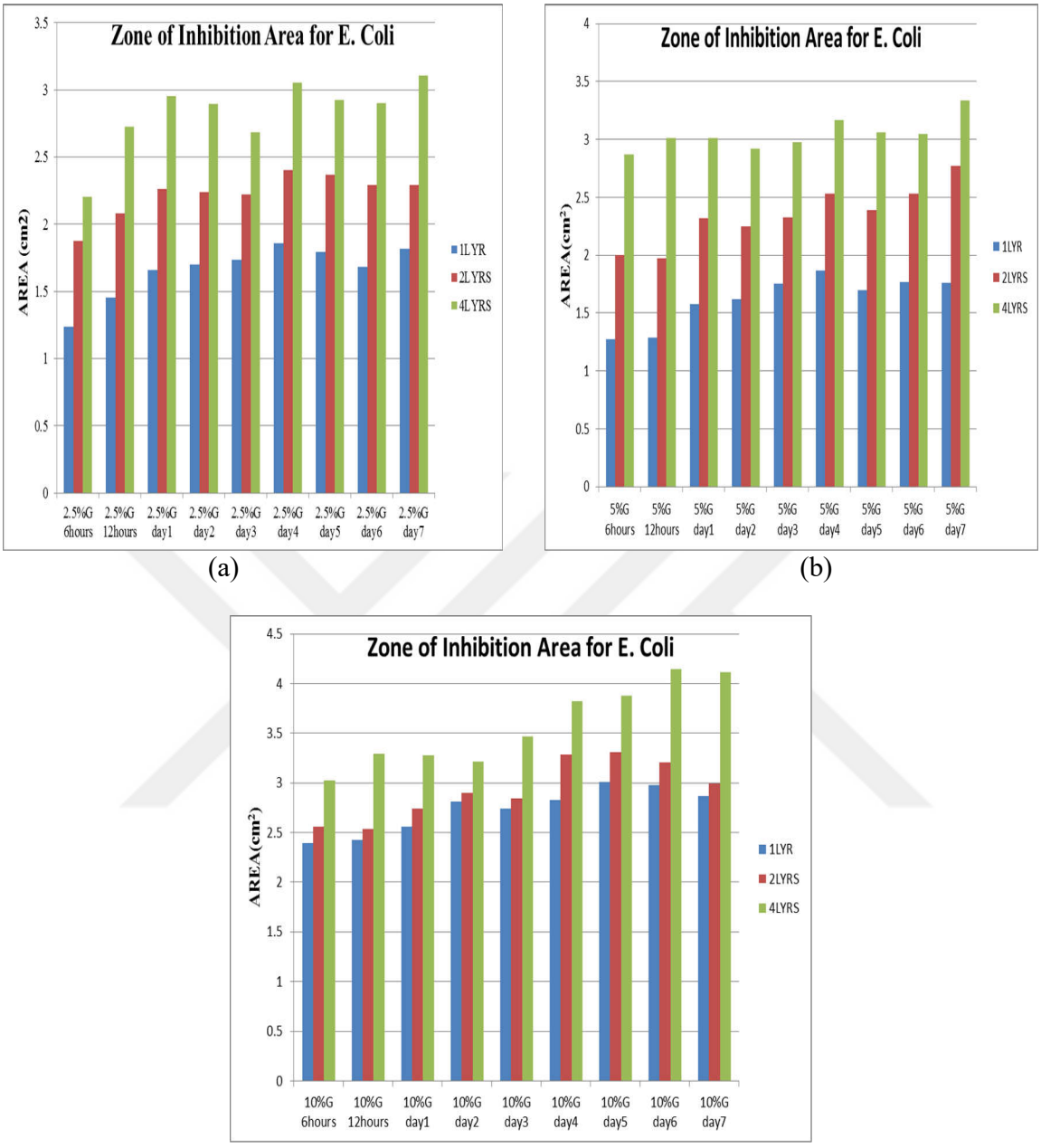


Figure 3.9: *E. coli* bacterial inhibition zones/areas of PCL nanofibers containing different concentrations of gentamicin: (a) 2.5 wt%, (b) 5 wt%, and (c) 10 wt%.

Figure 3.10 shows the *Salmonella* bacterial inhibition area of nanofibers containing 2.5, 5, and 10 wt% gentamicin contents. Zones of inhibitions can be seen due to the fact that all samples contain gentamicin. The area with 10 wt% gentamicin shows a larger inhibition zone compared to the areas with 2.5 wt% and 5 wt% gentamicin. It can be seen that the 2.5 wt%

sample show a larger inhibition zone than the 5 wt% sample, which could be attributed to the non-uniformity in thickness of the fiber layer.

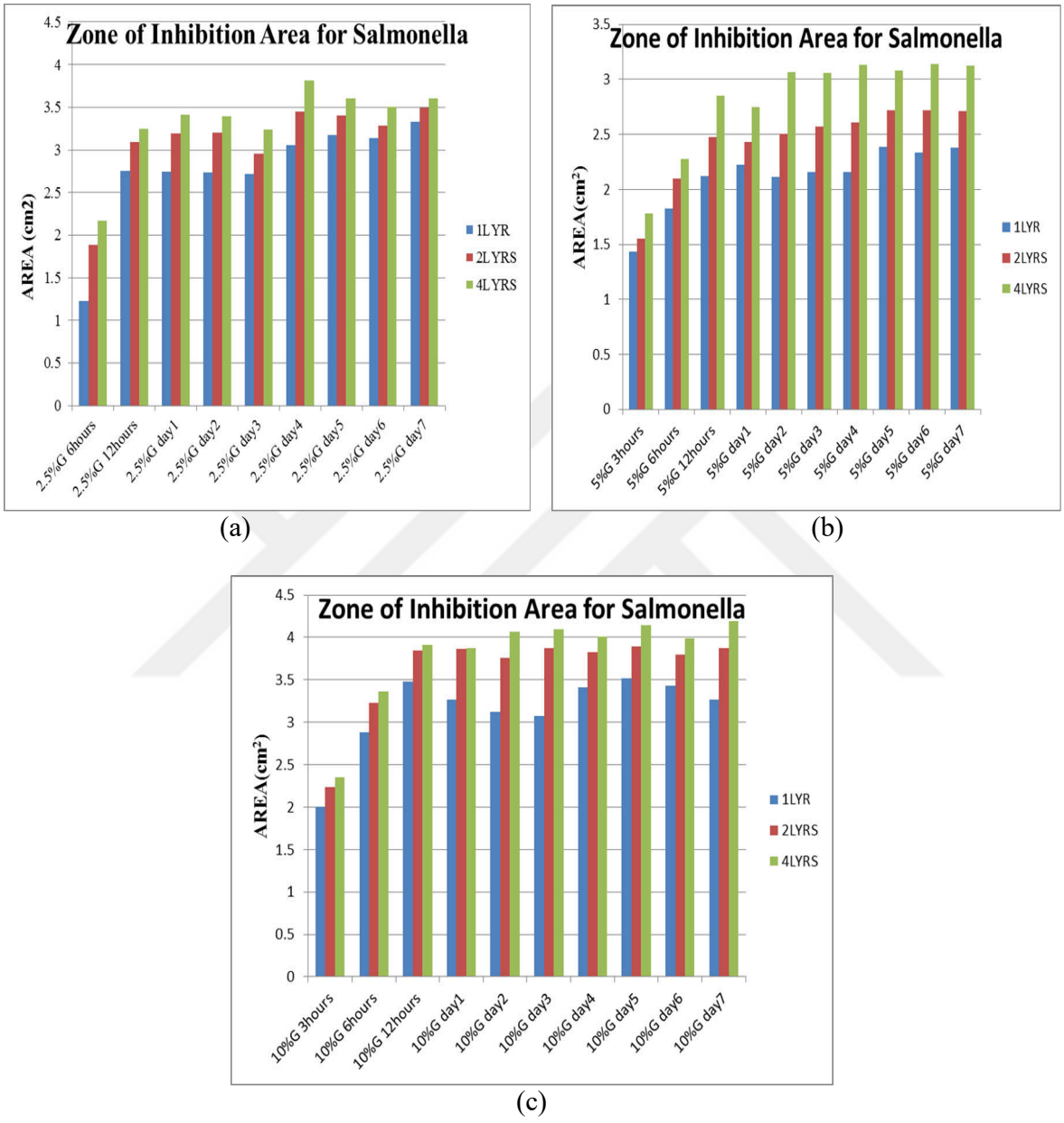


Figure 3.10: *Salmonella* bacterial inhibition zones/areas of PCL nanofibers containing different concentrations of gentamicin: (a) 2.5 wt%, (b) 5 wt%, and (c) 10 wt%.

Figure 3.11 shows the *S. Epidermidis* bacterial inhibition area of nanofibers containing 2.5, 5, and 10 wt% gentamicin contents. Zones of inhibitions can be seen due to the fact that all samples contain gentamicin. The 10 wt% gentamicin sample shows a larger inhibition zone

compared to the 2.5 wt% and 5 wt% gentamicin samples. It can be seen that the 2.5 wt% sample shows a larger inhibition zone than the 5 wt% sample, which could be attributed to the non-uniformity in thickness of the fiber layer.

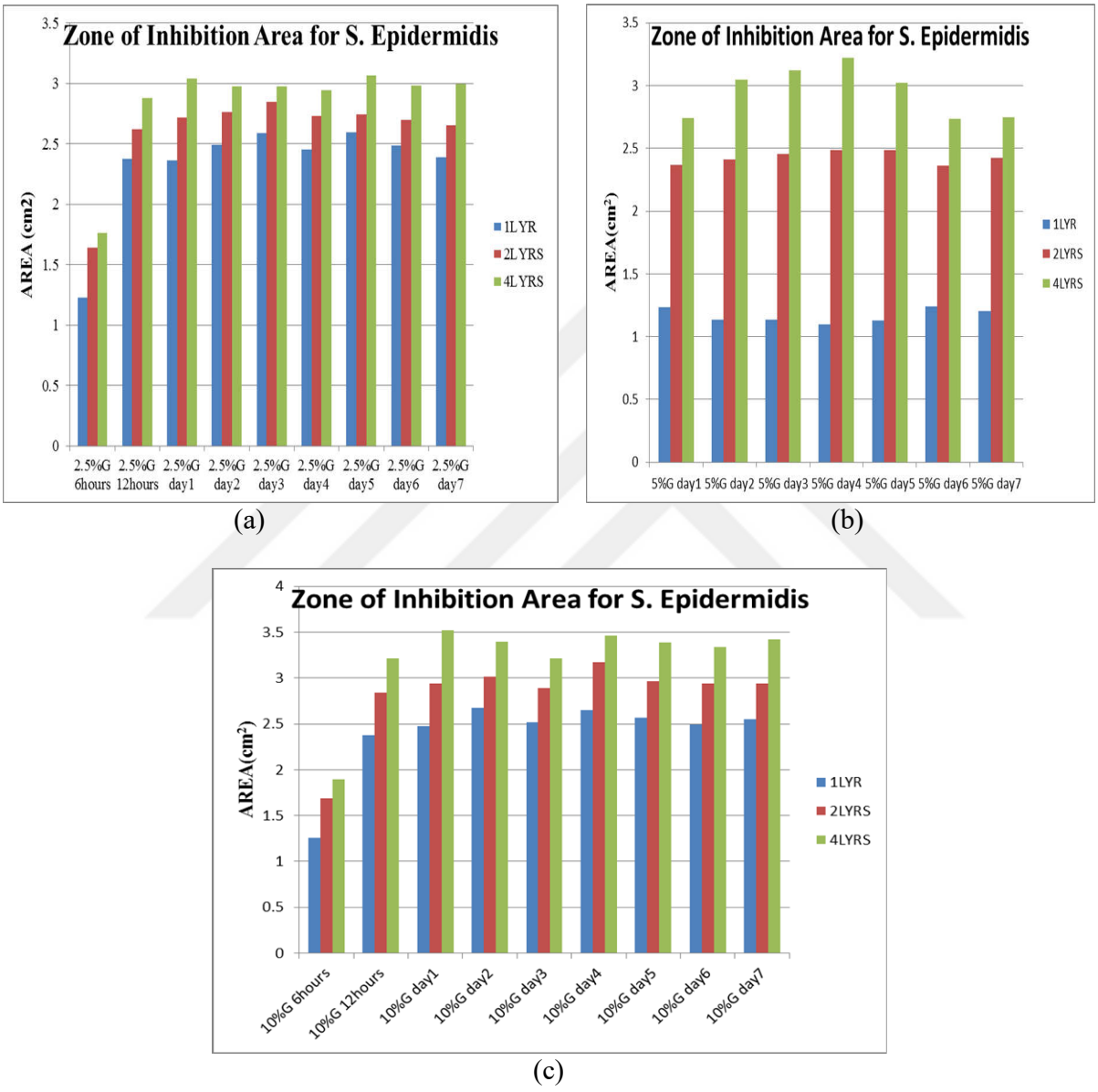


Figure 3.11: *S. Epidermidis* bacterial inhibition zones/areas of PCL nanofibers containing different concentrations of gentamicin: (a) 2.5 wt%, (b) 5 wt%, and (c) 10 wt%.

3.5 Conclusions

Gentamicin-loaded PCL nanofibers were successfully fabricated via the electrospinning process and characterized using SEM. The PCL nanofibers (below 100 nm) at different thicknesses (1, 2, and 4 layers) were used against the *E. coli*, *Salmonella* and *S. Epidermidis* bacteria. These bacterial studies indicated that the gentamicin molecules in the nanofibers were gradually released from the PCL nanofibers during the in vitro tests and prevented the bacterial growth for more than seven days. The increase in gentamicin concentration and layers of fibers showed better antibacterial properties. As a result, this study confirmed that antibacterial agent concentrations, thicknesses of nanofiber layers, and time were important factors, which may be useful for several biomedical applications, such as scaffolding; drug, DNA, and protein delivery; and wound healing.

Acknowledgments

The author greatly acknowledges the Flossie E. West Foundation and Wichita State University for the financial support of this work. The author also wishes to thank Ms. Zheng Song, Jimmy Nguyen ,Jianhoa Jiang, Jacqueline Weber, Seyed Soltani, and Dr. Suresh Raju for their excellent technical assistance.

3.6 References

[1] Nuraje, N., Asmatulu, R., Cohen, R. E., and Rubner, M. F. (2011). Durable antifog films from layer-by-layer molecularly blended hydrophilic polysaccharides. *Langmuir*, *27*(2), 782-791.

[2] Nuraje, N., Khan, W. S., Lei, Y., Ceylan, M., and Asmatulu, R. (2013). Superhydrophobic electrospun nanofibers. *Journal of Materials Chemistry A*,*1*(6), 1929-1946.

[3] Asmatulu, R., Ceylan, M., and Nuraje, N. (2011). Study of superhydrophobic electrospun nanocomposite fibers for energy systems. *Langmuir*, *27*(2), 504-507.

[4] Huang, Z. M., Zhang, Y. Z., Kotaki, M., and Ramakrishna, S. (2003). A review on polymer nanofibers by electrospinning and their applications in nanocomposites. *Composites Science and Technology*, *63*(15), 2223-2253.

[5] Sill, T. J., and von Recum, H. A. (2008). Electrospinning: Applications in drug delivery and tissue engineering. *Biomaterials*, *29*(13), 1989-2006.

[6] Dersch, R., Steinhart, M., Boudriot, U., Greiner, A., and Wendorff, J. H. (2005). Nanoprocessing of polymers: Applications in medicine, sensors, catalysis, photonics. *Polymers for Advanced Technologies*, *16*(2-3), 276-282.

[7] Gopal, R., Kaur, S., Ma, Z., Chan, C., Ramakrishna, S., and Matsuura, T. (2006). Electrospun nanofibrous filtration membrane. *Journal of Membrane Science*,*281*(1), 581-586.

[8] Gopal, R., Kaur, S., Feng, C. Y., Chan, C., Ramakrishna, S., Tabe, S., and Matsuura, T. (2007). Electrospun nanofibrous polysulfone membranes as pre-filters: Particulate removal. *Journal of Membrane Science*, *289*(1), 210-219.

[9] Yu, H., Matthew, H. W., Wooley, P. H., and Yang, S. Y. (2008). Effect of porosity and pore size on microstructures and mechanical properties of poly-ε-caprolactone-hydroxyapatite composites. *Journal of Biomedical Materials Research Part B: Applied Biomaterials*, *86*(2), 541-547.

[10] Agarwal, S., Wendorff, J. H., and Greiner, A. (2008). Use of electrospinning technique for biomedical applications. *Polymer*, *49*(26), 5603-5621.

[11] Duan, Y. Y., Jia, J., Wang, S. H., Yan, W., Jin, L., and Wang, Z. Y. (2007). Preparation of antimicrobial poly (ϵ-caprolactone) electrospun nanofibers containing silver-loaded zirconium phosphate nanoparticles. *Journal of Applied Polymer Science*, *106*(2), 1208-1214.

[12] Xie, J., Li, X., and Xia, Y. (2008). Putting electrospun nanofibers to work for biomedical research. *Macromolecular Rapid Communications*, *29*(22), 1775-1792.

[13] Kang, J., Chen, L., and Sukigara, S. (2012). Preparation and characterization of electrospun polycaprolactone nanofiber webs containing water-soluble eggshell membrane and catechin. *Journal of Fiber Bioengineering and Informatics*, *5*(2), 217-226.

[14] Lowery, J. L., Datta, N., and Rutledge, G. C. (2010). Effect of fiber diameter, pore size and seeding method on growth of human dermal fibroblasts in electrospun poly (ε-caprolactone) fibrous mats. *Biomaterials*, *31*(3), 491-504.

[15] Yohe, S. T., Herrera, V. L., Colson, Y. L., and Grinstaff, M. W. (2012). 3D superhydrophobic electrospun meshes as reinforcement materials for sustained local drug delivery against colorectal cancer cells. *Journal of Controlled Release*, *162*(1), 92-101.

[16] Joosten, U., Joist, A., Frebel, T., Brandt, B., Diederichs, S., and Von Eiff, C. (2004). Evaluation of an in situ setting injectable calcium phosphate as a new carrier material for gentamicin in the treatment of chronic osteomyelitis: Studies in vitro and in vivo. *Biomaterials*, *25*(18), 4287-4295.

[17] Takechi, M., Miyamoto, Y., Ishikawa, K., Nagayama, M., Kon, M., Asaoka, K., and Suzuki, K. (1998). Effects of added antibiotics on the basic properties of anti-washout-type fast-setting calcium phosphate cement. *Journal of Biomedical Materials Research*, *39*(2), 308-316.

[18] Ruckh, T. T., Oldinski, R. A., Carroll, D. A., Mikhova, K., Bryers, J. D., and Popat, K. C. (2012). Antimicrobial effects of nanofiber poly (caprolactone) tissue scaffolds releasing rifampicin. *Journal of Materials Science: Materials in Medicine*, *23*(6), 1411-1420.

[19] Liu, H., Leonas, K. K., and Zhao, Y. (2010). Antimicrobial Properties and Release Profile of Ampicillin from Electrospun Poly (ε-caprolactone) Nanofiber Yarns. *Journal of Engineered Fabrics and Fibers (JEFF)*, *5*(4).

[20] Francis, L., Meng, D., Knowles, J., Keshavarz, T., Boccaccini, A. R., and Roy, I. (2011). Controlled delivery of gentamicin using poly (3-hydroxybutyrate) microspheres. *International Journal of Molecular Sciences*, *12*(7), 4294-4314.

[21] Sirc, J., Kubinova, S., Hobzova, R., Stranska, D., Kozlik, P., Bosakova, Z., Marekova, D., Holan, V., Sykova, E., and Michalek, J. (2012). Controlled gentamicin release from multi-layered electrospun nanofibrous structures of various thicknesses. *International Journal of Nanomedicine*, *7*, 5315-5325.

[22] Shawki, M. M., Hereba, A. M., and Ghazal, A.(2010). Formation and characterisation of antimicrobial dextran nanofibers. *Romanian Journal of Biophysics*, *20*, 335-346.

[23] Sezer, U. A., Aksoy, E. A., Durucan, C., and Hasirci, N. (2012). Gentamicin loaded β-tricalcium phosphate/gelatin composite microspheres as biodegradable bone fillers. *Polymer Composites*, *33*(9), 1644-1651.

[24] Chakrapani, V. Y., Gnanamani, A., Giridev, V. R., Madhusoothanan, M., and Sekaran, G. (2012). Electrospinning of type I collagen and PCL nanofibers using acetic acid. *Journal of Applied Polymer Science*, *125*(4), 3221-3227.

[25] Bassi, A. K., Gough, J. E., Zakikhani, M., and Downes, S. (2011). The chemical and physical properties of poly (ε-caprolactone) scaffolds functionalised with poly (vinyl phosphonic acid-co-acrylic acid). *Journal of Tissue Engineering*, *2*(1).

3.7 Appendix B

Figures 3.12 to 3.32 show SEM images for PCL nanofibers and PCL composed with gentamicin fibers.

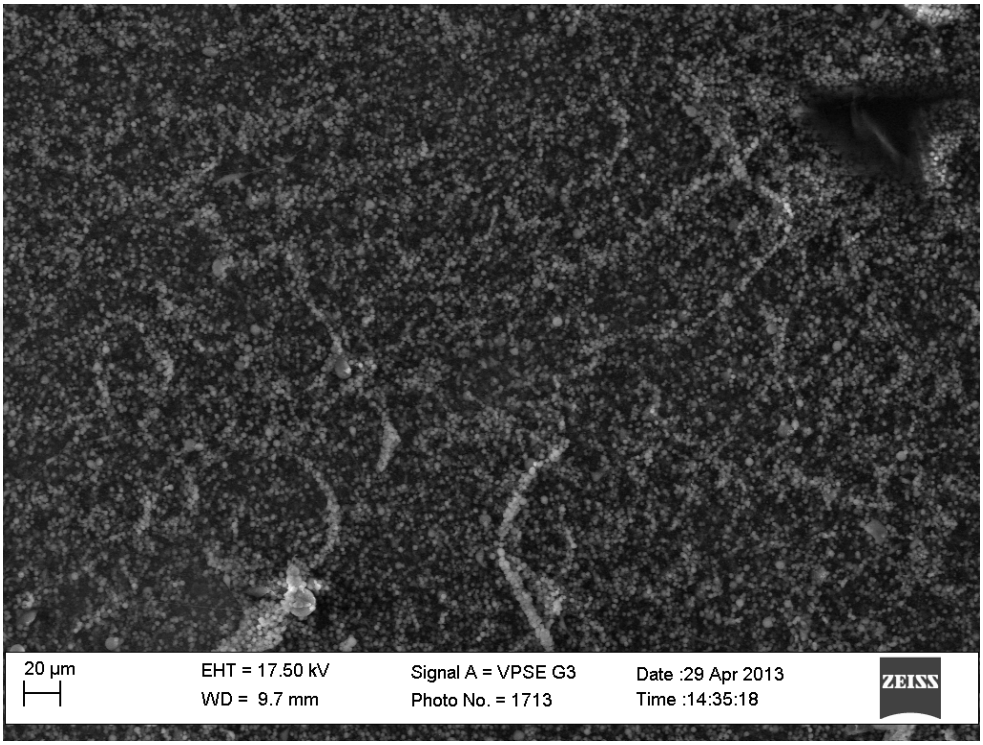


Figure 3.12: SEM image of PCL nanofibers without any inclusion.

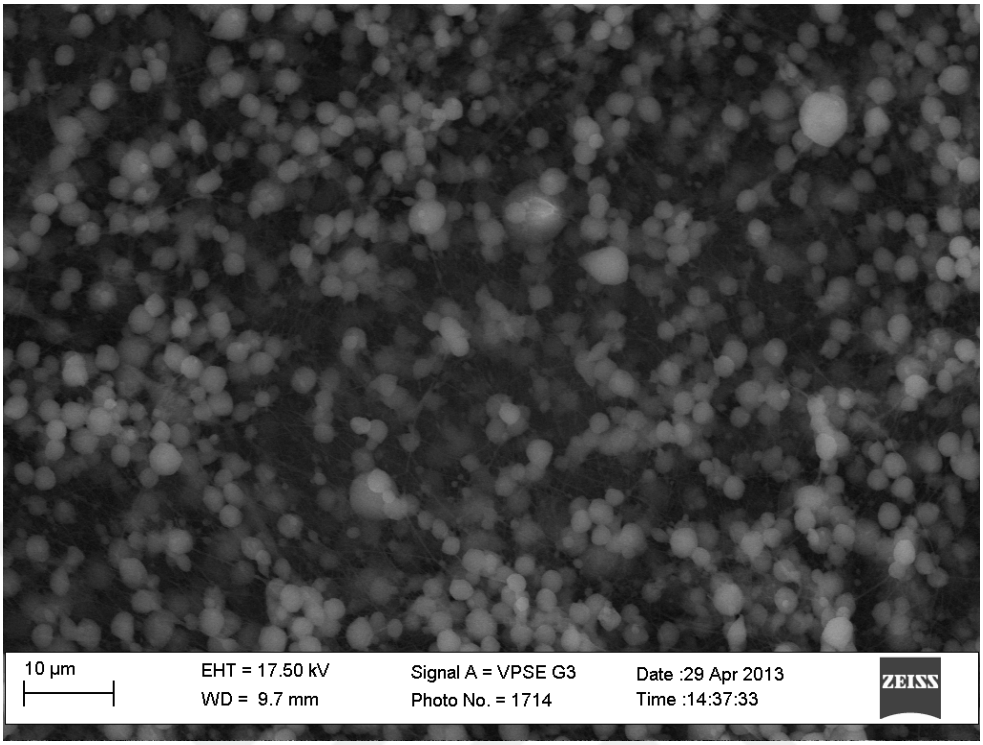


Figure 3.13: SEM image of PCL nanofibers without any inclusion.

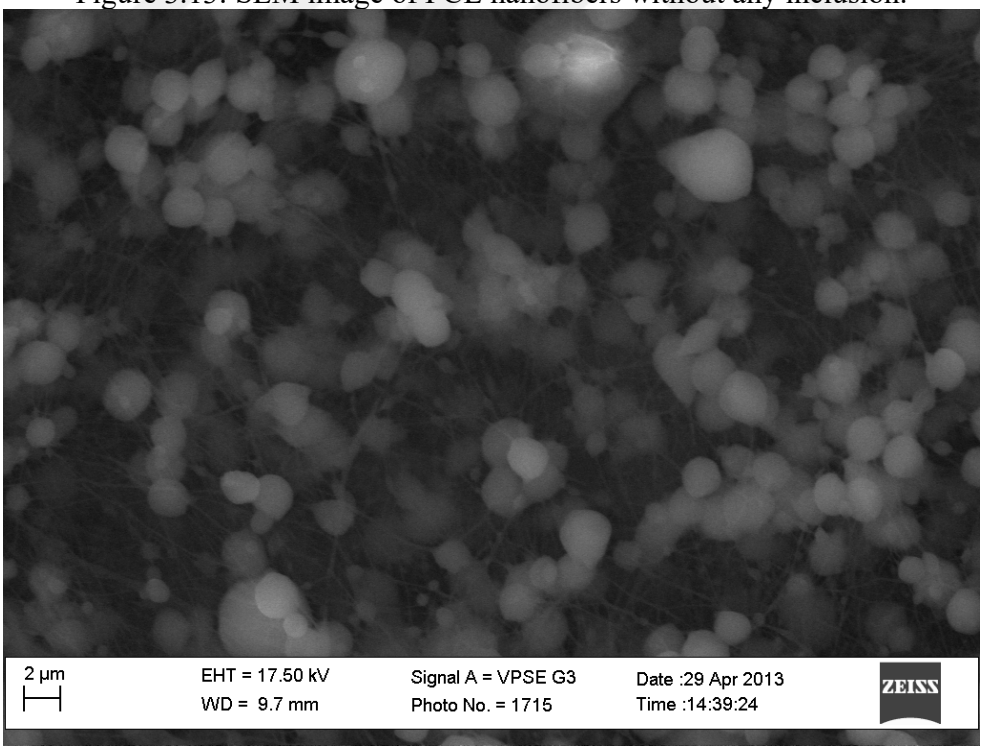


Figure 3.14: SEM image of PCL nanofibers without any inclusion.

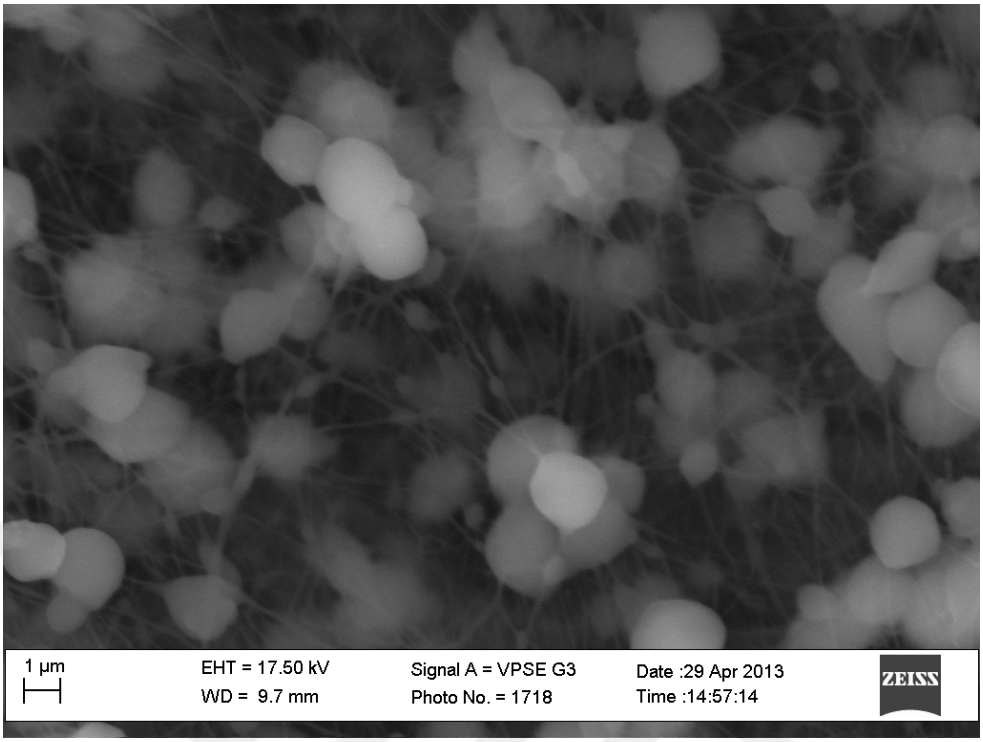


Figure 3.15: SEM image of PCL nanofibers without any inclusion.

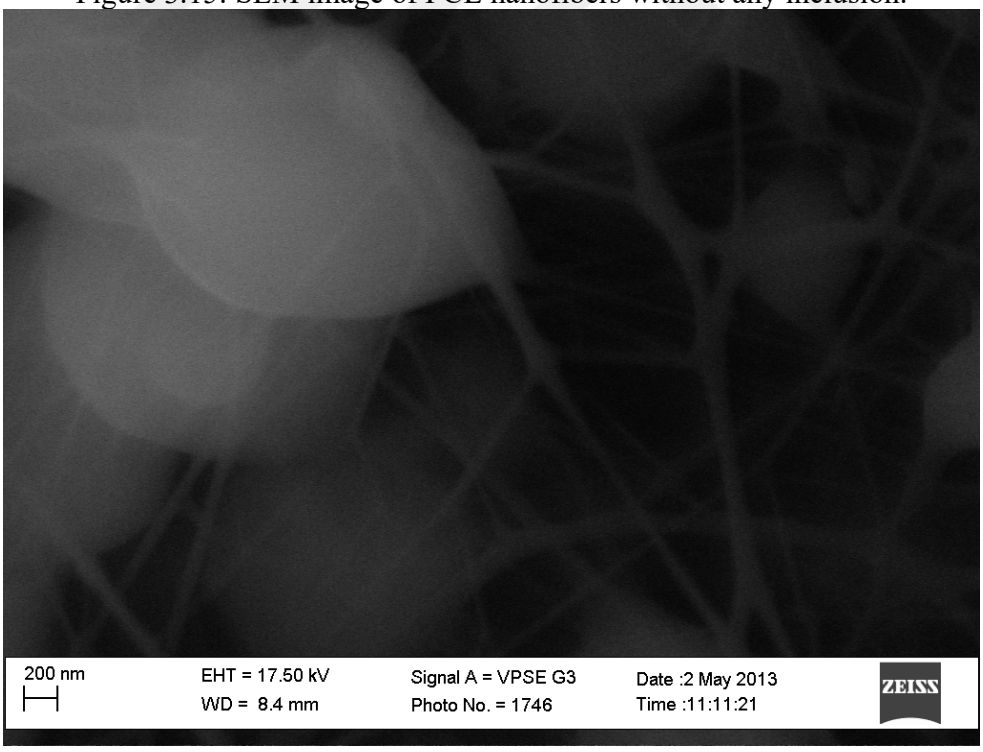


Figure 3.16: SEM image of PCL nanofibers without any inclusion.

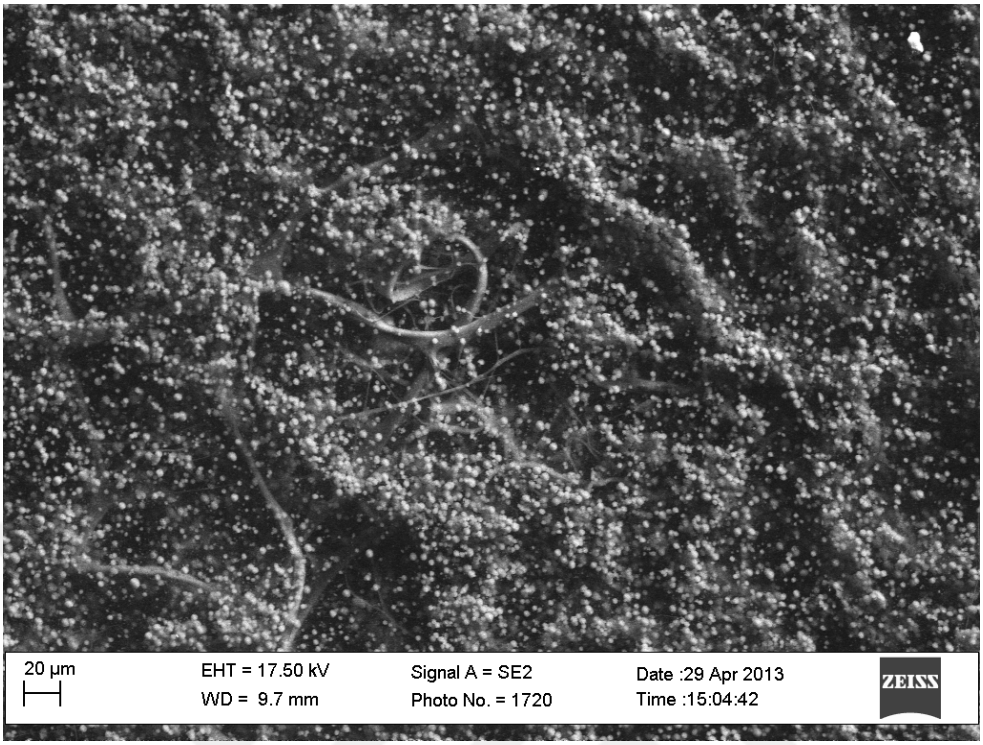


Figure 3.17: SEM image of PCL nanofibers with 2.5 wt% gentamicin.



Figure 3.18: SEM image of PCL nanofibers with 2.5 wt% gentamicin.

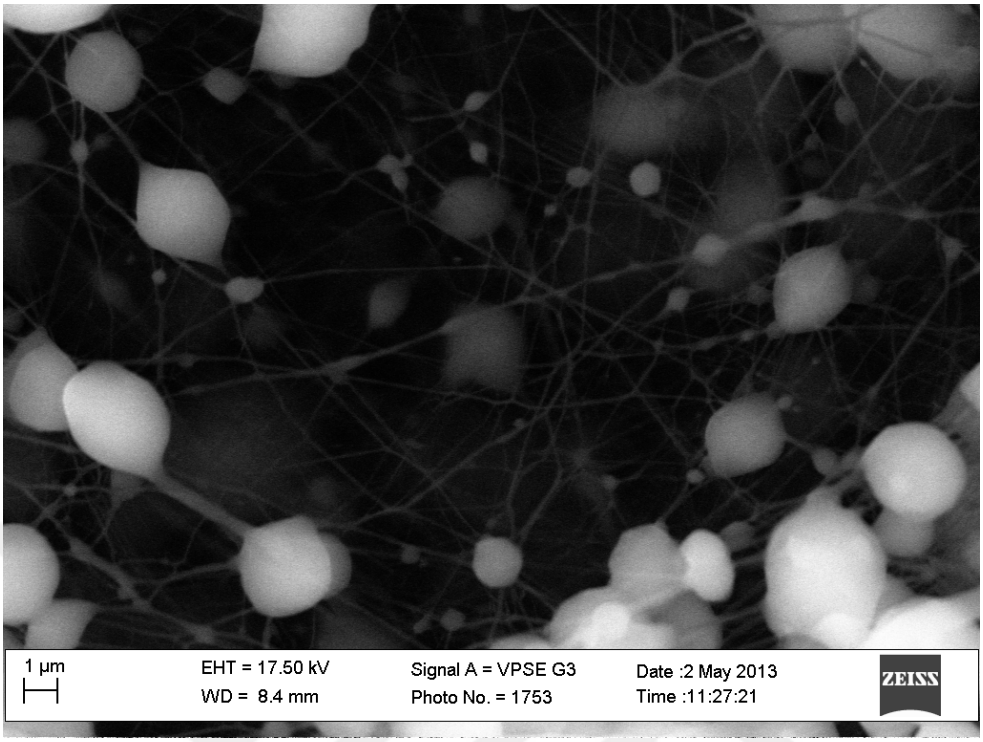


Figure 3.19: SEM image of PCL nanofibers with 2.5 wt% gentamicin.

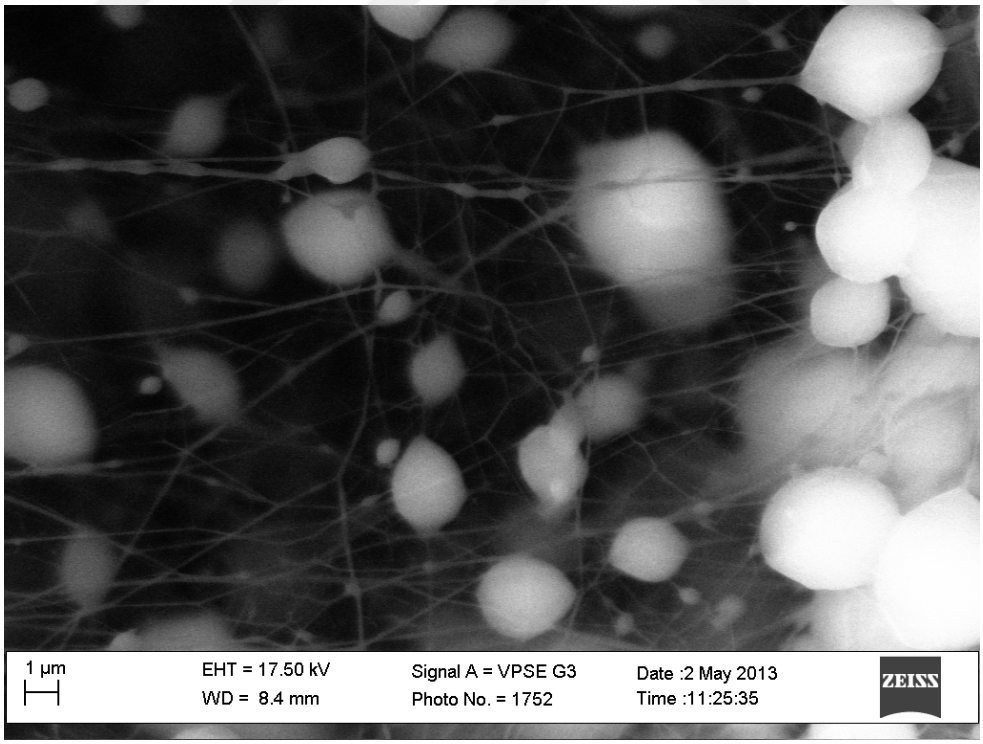


Figure 3.20: SEM image of PCL nanofibers with 2.5 wt% gentamicin.

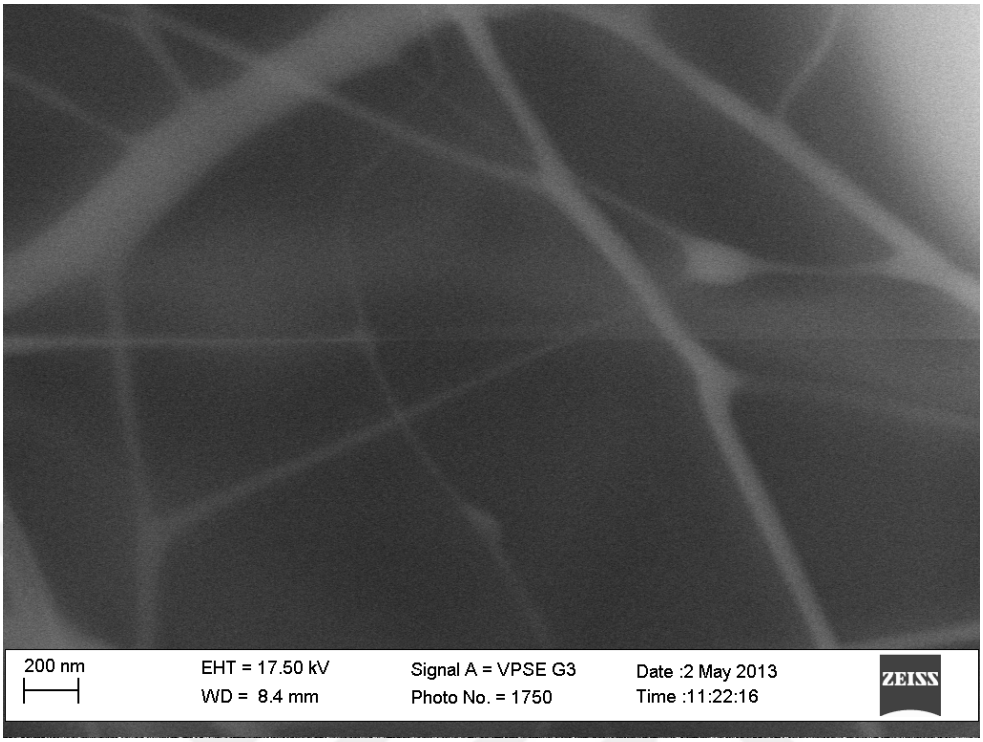


Figure 3.21: SEM image of PCL nanofibers with 2.5 wt% gentamicin.

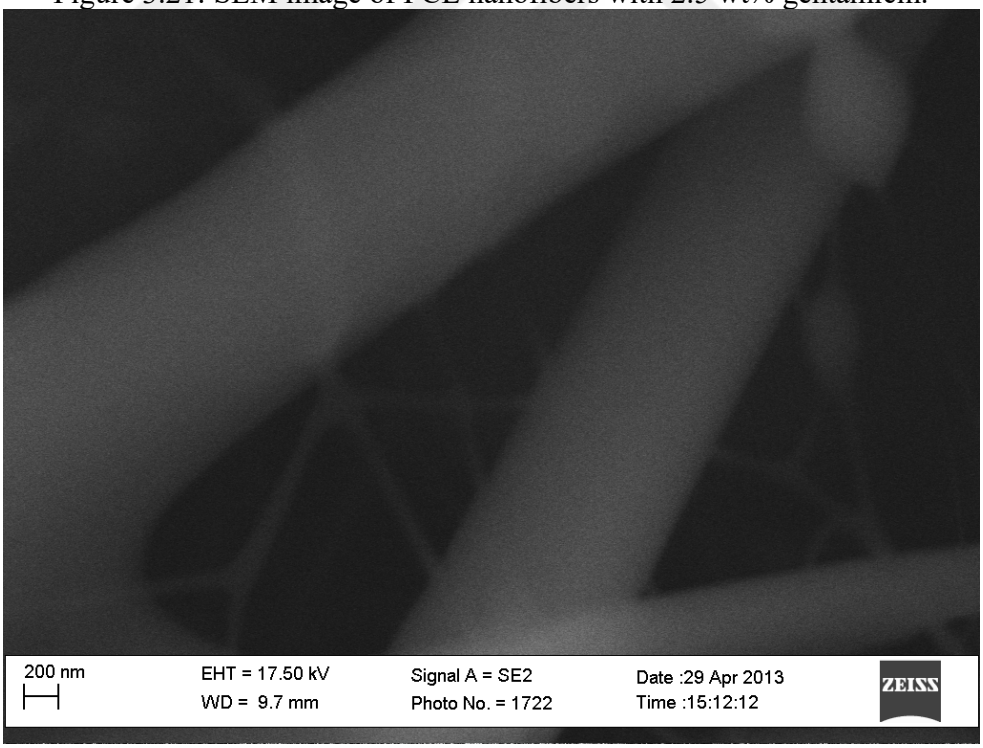


Figure 3.22: SEM image of PCL nanofibers with 2.5 wt% gentamicin.

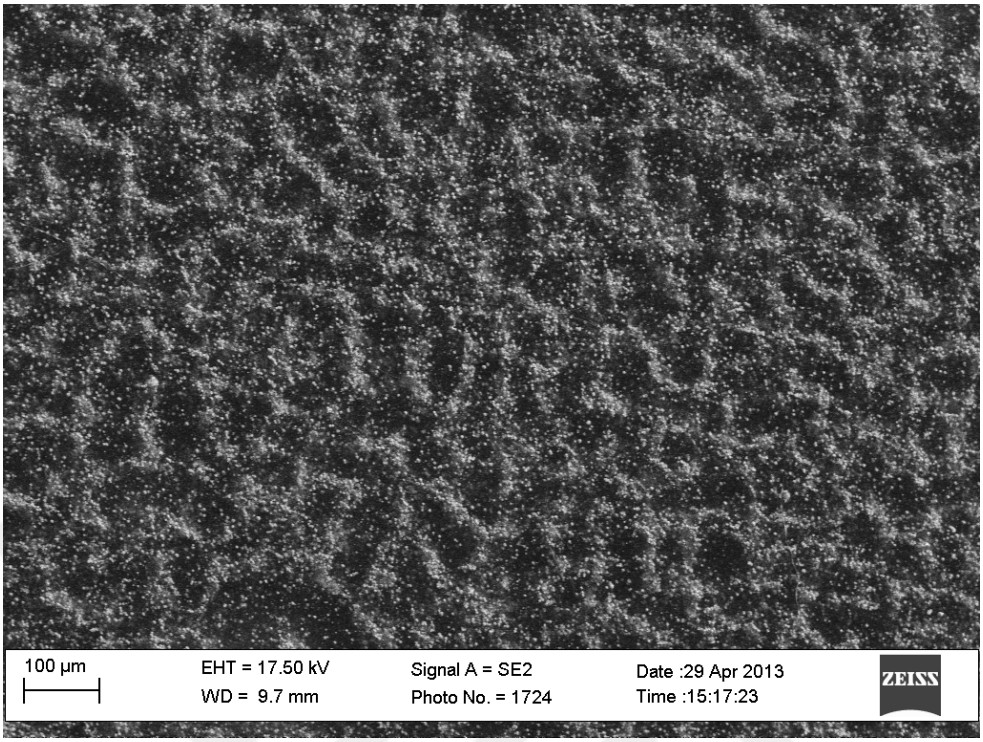


Figure 3.23: SEM image of PCL nanofibers with 5 wt% gentamicin.

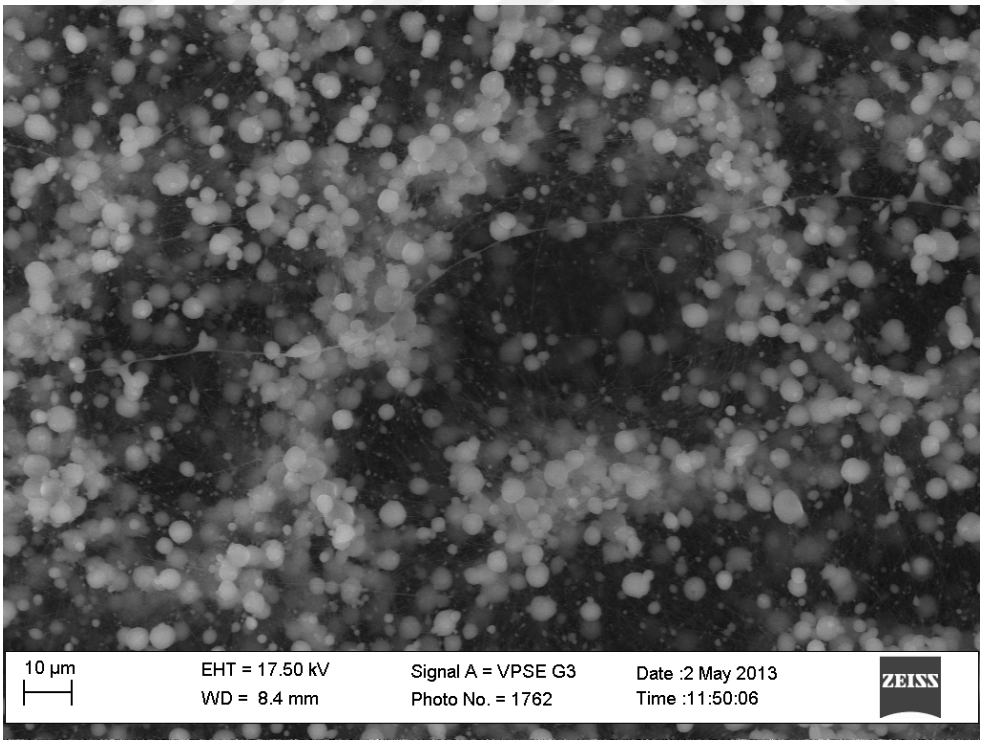


Figure 3.24: SEM image of PCL nanofibers with 5 wt% gentamicin.

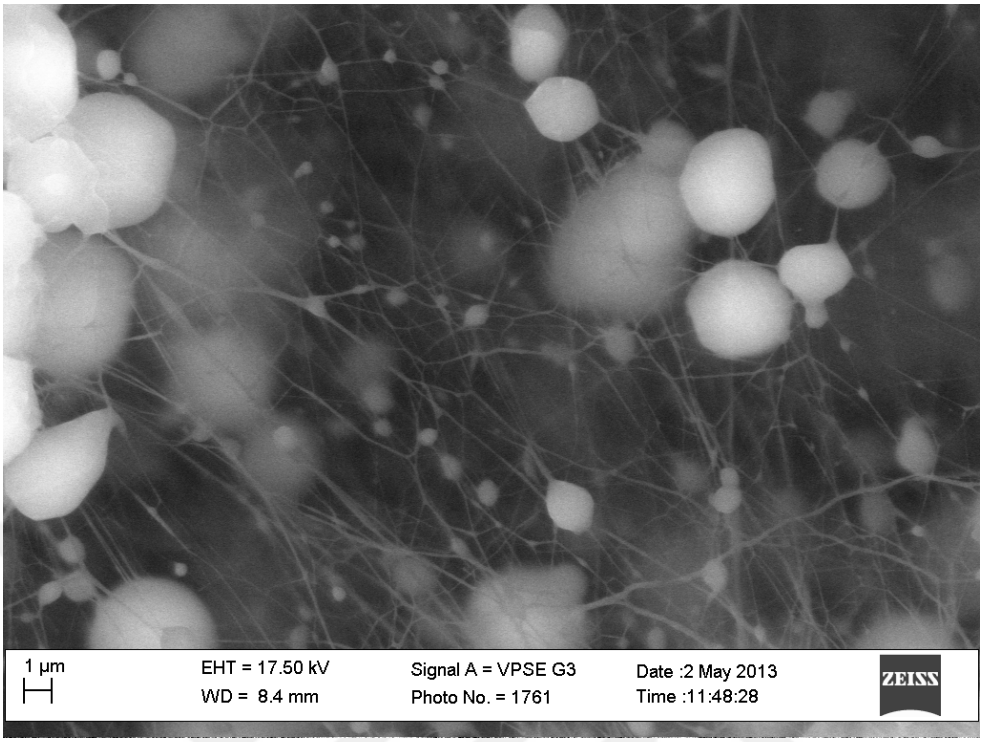


Figure 3.25: SEM image of PCL nanofibers with 5 wt% gentamicin.



Figure 3.26: SEM image of PCL nanofibers with 5 wt% gentamicin.

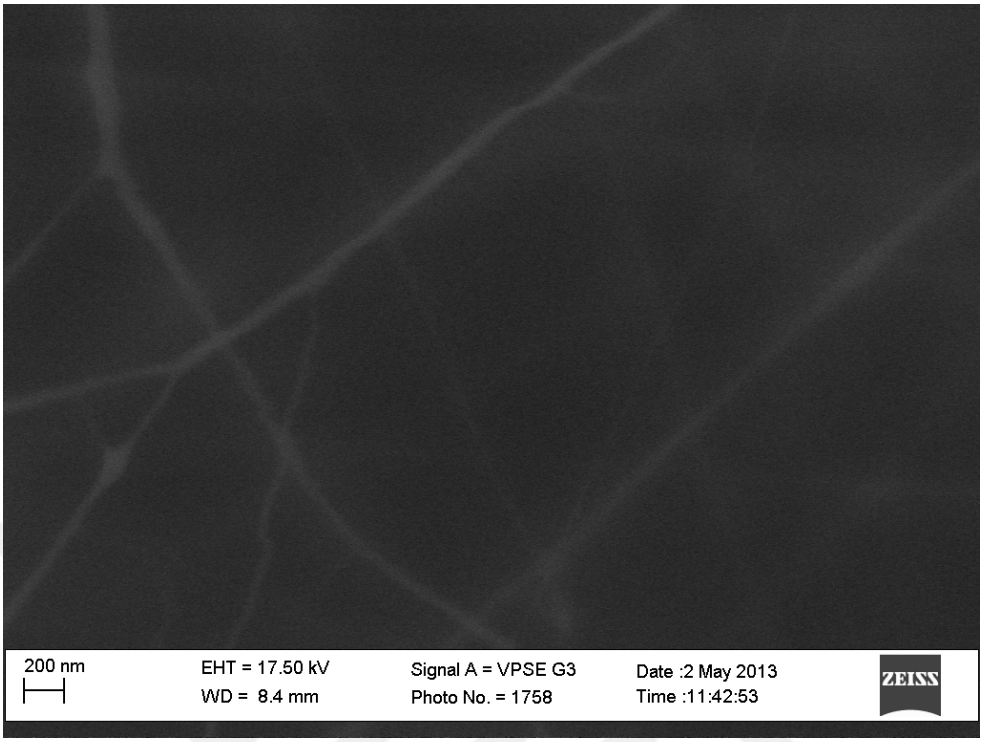


Figure 3.27: SEM image of PCL nanofibers with 5% gentamicin.

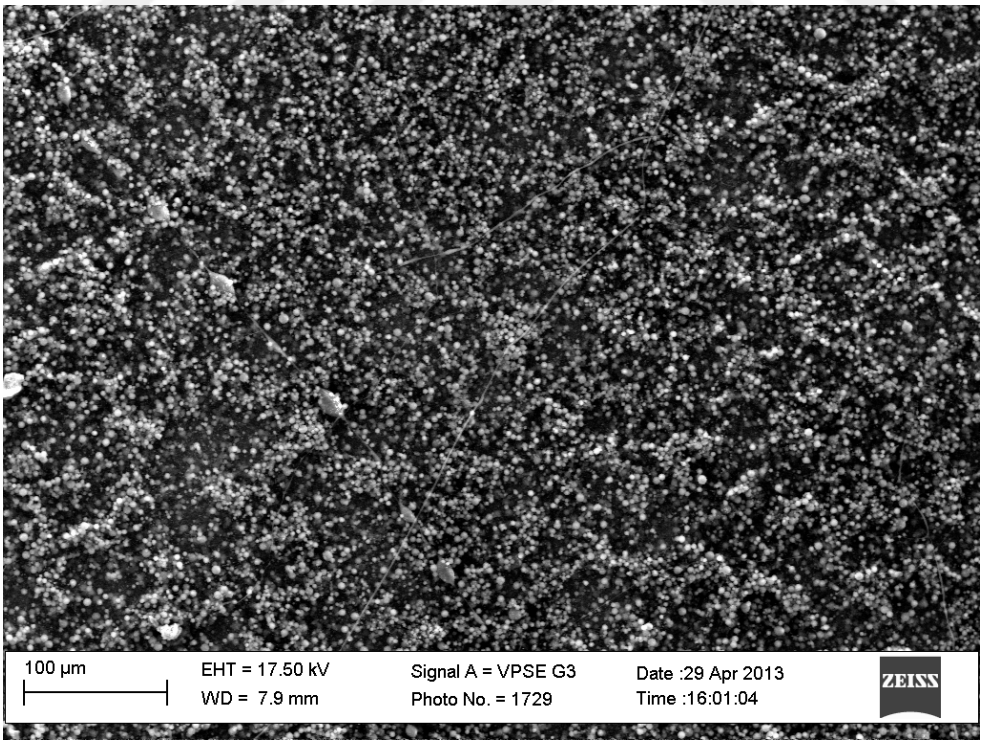


Figure 3.28: SEM image of PCL nanofibers with 10% gentamicin.

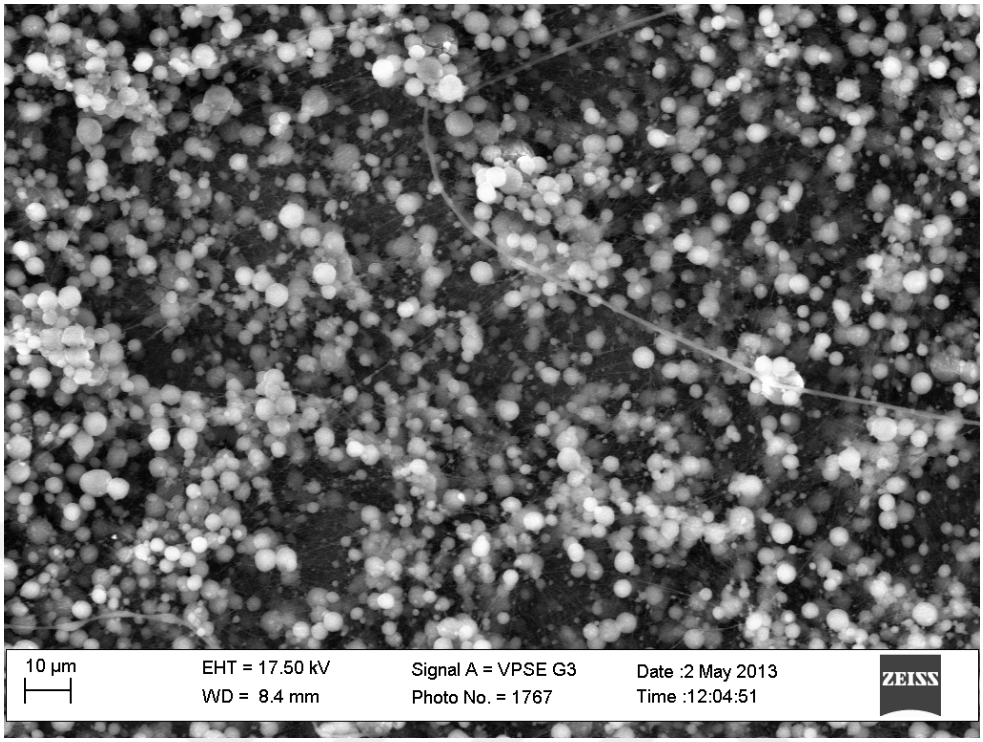


Figure 3.29: SEM image of PCL nanofibers with 10% gentamicin.

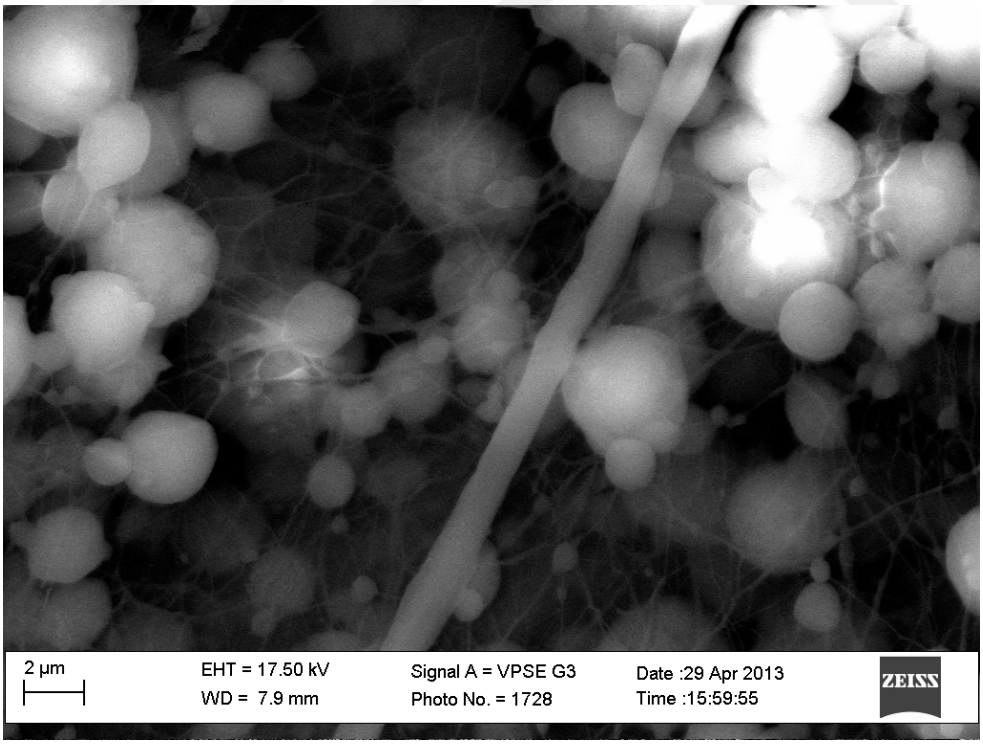


Figure 3.30: SEM image of PCL nanofibers with 10% gentamicin.

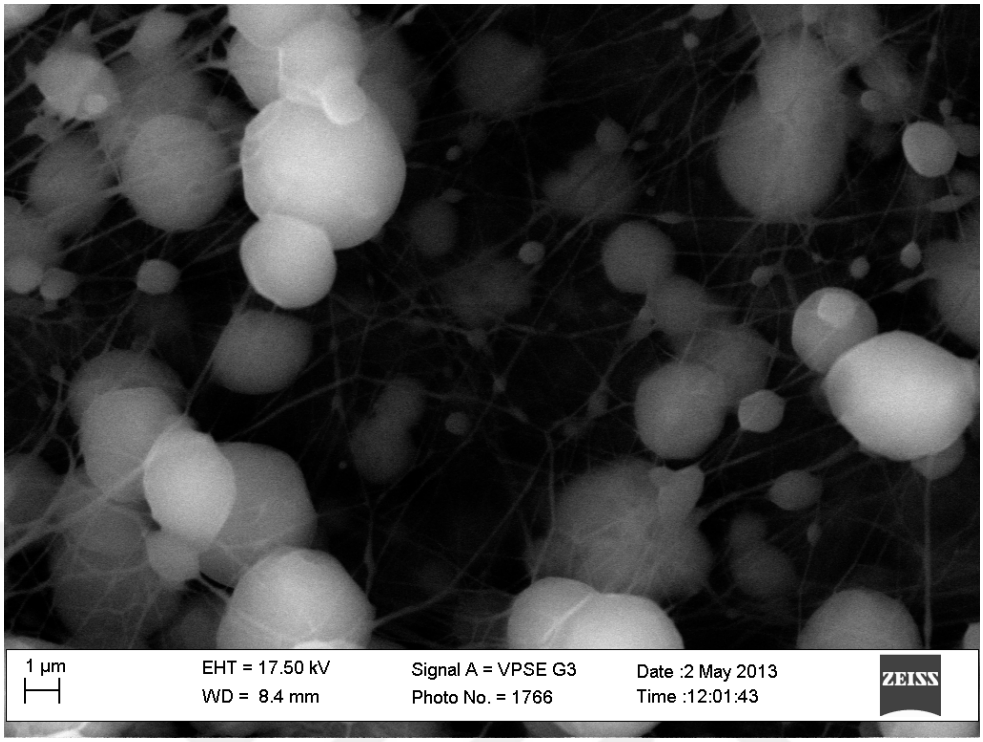


Figure 3.31: SEM image of PCL nanofibers with 10% gentamicin.

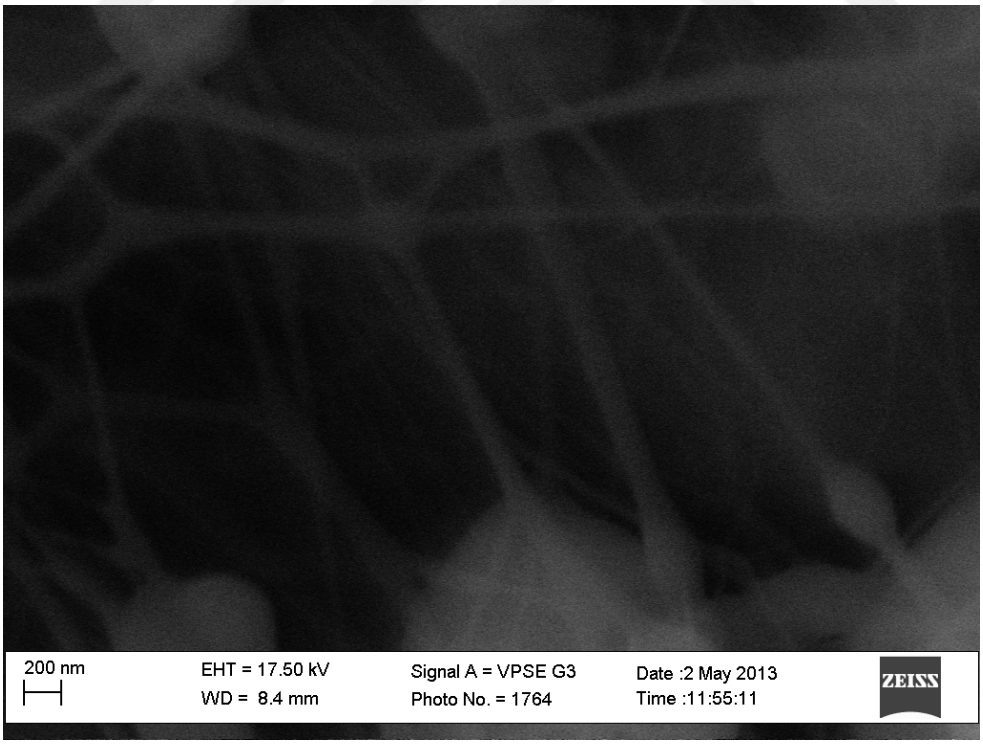


Figure 3.32: SEM image of PCL nanofibers with 10% gentamicin.

Figures 3.33 to 3.37 show FTIR spectroscopy results for PCL nanofibers and PCL nanofiber with gentamicin. Figure 3.38 shows DSC results for PCL nanofiber and PCL nanofiber with gentamicin. Figure 3.39 shows TGA results for PCL nanofiber and PCL nanofiber composed with gentamicin.

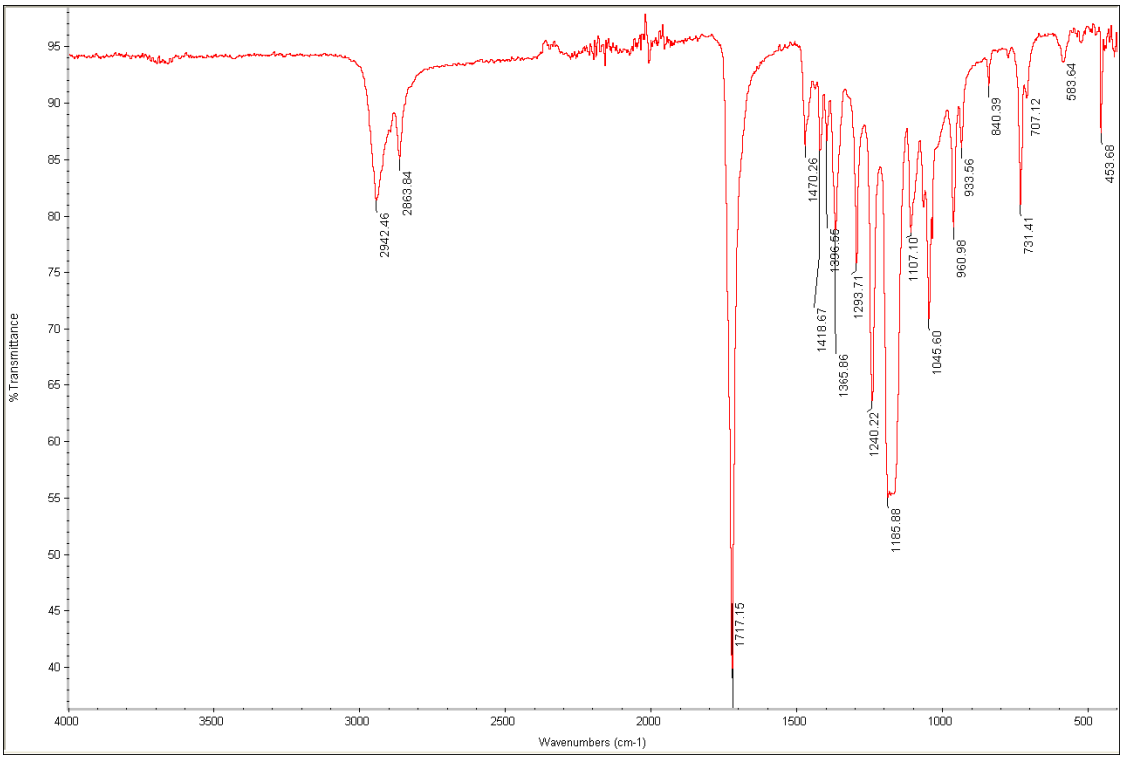


Figure 3.33: FTIR spectroscopy results for PCL nanofibers.

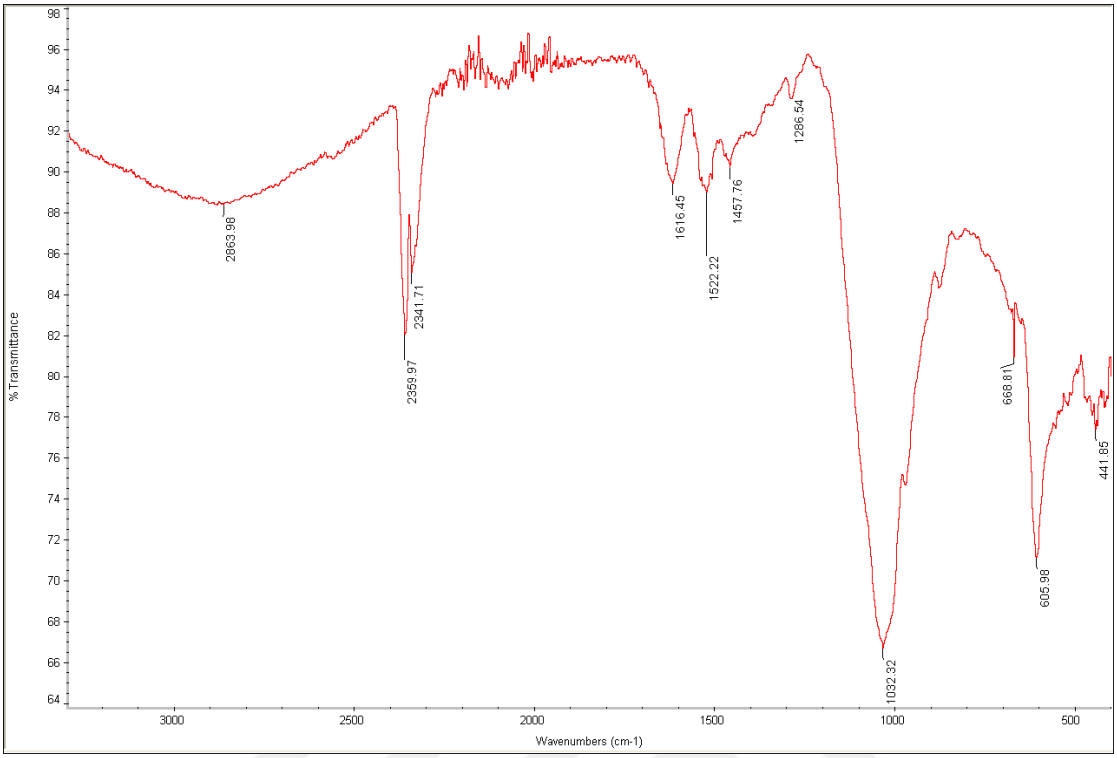


Figure 3.34: FTIR spectroscopy results for gentamicin only.

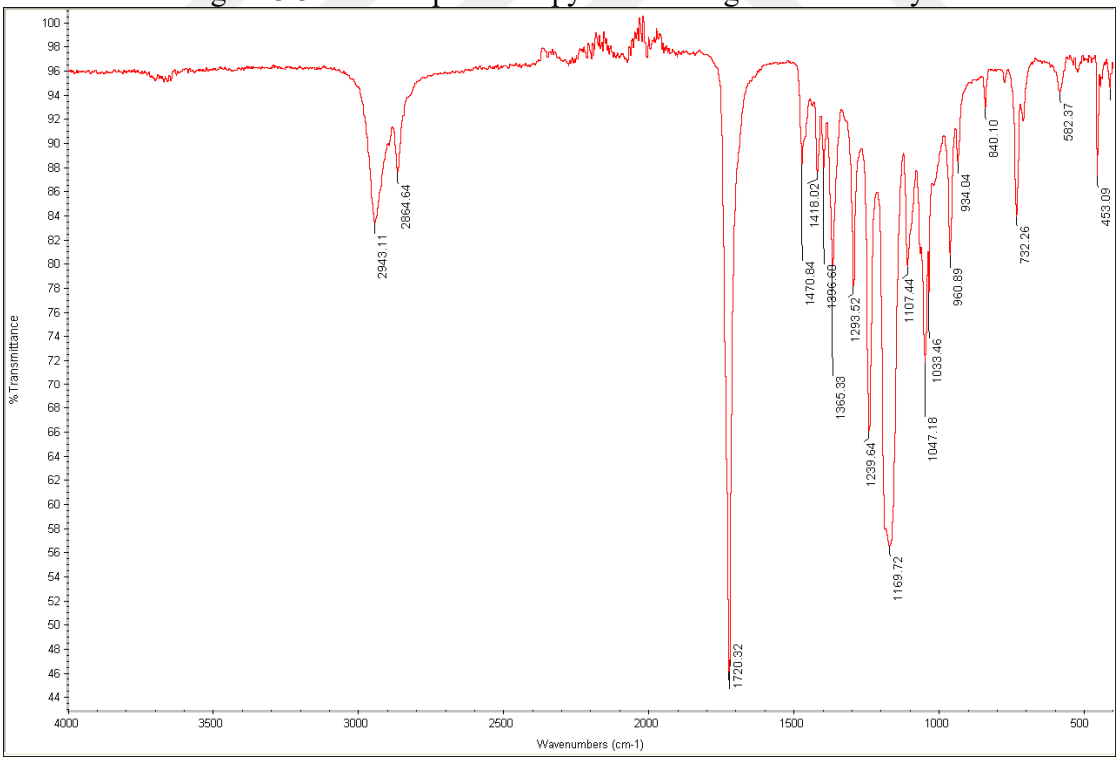


Figure 3.35: FTIR spectroscopy results for PCL nanofibers with 2.5 wt% gentamicin.

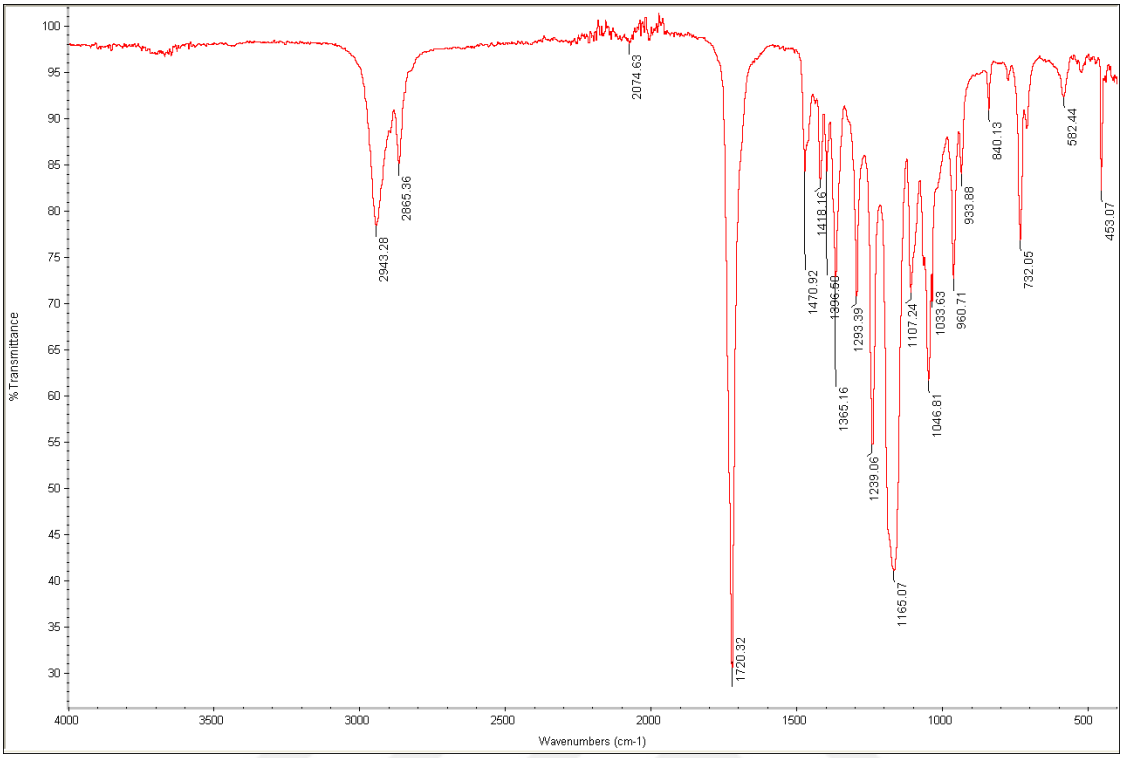


Figure 3.36: FTIR spectroscopy results for PCL nanofibers with 5 wt% gentamicin.

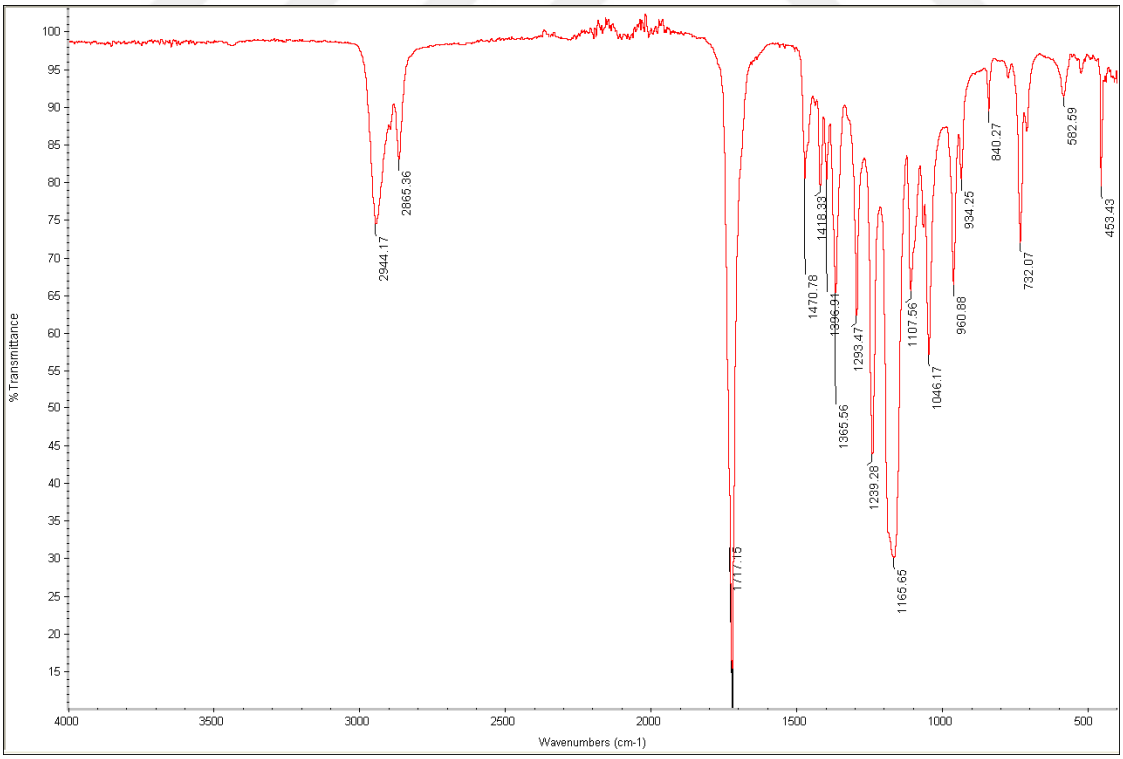


Figure 3.37: FTIR spectroscopy results for PCL nanofibers with 10 wt% gentamicin.

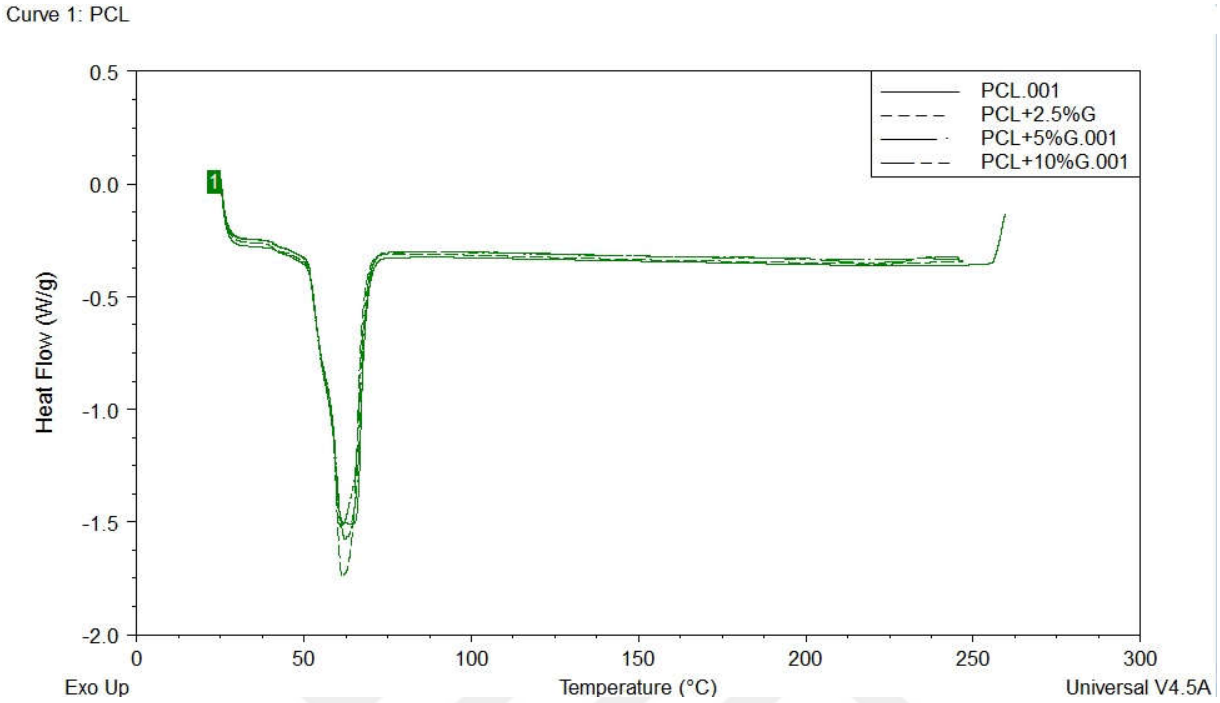


Figure 3.38: DSC results for PCL with 2.5, 5, and 10 wt% gentamicin.

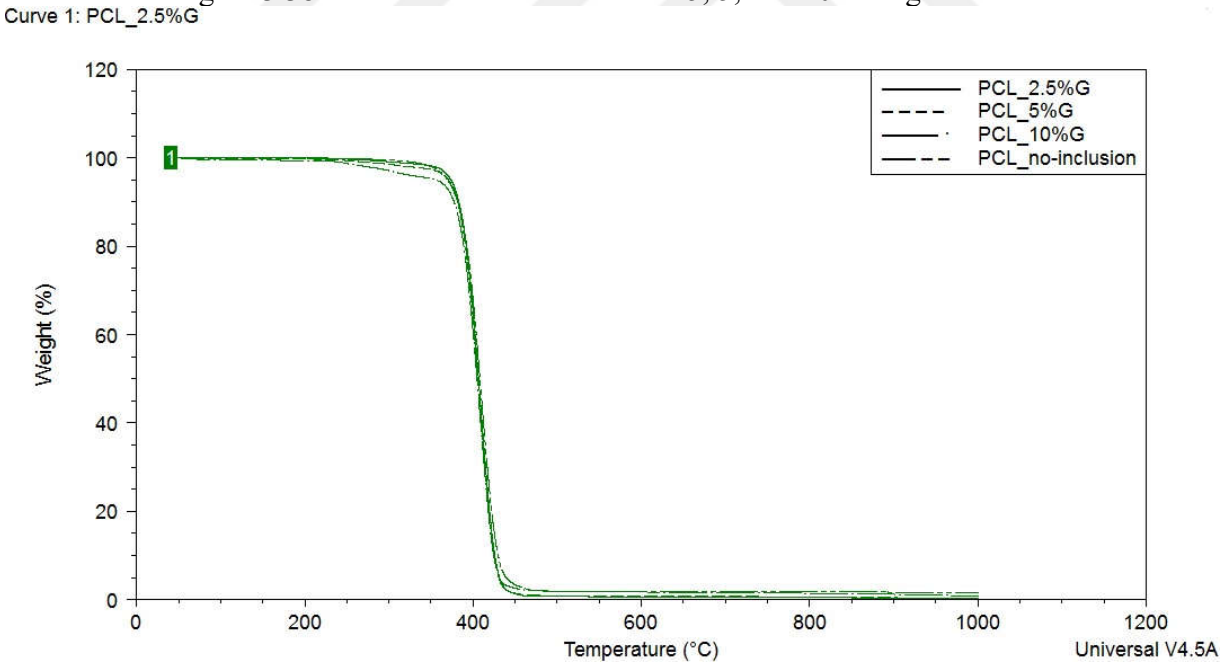


Figure 3.39: TGA results for PCL with 2.5, 5, and 10 wt% gentamicin.

CHAPTER 4

EFFECTS OF GENTAMICIN-LOADED PCL NANOFIBERS ON CELL VIABILITY AND RELEASE RATE OF PLASMID DNA

4.1 Abstract

Poly-ε-caprolactone (PCL) nanofibers were fabricated with the addition of a constant plasmid DNA and different concentrations of gentamicin. The nanofibers were designed using an electrospinning method and studied for their effect on cell viability and release rate. The plasmid DNA used in these PCL nanofiber was extracted from *E. coli*. Scanning electron microscopy (SEM) images show that the nanoscale fiber structures have an average diameter of 113.9 nm. The ultraviolet (UV) microplate reader confirmed the existence of plasmid DNA in the PCL nanofibers. An Elisa Reader study showed the addition of gentamicin in the fibers. Cell viability tests indicated that PCL nanofibers with 10% gentamicin on a fibroblast cell showed high cell viability, which is related to surface area and pore size of the electrospun fibers, in addition to the interaction with gentamicin, plasmid DNA, and electrospun fiber matrix.

Keywords: Electrospinning, PCL nanofibers, Cell viability, Wound dressing

4.2 Introduction

Popularity of the electrospinning process has improved in the past decade due to the diameter reduction of large fibers from micron to nanometer size. At the point when the diameters of the polymeric fibers could be reduced in size from micrometers to nanometers, this offered a few remarkable aspects, for instance, high surface-to-volume ratio, high porosity, adaptability in surface functionalities, and predominant mechanical properties. These exceptional properties of electrospun nanofibers make them ideal candidates for a wide area of significant

use in different areas, such as drug delivery, tissue engineering, scaffolding, wound dressing, sensors, and filters [1].

Electrospinning is the methodology of expelling a fine fiber from a charged polymer solution towards a grounded collector. The fiber is constantly elongated by electric static forces, and the solvent evaporates while traveling through air to the collector [2]. The history of electrospinning started with electrospraying about 100 years ago. Instead of fibers, polymer droplets were formed by electrostatic forces. In 1934, Formhals patented a device that effectively electrospun fibers [3]. Throughout the following few years, he kept improving his work, patenting minor, yet compelling, progressions, which eventually led to the electrospinning setup [4, 5]. In 1969, Taylor created a mathematical model to show the form of a liquid droplet under a electric field. This shape is known as the Taylor cone. In order to achieve successful jet formation, the droplet cone angle was 98.6 degrees [6]. In 1971, Baumgarten studied solution parameters and their effects on fiber diameter [7]. This study showed that increasing the viscosity of the solution increased the fiber diameters; therefore, electrospun fibers in nanometer range could be produced. Publications relative to electrospinning have increased since 2000 [2]. The production of fibers at nano size has turned into a promising feature for biomedical applications such as wound dressings, drug delivery, tissue engineering, and filtration [8,9].

The diameters of electrospun fibers formed have been attained from microns to nanometers size [10]. Electrospun fibers have a high surface-to-volume ratio, which allows for the improvement of cell reproduction. Electrospinning has promising applications including vasculature [11, 12], neural [13], bone tissue [14], antibacterial, filtration, and scaffolding. Natural and synthetic polymers, such as collagen [15], gelatin [16], and fibrinogen [17], have been electrospun. Inclusions include drugs, antibiotics, graphene, and TiO_2 nanoparticles.

Adding these inclusions to a polymer solution can increase the properties of an electrospun fiber. Electrospinning technology opens up new opportunities for the generation of fiber-based biomaterials, including antimicrobial fibers [18, 19].

PCL is a biodegradable, hydrophobic, and Food and Drug Administration (FDA)-approved polymer that has extensive uses in biomedical applications and shows biocompatibility [20]. In the present study, PCL nanofibers were examined, and antibiotic and plasmid DNA-loaded fibril structures that display various release characteristics for wound-healing applications were developed. Gentamicin was chosen as the drug to load onto PCL nanofibers because of its antibiotic ability to inhibit or kill germs and bacteria that are common as the result of surgical infection. The choice of polymer, distribution of plasmid DNA, and antibiotics within the nanofibers affect the morphology and release rate. Preliminary antibiotic effectiveness against fibroblast cells (L929) and neuroblast cells (B104) has been tested to determine the suitability of these nanofibers being applied in order to decrease the frequency and severity of post-surgery infections.

4.3 Experimental Procedure

4.3.1 Materials

PCL was purchased from Scientific Polymer Products Inc., acetonitrile from Sigma-Aldrich, and pCMVb-GFP DNA from Addgene. Plasmid DNA was amplified with *E. coli*., which is a typical way of handling plasmid DNA. These items were straightforwardly utilized for the electrospinning procedure without further purification. Fibroblast cells (L-929) and neuroblast cells (B104) were purchased from American Type Culture Collection (ATCC).

4.3.2 Methods

4.3.2.1 Electrospinning of Nanofibers

The electrospinning process is a complex system with multiple parameters. Using these parameters, various electrospun fibers can be produced for different applications. The electrospinning setup includes a syringe, charged polymer solution, pump, grounded collector, and high power supply, as shown in Figure 4.1.

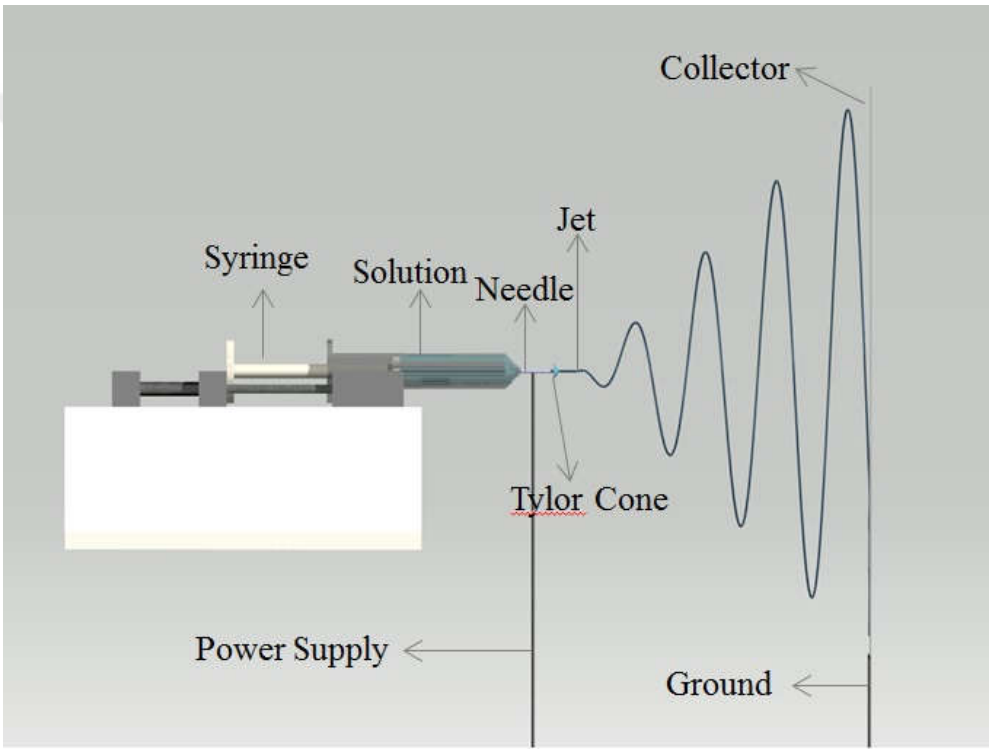


Figure 4.1: Schematic of electrospinning process.

The polymer solution is composed of melted polymer and a solvent. The solvent plays the role of bringing the polymer resin into solution, and then, when the solution is exposed to air, the solvent evaporates. In order to form a solid fiber, evaporation of the solvent is necessary. The pump holds the syringe containing the polymer solution and can be used to adjust the flow rate of the solution. The high power supply is in the range of 10–30 kV. An electrode from the high power supply is applied to the solution for most of the time through a syringe needle, or

conductive material is attached to the syringe and is in contact with polymeric solution. Collectors vary, depending on the application, such as for scaffolding, in order to obtain different-shaped fibers. Collectors can be a wire mesh, fluid bath, flat plate, or rotating drum around which the polymer wraps itself [21]. The distance between the tip of the needle to the collector is called the gap distance. The grounded collector and the charged polymer solution creates a static electric field. When voltage is applied to the needle, the solution droplet at the tip experiences Coulomb forces exerted by the electric field and electrostatic repulsion between the surface charges [2]. As the applied charges increases, the solution droplet changes from a round shape to a Taylor cone. When the charge overcomes the surface tension of the solution droplet, a thin polymer jet moves from the Taylor cone to the collector. As the jet travels through the air, a whipping instability occurs and causes the jet to progress in a conical or zigzag pattern. Before arrival to the collector, this will further thin the fiber diameter.

In the fabrication in this study, 15 wt% of PCL was dissolved in acetonitrile. Then 0, 2.5, 5, 10 wt% of gentamicin and 0.55 µg of plasmid DNA were added to the PCL solutions. The final solution was placed on a hot plate (stir plate) for 24 hours, which was heated to 54ºC at a speed of 500 rpm. The mixed solution was transferred into a 10 mL syringe and placed in a KD Scientific syringe pump at a flow rate of 2 mL/hr. The electrospinning process was completed in ambient conditions. Fibers were collected after drying for at least two days.

4.3.2.2 Materials Characterization

Scanning electron microscopy (ZEISS) was used to analyze the morphology of the PCL electrospun fibers. The Elisa Reader was used for the cytotoxicity reading plate at OD 590 nm. A UV microplate reader (CytoFlour Series 4000, Perceptive Biosystems) was used for the release-rate study.

4.3.2.3 Isolation of pCMVb-GFP Plasmid DNA

Plasmid DNA enhanced green fluorescent protein (EGFP) with cytomegalovirus (CMV) promoter was amplified with *E. coli* and grown on a shaker at 37ºC overnight. Micro-centrifuge tubes were filled with the saturated bacterial culture grown in lysogeny broth (LB) containing ampicillin and centrifuged at a speed of 4,000 rpm at 4ºC for 3 min, followed by the addition of 0.2 ml ice-cold solution I (50 mM glucose, 25 mM Tris-Hcl pH 8.0, 10 mM EDTA Ph 8.0), 0.4 ml solution II (1% sodium dodecyl sulfate(SDS), 0.2 N NaOH), and 0.3 ml ice-cold solution III (3 M K+ 5 M Acetate). Next, the micro-centrifuge tubes were put on ice for 10 min and then centrifuged at 12,000 rpm at 4ºC for 5 min, and the supernatant was transferred to a fresh micro-centrifuge tube. Then isopropanol was added to fill the remainder of the centrifuge tubes, which were put on ice for 10 min, followed by centrifuging at 12,000 rpm at 4ºC for 5 min. Followin this, 1 ml ice-cold 70% ethanol was added to each of the micro-centrifuge tubes, which were then centrifuged at a speed of 7,500 rpm at 4ºC for 2 min. Finally, 50µl TE buffer (10 mM Tris-HCl, 1 mM EDTA, pH 8.0) was added to each tube. Using the Elisa Reader, the concentration of plasmid DNA was detected from the UV absorbance at a wavelength of 260 nm (A260).

4.3.2.4 Biocompatibility and Cytotoxicity Assay of PCL Nanofibers

Sterile nanofibers in a 2 ml Eppendorf tube were submerged with Dulbecco's Modified Eagle's Medium (DMEM) (ATCC) containing 5% fetal bovine serum (FBS), 2 mM glutamine, 100 µ/ml penicillin, and 0.1 mg/ml streptomycin. The medium was collected on the first, fourth, and seventh days, and the tubes were refilled with fresh medium. Cells were seeded in a 96-well plate at a density of $5x10^4$ cells/well and cultured in a standard incubator (37ºC, 5% CO_2) for three days. Then 20 µl 3-(4, 5-dimethylthiazol-2-yl)-2, 5-diphenyltetrazolium bromide (MTT)

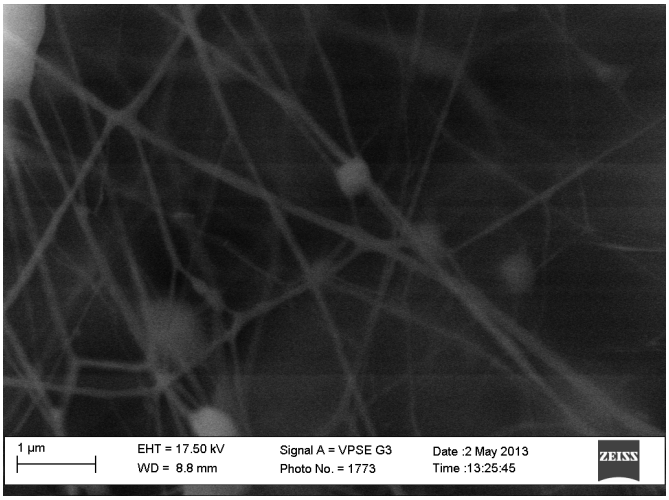
was added to each well. After six hours, the cells were cracked by 10% sodium dodecyl sulfonate (SDS) solution, followed by a reading plate at OD 590 nm using an Elisa Reader.

4.3.2.5 DNA Release Rates

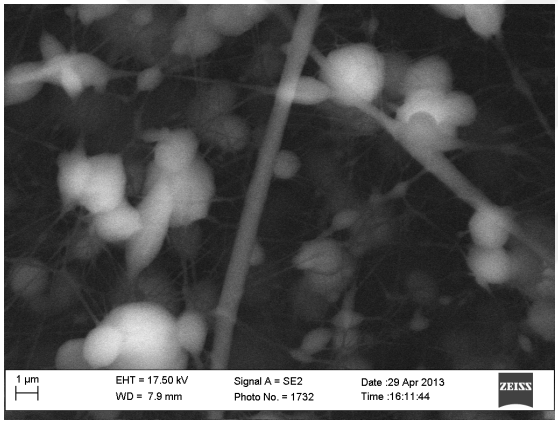
The electrospun nanofibers were cut into quarter sizes and each immersed in 1 ml TE buffer in Eppendorf tubes at 37ºC. The amount of DNA released into solution was quantified using a PicoGreen assay, according to the manufacture's protocol. Briefly, the elution TE buffers were collected at 1 hr, 4 hr, 1 day, 4 days, and 7 days, and labeled with PicoGreen to detect DNA content. For each time point, there were six samples. The DNA standard solution (100 µg/ml in TE(10 mM Tris-HCl, 1 mM EDTA, pH 7.5) buffer) was diluted into 2 µg/ml stock solution, which was a dilution of 1:2. Based on the concentration of DNA in the standard solution, it is possible to calculate how much double-strand DNA was released into the TE buffer. PicoGreen reagent was diluted 200 fold in the TE buffer. The elution solutions were measured at 520 nm (with excitation at 480 nm) in a UV Microplate Reader (CytoFlour Series 4000, Perceptive Biosystems). According to the standard curve, the plasmid DNA concentration in each sample can be calculated.

4.4 Results and Discussion

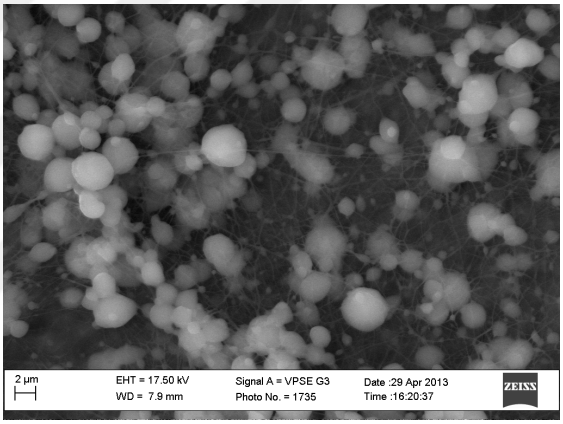
PCL nanofibers with the addition of gentamicin and plasmid DNA were produced using electrospinning. From the SEM images, it can be seen that the fiber diameter was around 113.9 ± 36.60 nm. Figure 4.2 shows SEM images for the following combinations of plasmid DNA and gentamicin: 0% plasmid DNA and 0% gentamicin, plasmid DNA, 2.5% gentamicin and plasmid DNA, 5% gentamicin and plasmid DNA, and 10% gentamicin and plasmid DNA.



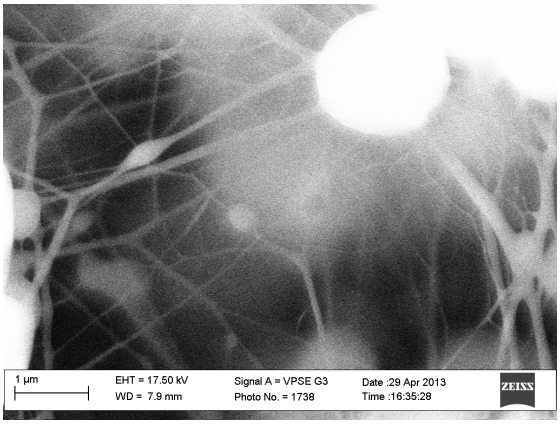
(a)



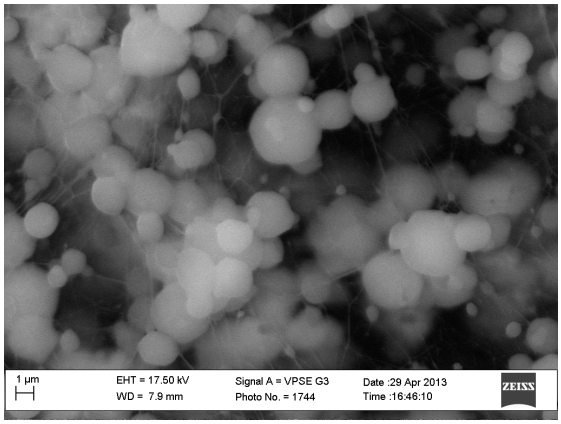
(b)



(c)



(d)



(e)

Figure 4.2: SEM images of PCL nanofiber composed of the following materials: (a) 0% gentamicin and 0% plasmid DNA, (b) 0% gentamicin and plasmid DNA, (c) 2.5% gentamicin and plasmid DNA, (d) 5% gentamicin and plasmid DNA, and (e) 10% gentamicin and plasmid DNA.

Nanofiber diameters were calculated using two SEM images from each sample; the results are shown in Figure 4.3. It can be seen that the addition of 10% gentamicin and plasmid DNA produced nanofibers with the smallest diameters. However, there was no significant change by adding gentamicin and plasmid DNA into the PCL.

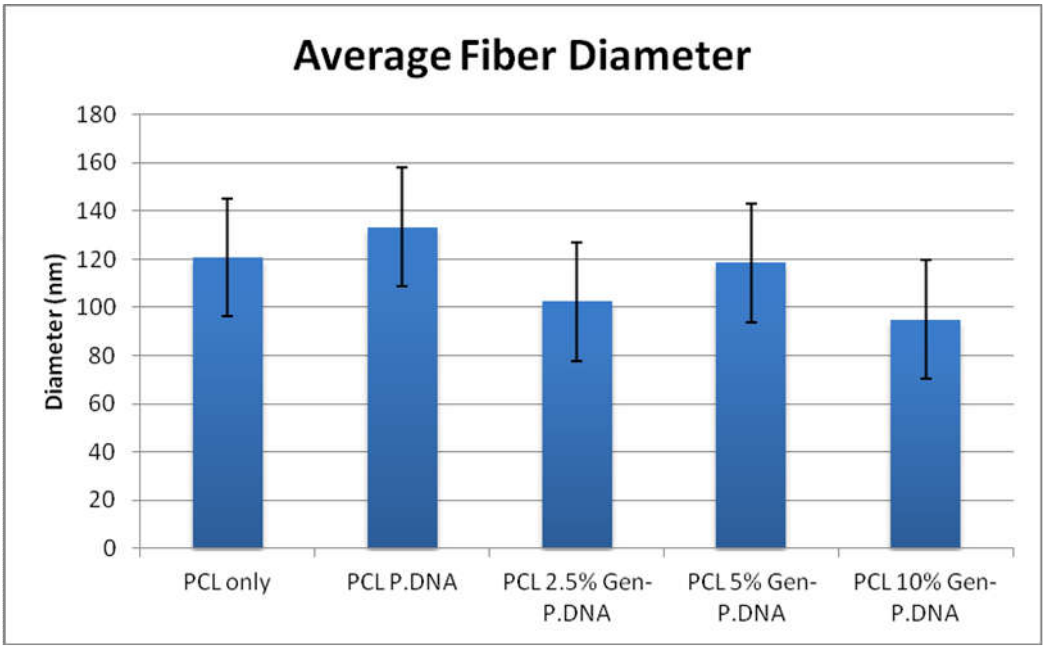


Figure 4.3: Average fiber diameter of PCL nanofibers with different percentages of gentamicin and plasmid DNA.

PCL nanofibers were investigated using the UV Elisa Reader. Figure 4.4 shows DNA release as a function of time for PCL nanofibers composed of gentamicin and plasmid DNA. As shown, 2.5% gentamicin-loaded PCL nanofiber had a good amount of release. However, there is no significant change in DNA release by adding gentamicin into the PCL nanofiber.

For the evaluation of the antimicrobial properties of the PCL nanofibers with various concentrations of gentamicin and plasmid DNA nanofibers evaluated through cell viability, B104 and L929 cells were used for both cases of cell viability above 70%. Generated using the Elisa Reader, Figures 4.5 and Figure 4.6 show the cell viability of neuroblast and fibroblast cell viability, respectively. As shown in Figure 4.5, gentamicin does not significantly affect

neuroblast cell viability but does significantly affect fibroblast cell viability. The addition of 5% gentamicin shows the highest cell viability among other gentamicin additions.

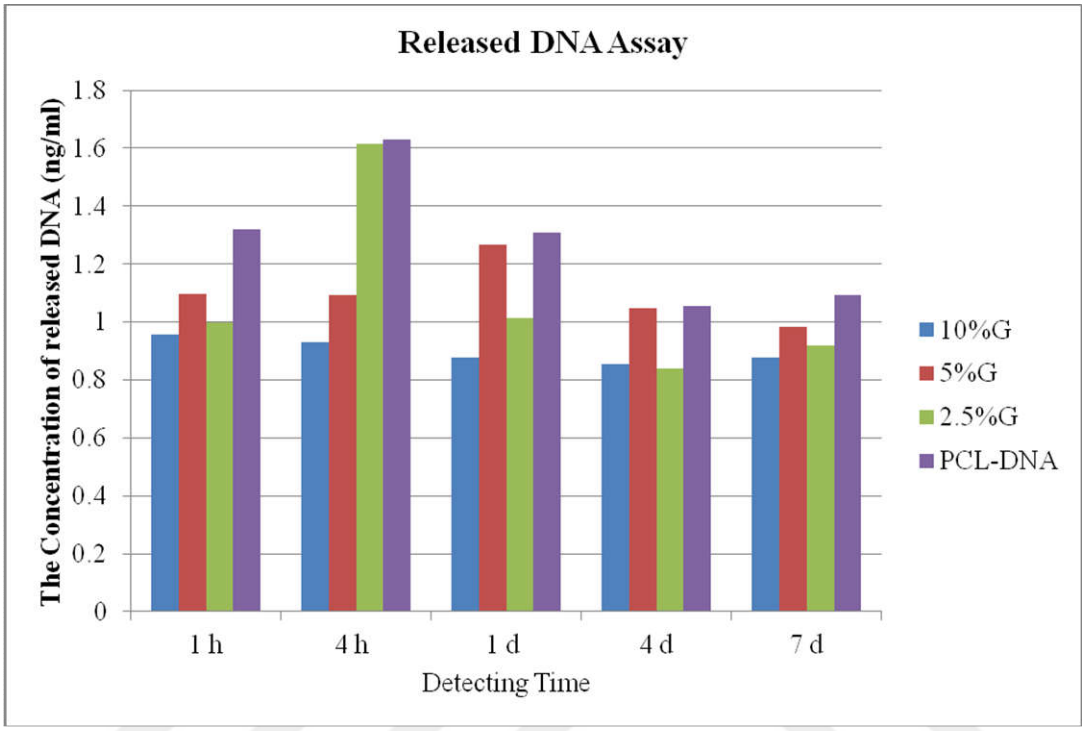


Figure 4.4: DNA release rates as function of time for different PCL nanofibers.

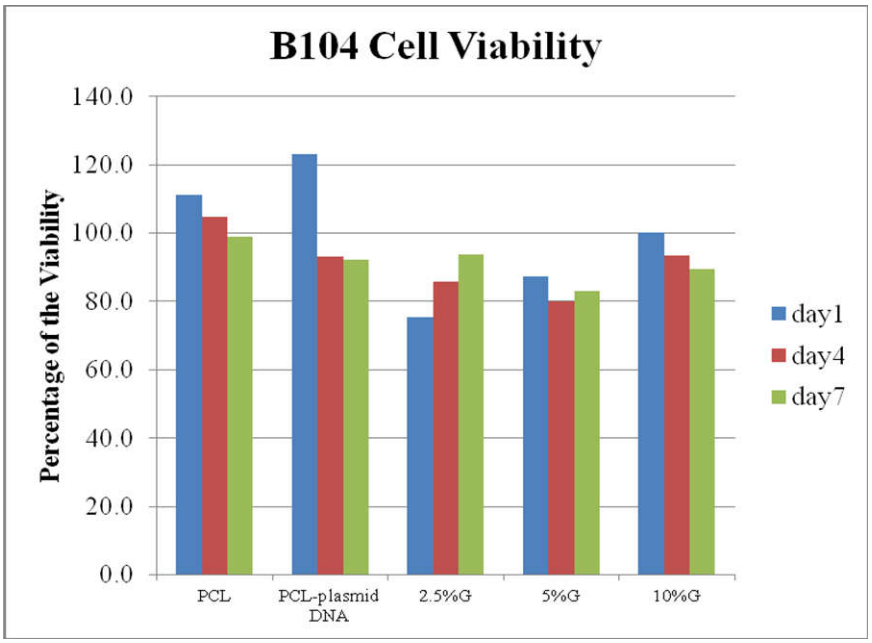


Figure 4.5: Cell viability of B104 neuroblast cells.

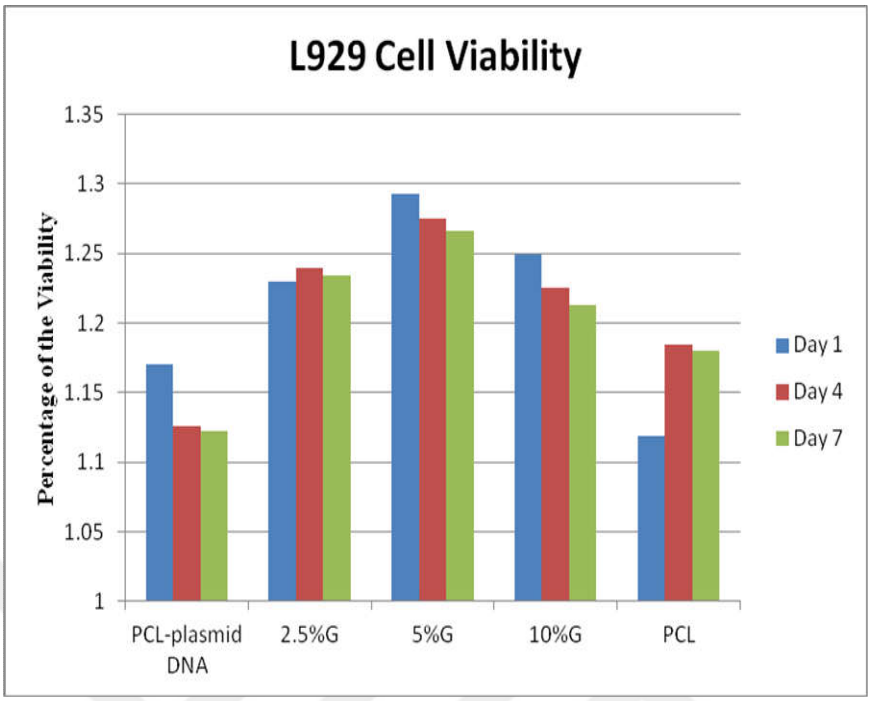


Figure 4.6: Cell viability of L929 fibroblast cells.

Results shows that L929 cells are more susceptible to gentamicin than B104 cells. This result is comparable to that demonstrated by Ozdemir et al., although they demonstrated the cytotoxicity of soft lining material with L929 cells [22]. Furthermore, a study by Lanbeck et al. involved four antibiotics tests with endothelial cells. The antibiotics used for their testing were erythromycin, dicloxacillin, cefuroxime, and benzylpenicillin. Their results show that in a time-related manner, erythromycin and dicloxacillin reduced DNA synthesis in all types of cells; however, cefuroxime and benzylpenicillin did not show any effects [23]. The results in this dissertation study show that the PCL nanofibers in fibroblast cells without gentamicin did not show high cell viability as compared to those with the addition of the antibiotic. The release of gentamicin depends on a variety of factors including the nature of the polymer matrix such as chemical composition of the polymer and water solubility. Also, the distribution of nanofibers, matrix design, capacity of loading, interaction between the drug and the matrix, diameter of

fibers, surface area, and pore structure of fibers are all important factors in gentamicin release.

From Figure 4.6, it can be seen that the addition of gentamicin to PCL nanofibers affects cell viability. When the gentamicin reaches 10 percent in the nanofibers, the nanofibers do not show higher cell viability, which may be because of strong interactions among the PCL, plasmid DNA, and gentamicin, low surface areas, and volumes of the PCL nanofibers. However, as gentamicin in the PCL nanofiber reaches 5%, a higher cell viability show is displayed. From Figure 4.5, it can be seen that there is not much effect on cell viability with the inclusion of gentamicin. This may be because of the cell type or strong interactions between PCL, plasmid DNA, and gentamicin as well as the low surface area and volume size. These results confirm that PCL nanofibers are potential candidates for the wound dressing application. These findings encourage further future work correlating the mechanical properties and porosity of nanofibers.

Lately, various types of nanotechnology and its products have been utilized to increase the efficiencies of new materials and systems. Nevertheless, novel developments also bring uncertainty and danger to human health and the environment. Consequently, the future of nanotechnology depends mainly on public acceptance of the benefits and risks related to the applications of the nanomaterials and devices. Additional studies will be needed to identify the nanosafety concerns of this new class of materials [24].

4.5 Conclusions

PCL nanofibers were successfully produced using electrospinning with the addition of gentamicin and plasmid DNA. SEM images show that the electrospun fibers are truly on a nanoscale and contain the plasmid DNA and gentamicin within the fiber. The UV Elisa Reader confirmed the presence of both plasmid DNA and gentamicin in the PCL nanofiber. Biological tests showed that the gentamicin successfully remained active and was effective with fibroblast

cells as an antimicrobial agent. Fibroblast cells showed that the increase of gentamicin concentration in the nanofibers resulted in better cell viability. PCL nanofibers with the addition of gentamicin showed significant cell viability in the fibroblast cells, compared to those fibers without gentamicin inclusion. These results further confirmed that PCL nanofibers are potential candidates for wound dressing antimicrobial applications.

Acknowledgments

The author wishes to thank Ms. Zheng Song, Li Yongchao, Li Yao, Jimmy Nguyen, and Jianhoa Jiang for their excellent technical assistance.

4.6 References

[1] Fujihara, K., Teo, W. E., Lim, T. C., and Ma, Z. (2005). *An introduction to electrospinning and nanofibers* v. 90. World Scientific, Singapore.

[2] Doshi, J., and Reneker, D. H. (1995). Electrospinning process and applications of electrospun fibers. *Journal of Electrostatics*, *35*(2), 151-160.

[3] Anton, F. (1938). *U.S. Patent No. 2,116,942*. Washington, DC: U.S. Patent and Trademark Office.

[4] Anton, F. (1940). *U.S. Patent No. 2,187,306*. Washington, DC: U.S. Patent and Trademark Office.

[5] Anton, F. (1939). *U.S. Patent No. 2,158,416*. Washington, DC: U.S. Patent and Trademark Office.

[6] Taylor, G. (1969). Electrically driven jets. *Proceedings of the Royal Society of London. A. Mathematical and Physical Sciences*, *313*(1515), 453-475.

[7] Baumgarten, P. K. (1971). Electrostatic spinning of acrylic microfibers. *Journal of Colloid and Interface Science*, *36*(1), 71-79.

[8] Sill, T. J., and von Recum, H. A. (2008). Electrospinning: Applications in drug delivery and tissue engineering. *Biomaterials*, *29*(13), 1989-2006.

[9] Deitzel, J. M., Kleinmeyer, J., Harris, D. E. A., and Beck Tan, N. C. (2001). The effect of processing variables on the morphology of electrospun nanofibers and textiles. *Polymer*, *42*(1), 261-272.

[10] Huang, C., Chen, S., Lai, C., Reneker, D. H., Qiu, H., Ye, Y., and Hou, H. (2006). Electrospun polymer nanofibres with small diameters. *Nanotechnology*, *17*(6), 1558.

[11] Heydarkhan-Hagvall, S., Schenke-Layland, K., Dhanasopon, A. P., Rofail, F., Smith, H., Wu, B. M., Shemin R., Beygui R.E., and MacLellan, W. R. (2008). Three-dimensional electrospun ECM-based hybrid scaffolds for cardiovascular tissue engineering. *Biomaterials*, *29*(19), 2907-2914.

[12] Balguid, A., Mol, A., van Marion, M. H., Bank, R. A., Bouten, C. V., and Baaijens, F. P. (2008). Tailoring fiber diameter in electrospun poly (ε-caprolactone) scaffolds for optimal cellular infiltration in cardiovascular tissue engineering. *Tissue Engineering Part A*, *15*(2), 437-444.

[13] Yang, F., Murugan, R., Wang, S., and Ramakrishna, S. (2005). Electrospinning of nano/micro scale poly (L-lactic acid) aligned fibers and their potential in neural tissue engineering. *Biomaterials*, *26*(15), 2603-2610.

[14] Yoshimoto, H., Shin, Y. M., Terai, H., and Vacanti, J. P. (2003). A biodegradable nanofiber scaffold by electrospinning and its potential for bone tissue engineering. *Biomaterials*, *24*(12), 2077-2082.

[15] Matthews, J. A., Wnek, G. E., Simpson, D. G., and Bowlin, G. L. (2002). Electrospinning of collagen nanofibers. *Biomacromolecules*, *3*(2), 232-238.

[16] Li, Y., Ceylan, M., Shrestha, B., Wang, H., Lu, Q. R., Asmatulu, R., and Yao, L. (2013). Nanofibers Support Oligodendrocyte Precursor Cell Growth and Function as a Neuron-Free Model for Myelination Study. *Biomacromolecules*,15(1),319–326.

[17] McManus, M. C., Boland, E. D., Simpson, D. G., Barnes, C. P., and Bowlin, G. L. (2007). Electrospun fibrinogen: Feasibility as a tissue engineering scaffold in a rat cell culture model. *Journal of Biomedical Materials Research Part A*, *81*(2), 299-309.

[18] Nuraje, N., Khan, W. S., Lei, Y., Ceylan, M., and Asmatulu, R. (2013). Superhydrophobic electrospun nanofibers. *Journal of Materials Chemistry A*,*1*(6), 1929-1946.

[19] Asmatulu, R., Ceylan, M., and Nuraje, N. (2010). Study of superhydrophobic electrospun nanocomposite fibers for energy systems. *Langmuir*, *27*(2), 504-507.

[20] Orozco-Castellanos, L. M., Marcos-Fernández, A., and Martínez-Richa, A. (2011). Hydrolytic degradation of poly (ε-caprolactone) with different end groups and poly (ε-caprolactone-co-γ-butyrolactone): Characterization and kinetics of hydrocortisone delivery. *Polymers for Advanced Technologies*, *22*(4), 430-436.

[21] Boland, E. D., Matthews, J. A., Pawlowski, K. J., Simpson, D. G., Wnek, G. E., and Bowlin, G. L. (2004). Electrospinning collagen and elastin: Preliminary vascular tissue engineering. *Frontiers in Bioscience: A Journal and Virtual Library*,*9*, 1422-1432.

[22] Ozdemir, K. G., Yılmaz, H., and Yılmaz, S. (2009). In vitro evaluation of cytotoxicity of soft lining materials on L929 cells by MTT assay. *Journal of Biomedical Materials Research Part B: Applied Biomaterials*, *90*(1), 82-86.

[23] Lanbeck, P., and Paulsen, O. (2001). Short-Term Effects of Four Antibiotics on DNA Synthesis in Endothelial Cells. *Pharmacology and Toxicology*, *88*(4), 204-208.

[24] Asmatulu, R. (Ed.). (2013). *Nanotechnology Safety*. Elsevier, San Diego, CA.

CHAPTER 5

NANOFIBER SUPPORT OF OLIGODENDROCYTE PRECURSOR CELL GROWTH AND FUNCTION AS A NEURON-FREE MODEL FOR MYELINATION STUDY

5.1 Abstract

Nanofiber-based scaffolds may simultaneously provide immediate contact guidance for neural regeneration and act as a vehicle for therapeutic cell delivery to enhance axonal myelination. Furthermore, electrospun fibers can serve as a neuron-free model to study the myelination of oligodendrocytes. In the current study, nanofibers were produced using a polycaprolactone (PCL) and gelatin co-polymer. The ratio of the gelatin component in the fibers was confirmed by energy dispersive x-ray spectroscopy (EDS). PCL has a hydrophobic property, and the addition of gelatin into the electrospun fiber production decreased the contact angle. It was shown that both PCL nanofibers as well as PCL and gelatin co-polymer nanofibers can support oligodendrocyte precursor cell (OPC) growth and differentiation. OPCs maintained their phenotype and viability on nanofibers and were induced to differentiate into oligodendrocytes. The differentiated oligodendrocytes extended their processes along the nanofibers and ensheathed the nanofibers. Oligodendrocytes (OLs) formed significantly more myelinated segments on the PCL and gelatin co-polymer electrospun fiber compared to PCL fibers alone.

Keywords: Oligodendrocyte precursor cells, Nanofibers, Myelination, Differentiation

5.2 Introduction

The repair of a harmed spinal cord presents a huge medicinal challenge. The advancement of biomaterial development has offered a promising result for the repair of injured neural tissue. In neural recovery investigations using animal models, the transected or incompletely injured spinal cord has been recreated by filling the imperfection with hydrogels

[1–3]. The contact interceded direction given by biomaterial scaffolds may control axonal regrowth over the site of harm into the distal host tissue and possibly could bring about functional recuperation.

OLs experience both necrosis and apoptosis not long after spinal cord injury (SCI). Because of demyelination, OPCs are enlisted from gray and white matter and moved to the injury to myelinate the recreated axon; this procedure is constrained by the amount of endogenous OPCs [4, 5]. The focal transfer of OPCs provides another path to axonal myelination. A biomaterial scaffold can concurrently intercede the contact control of neural tissue progress and act as a vehicle for therapeutic cell transfer to improve axonal myelination [6–9]. The nanofibers and consistent porous structure produced by electrospinning may improve neural reconstruction due to the nanofibers mimicking the extracellular matrix and providing guidance to axonal growth at nano-levels. Past studies have indicated that electrospun aligned fibers can manage neurite growth in vitro [10–12] and could be useful in spinal cord and peripheral nerve regrowth [13–16]. PCL has been used as a biomaterial scaffold for neural reconstruction on account of its biodegradable and biocompatible properties [15, 16]. PCL nanofibers can be produced by electrospinning, and their biocompatibility could be improved by adding extracellular protein to the electrospun fibers. Gelatin, a heterogeneous mixture of polypeptides structured by thermal denaturation of collagen, retains the biological properties of collagen and together with PCL has been studied to produce electrospun fibers [17]. However, none has studied whether PCL nanofibers can support oligodendrocyte precursor cells.

Myelination is a serious step in neural reconstruction. The axonal signaling to oligodendrocytes and the close contact between the axons and oligodendrocytes are difficult processes that direct myelination formation of the reconstructed axons [18–20]. Lately it was

discovered that oligodendrocytes can myelinate electrospun fibers of artificial polymers, and the fibers can serve as a simplified without-neuron model for myelination study [21, 22]. The capacity of a specific biological molecule in the myelination procedure might be studied by joining the molecules into the synthesized fibers. In the present study, PCL nanofibers and PCL-gelatin co-polymer nanofibers were produced. First, the growth and distinction of OPCs on both electrospun PCL nanofibers and PCL-gelatin co-polymer nanofibers were examined. Second, the capacity of gelatin as a biological molecule on oligodendrocyte myelination for nanofibers was examined. This work has provided new understanding to the examination of biological molecules in axonal myelination.

5.3 Materials and Methods

5.3.1 Generation of PCL and Gelatin Electrospun Nanofibers

PCL (molecular weight of 70,000, Scientific Polymer Products, Inc., New York) nanofibers were generated by electrospinning a PCL solution (35 wt% in acetonitrile). To fabricate the PCL-gelatin nanofibers, gelatin (Sigma-Aldrich, St. Louis, MO) and PCL (mixing ratio: 50 wt% of gelatin to PCL) in a mixture of acetic acid and acetonitrile (50:50 (v/v)) were used to generate fibers by electrospinning. The solvent-to-solute ratio for the mixtures was 85:15 by weight. Fibers were collected on a stationary collector placed 20–30 cm from the infusion syringe at an infusion speed of 2 ml/hour at 20–25 kV. To study the growth and differentiation of the OPCs, films of dense fibers were electrospun onto aluminum foil or round glass coverslips. Loose nanofibers were also fabricated on coverslips to study the myelination of the differentiated OPCs to the fibers.

5.3.2 Contact Angle of Nanofibers.

The contact angle values of the electrospun nanofibers were measured with an optical contact angle goniometer (CAM 100, KSV Instruments Ltd., Helsinki, Finland). This compact video-based instrument measures contact angles between 1º and 180º with an accuracy of ±1º. Computer software provided by KSV Instruments Ltd. precisely recorded and measured the contact angles and also took pictures of the measured contact angle values on the surfaces of the nanofibers.

5.3.3 Isolation and Culture of OPCs on Electrospun Nanofibers

The process for confining OPCs from neonatal rats was approved by the Institutional Animal Care and Use Committee (IACUC) and finished at Wichita State University, Wichita, KS. The culturing of OPC cells was executed as reported previously [23]. In short, cerebral cortexes were detached from the brains of neonatal rats (postnatal day P1–2 rats) after they were sacrificed. The cortex tissues were triturated tenderly through a 5 ml syringe with needle. The tissue suspension was passed through a 70-mm nylon cell strainer (BD Falcon™, Durham, NC), and the flow through was gathered with a 50-ml cylindrical tube. The cells were cultured for about seven days. The OPCs were then confined from the mixed cell culture layer by mechanically shaking the cell culture flasks for about 24 hours in an incubator at 37ºC. The collected OPCs were cultured in an OPC growth medium (DMEM, Lifetechnologies™, Grand Island, NY) with Sato media (DMEM, 100 µg/ml transferrin, 100 µg/ml BSA, 0.2 µm progesterone, 16 µg/ml putrescine, 40 ng/ml sodium selenite [sigma-Aldrich, St. Louis, MO]), 1% penicillin-streptomycin, 2 mM L-glutamine (Lifetechnologies™, Grand Island, NY), 5 µg/ml insulin, 10 nM D-biotin, 1 mM sodium pyruvate, 5 µg/ml N-acetyl cysteine (Sigma-Aldrich, St. Louis, MO), trace elements B (1x, Mediatech Inc., Manassas, VA), 10 ng/ml PDGF, and 10

ng/ml bFGF (Peprotech, Rocky Hill, NJ). Next the OPCs were grown on the electrospun nanofibers.

5.3.4 Growth of OPCs on Electrospun Nanofibers and Cell Viability Assay

To study their growth and distinction on electrospun nanofibers, OPCs were grown in cell culture wells or the films of thick electrospun nanofibers set in 24-well plates with a cell quantity of 15,000 cells/well. The cells were either cultured in OPC growth medium or oligodendrocyte growth medium (OL medium) for OPC distinction (DMEM with Sato media, 1% penicillin-streptomycin, 2 mM L-glutamine, 5 µg/ml insulin, 10 nM D-biotin, 1 mM sodium pyruvate, 5 µg/ml N-acetyl cysteine, trace components B, 15 nM triiodothyronine, and 10 ng/ml CNTF [Peprotech, Rocky Hill, NJ]). After 4 days, the cells were set with 4% paraformaldehyde in phosphate-buffered saline (PBS) solution for the immunostaining analysis.

The viability and reproduction of OPCs, which were seeded on the electrospun nanofibers, were examined by following their metabolic activity utilizing the alamarBlue analysis (Pierce Biotechnology, Rockford, IL). To perform this test, the electrospun nanofibers were cut into round shapes and put in 24-well plates to cover the base of the wells. The cells, with a quantity of 25,000 cells/well, were cultured for 4 days. After that they were incubated with OPC culture medium holding 10% (v/v) alamarBlue reagent for 2 hr. Absorbance was measured at a wavelength of 570 nm and 600 nm with a microplate reader (Synergy Mx Monochromator-Based Multi-Mode Microplate Reader, Winooski, VT).

5.3.5 Myelination Study of Oligodendrocytes for Nanofibers

In this investigation of the myelination of OPCs for electrospun fibers, coverslips with PCL or PCL-gelatin nanofibers were placed in 24-well plates for the culture of OPCs. The OPCs (20,000 cells/well) were seeded on these coverslips for 3 or 8 days. The medium for the

myelination study was reported previously [22, 23]. In short, the myelination medium consisted of DMEM containing 1 × B27, 1 × N2 (Lifetechnologies™, Grand Island, NY), 5 μg/ml of N-acetyl cysteine (NAC, Sigma-Aldrich, St. Louis, MO), and 5 μM of forskolin (Minneapolis, MN). The cell culture medium was changed every 3 days. Following 3 or 8 days of culturing, the cultured cells on the electrospun fibers were set with 4% paraformaldehyde in a PBS solution for immunostaining.

5.3.6 Immunocytochemistry

The phenotype of the well-cultured OPCs was resolute anti-A2B5 immunizer (produced in Dr Q. Richard Lu's laboratory, Cincinnati Children's Center) and anti-PDGFR-α antibody (Santa Cruz Biotechnology, Inc., Dallas, TX). The distinction OPCs were named with anti-O4 antibody (Dr Q. Richard Lu's laboratory, Cincinnati Children's Medical Center). The myelination of OPCs for the electrospun fibers was marked with an anti-myelin basic protein (MBP) antibody (Millipore, Billerica, MA). Pictures were taken with a Zeiss Axio Observer microscope (Carl Zeiss Microscopy, LLC, Thornwood, NY).

5.3.7 Scanning Electron Microscopy for Nanofibers

Nanofiber images were taken by scanning electron microscopy (SEM) with a model of ZEISS SIGMA VP and EDS (Carl Zeiss Microscopy, LLC, Thornwood, NY). These images were used to measure the fiber diameter with NIH ImageJ software (National Institutes of Health, Bethesda, MD). To quantify the fiber diameter, 150 fibers from each type of fiber were measured. The nanofibers with oligodendrocytes were washed with PBS and placed in 2% glutaraldehyde-PBS for 2 hr. The samples were then dried out with evaluated ethanol and hexamethyldisilazane. The frameworks were air-dried and thusly covered with gold. At that

point, the oligodendrocyte morphology and ensheathed nanofibers were investigated utilizing the SEM pictures.

5.3.8 Energy Dispersive X-Ray Spectroscopy for Nanofibers

EDS was used to analyze the composition of the nanofibers. An electron beam that scans across the surface during SEM causes shell transitions that result in the emission of an x-ray. Detection and measurement of the energy from the emitted x-ray permit qualitative and quantitative elemental analyses. Gelatin is a heterogeneous mixture of polypeptides formed by thermal denaturation of collagen. These polypeptides primarily contain glycine, proline, and 4-hydroxyproline residues. Polycaprolactone is a biodegradable polyester with the molecular formula $C_6H_{10}O_2$. PCL contains more carbon per oxygen than gelatin. An increase of PCL in nanofibers would result in an increase in carbon.

5.3.9 Statistical Analysis

Statistical analysis was conducted using a two-tailed Student's t-test. A p value of 0.05 was considered to be statistically significant. Data are expressed as means ± standard deviation.

5.4 Results

5.4.1 Characterization of Electrospun Fibers of PCL and Gelatin Co-Polymer

SEM images of films of dense PCL fibers and PCL-gelatin fibers are shown in Figures 5.1A and 5.1B. The fiber diameters for the PCL fibers and PCL-gelatin fibers are 163.5 ± 126.8 nm and 214.9 ± 58.7 nm, respectively (Figure 5.1C). EDS assay was used to analyze the composition of the PCL-gelatin nanofibers. Carbon is the major element in both gelatin and PCL. The carbon atomic ratio and the carbon weight ratio of gelatin fibers, PCL fibers, and PCL-gelatin fibers were measured. The carbon atomic ratio and carbon weight ratio of PCL-gelatin fibers are 60.2 ± 0.9% and 54 2 ± 0.7%, respectively, which are close to the mean ratio of PCL

fibers (69.7 ± 1.0% and 59.7 ± 1.1%, respectively) and gelatin fibers (50.0 ± 3.5% and 38.4 ± 2.3%, respectively) (Figure 5.1D).

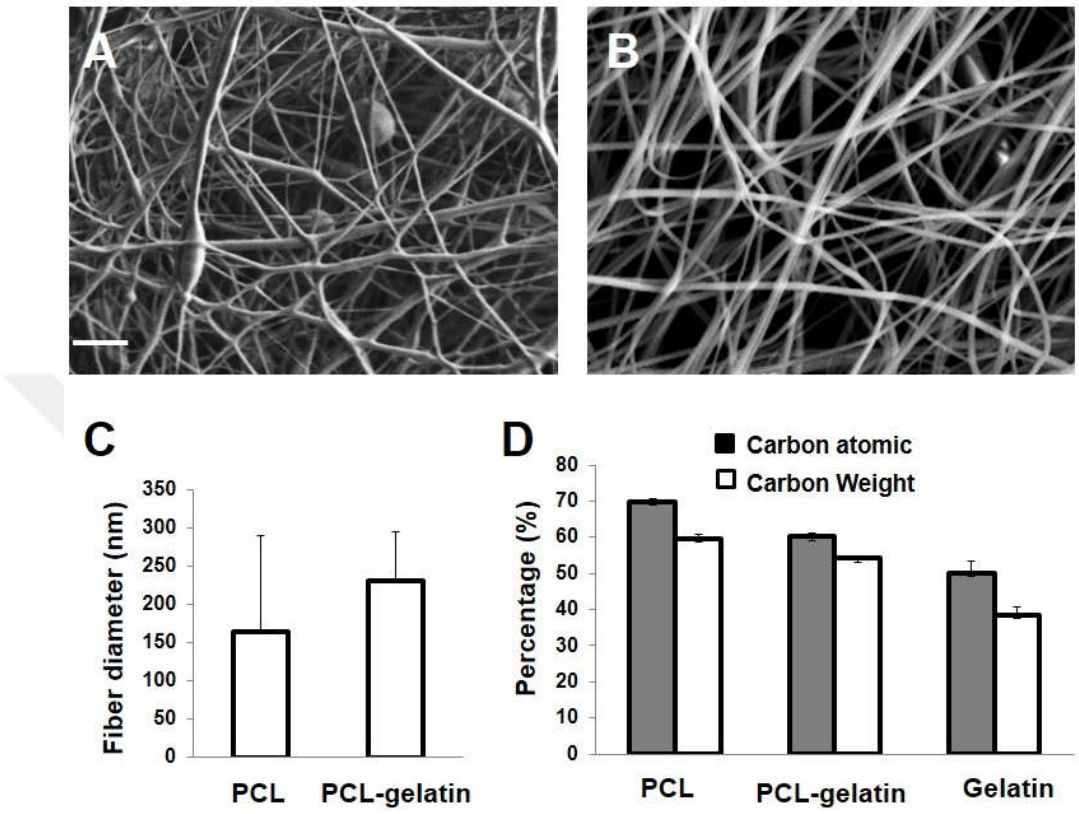


Figure 5.1: Characterization of electrospun fibers: (A) SEM image of electrospun PCL fibers, (B) SEM image of PCL-gelatin fibers, (C) quantification of fiber diameter, and (D) carbon atomic and carbon weight ratio in nanofibers. Scale bar: 2 μm.

The contact angles of the fiber surface were measured to show the hydrophilicity of the fibers. Gelatin in the electrospun fibers decreased the surface contact angle. Contact angles for the PCL fibers, PCL-gelatin fibers, and gelatin fibers are 133.5º ± 2.3º, 78.6º ± 3.1º, and 63.3º ± 2.2º, respectively. The decrease in contact angle indicates the increase of hydrophilicity of the electrospun fibers. Contact angle results are shown in Figure 5.2.

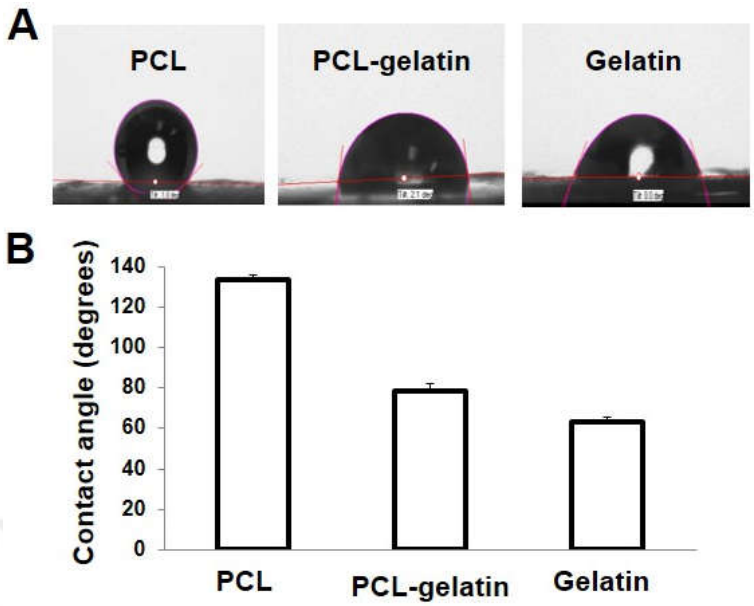


Figure 5.2: Measurement of contact angle of PCL nanofibers, PCL-gelatin nanofibers, and gelatin nanofibers: (A) droplet profiles and contact angle evaluation on different films of dense PCL nanofibers, PCL-gelatin nanofibers, and gelatin nanofibers; (B) quantification of contact angle of PCL nanofibers, PCL-gelatin nanofibers, and gelatin nanofibers.

5.4.2 Electrospun Nanofibers Support OPCs Growth and Differentiation

OPCs were seeded on the electrospun fibers and cultured with OPC culture medium for 4 days. The OPCs grown on electrospun fibers were marked with anti-A2B5 and anti-PDGFα antibodies. Immuno-labeling demonstrated that the OPCs grown on both PCL electrospun fibers and PCL-gelatin fibers expressed A2B5 and PDGFRα (Figure 5.3). OPCs were additionally seeded on the electrospun fibers and cultured with OL medium for 4 days. Immnostaining with anti-O4 immunizer on the fibers indicated that OPCs distinction into oligodendrocytes and created different processes (Figures 5.3F and 5.3J).

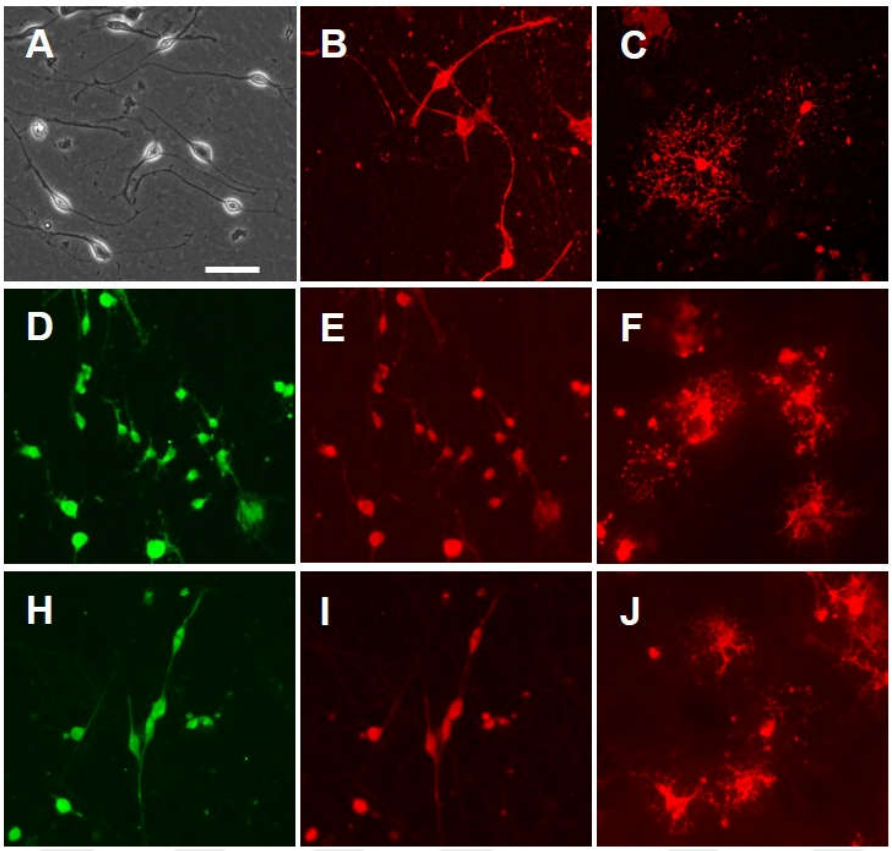


Figure 5.3: Growth and differentiation of OPCs on films of dense electrospun nanofibers: Growth of OPCs on tissue culture plate (A, B), PCL nanofibers (D, E), and PCL-gelatin nanofibers (H, I). OPCs differentiated into OL cells on tissue culture plate (C), PCL nanofibers (F), and PCL-gelatin nanofibers (J). OPCs labeled with anti-PDGFα antibody (D, H) or anti-A2B5 antibody (B, E, I). OL cells labeled with anti-O4 antibody (C, F, J). Scale bar: 100 μm. Experiment performed and data collected by Dr. Yongchao and Dr.Yao.

The alamarBlue analysis demonstrated that OPCs proliferated on both PCL nanofibers and PCL-gelatin nanofibers; no critical change in OPC proliferation was found. The decrease of alamarBlue reagent for OPCs grown on PCL, PCL-gelatin electrospun fibers, and tissue culture plates is 47.9 ± 3.4%, 42.6 ± 5.6%, and 54.9 ± 6.2%, individually (Figure 5.4).

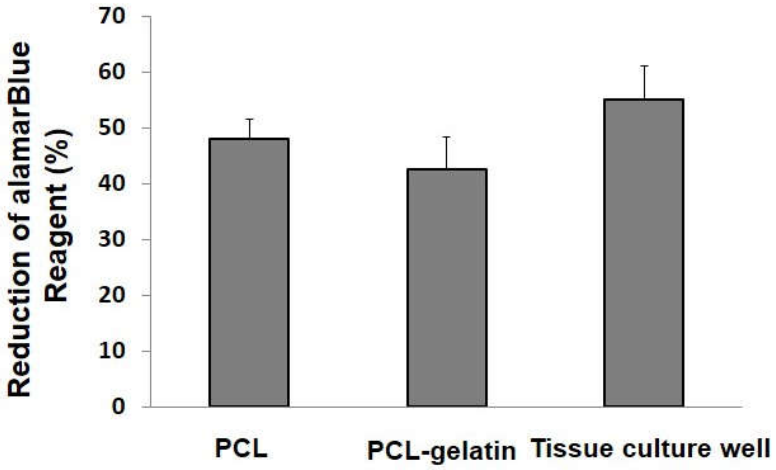


Figure 5.4: Cell viability assay (alamarBlue) of OPCs growing on films of dense electrospun PCL nanofibers, PCL-gelatin nanofibers, and gelatin nanofibers. Experiment performed and data collected by Dr. Yongchao, Dr.Yao, and Bikesh Shrestha.

5.4.3 Differentiated Oligodendrocyte Ensheathed Nanofibers

To study the capacity of OPC distinction and wrapping of the electrospun fibers, OPCs were grown on coverslips with PCL and PCL-gelatin electrospun fibers (Figures 5.5 and 5.6). The PCL and PCL-gelatin electrospun fibers were 731 ± 198.9 nm and 801.2 ± 188.4 nm, respectively (Figure 5.5). To study the myelin structure around the individual electrospun fibers, PCL and PCL-gelatin fibers were electrospun on the coverslips using the electrospinning method. This time, fibers were not dense on coverslips. The coverslips with electrospun fibers were set in 24-well plates, and the OPCs were seeded on the nanofibers with a cell quantity of 20,000 cells/well.

After the OPCs were cultured on PCL and PCL-gelatin electrospun fibers with myelination medium for 3 days, with short process PDGFα positive cells grown, some of them were associated with fibers, as it can be seen in Figure 5.5. After the OPCs were cultured on PCL and PCL-gelatin fibers with myelination medium for 8 days, the OPCs distinction and created numerous processes. For both PCL and PCL-gelatin electrospun fibers, distintive OPCs

wrapping the nanofibers were investigated (Figure 5.6). The OPCs shaped much more myelin sections for PCL-gelatin fibers than those for PCL fibers. The percentages of MBP positive cells wrapping fiber and myelin sections for PCL-gelatin fibers are 70.7 ± 8.8% and 48.9 ± 10.9%, respectively, which are much higher than those for PCL fibers alone (27.7 ± 7.2% and 15.4 ± 3.2, $p < 0.01$). SEM pictures indicate the morphology of oligodendrocytes and the myelination formation all around the electrospun fibers. Oligodendrocytes expanded various techniques on the coverslips along the electrospun fibers (Figure 5.7A). Oligodendrocytes were wrapped around the electrospun fibers. The ensheathed and not-ensheathed electrospun fibers are shown in Figure 5.7.

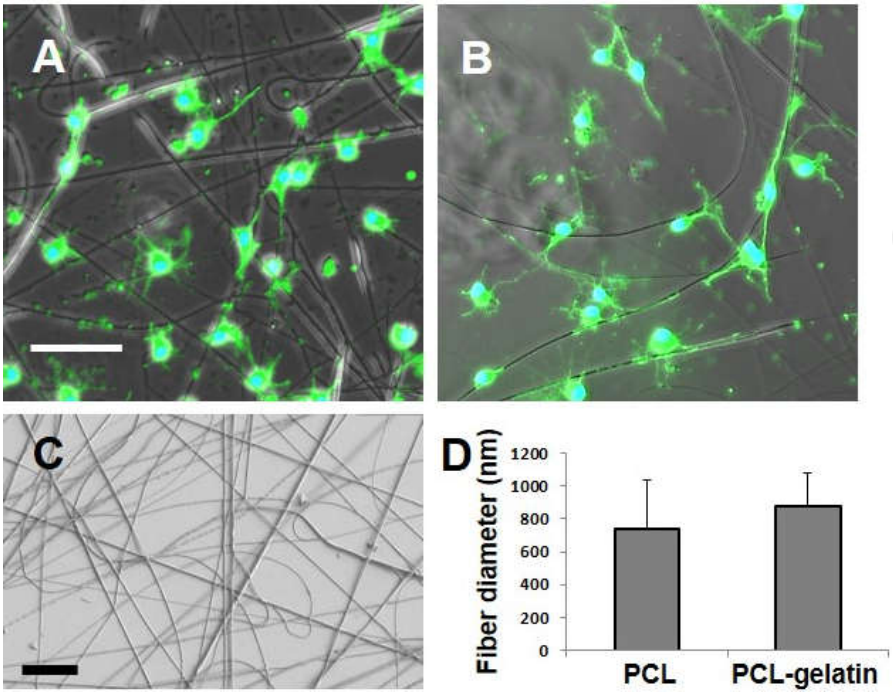


Figure 5.5: Growth of OPCs on coverslips with electrospun nanofibers. After culturing for 3 days, OPCs developed short processes on coverslips with PCL nanofibers (A) and PCL-gelatin nanofibers (B). OPCs were labeled with anti-PDGFα antibody. Some cells were associated with nanofibers. Scale bar: 100 μm. (C) SEM images of PCL-gelatin nanofibers. Scale bar: 20 μm. (D) Analysis of nanofiber diameter. Experiment performed and data collected by Dr. Yongchao and Dr.Yao).

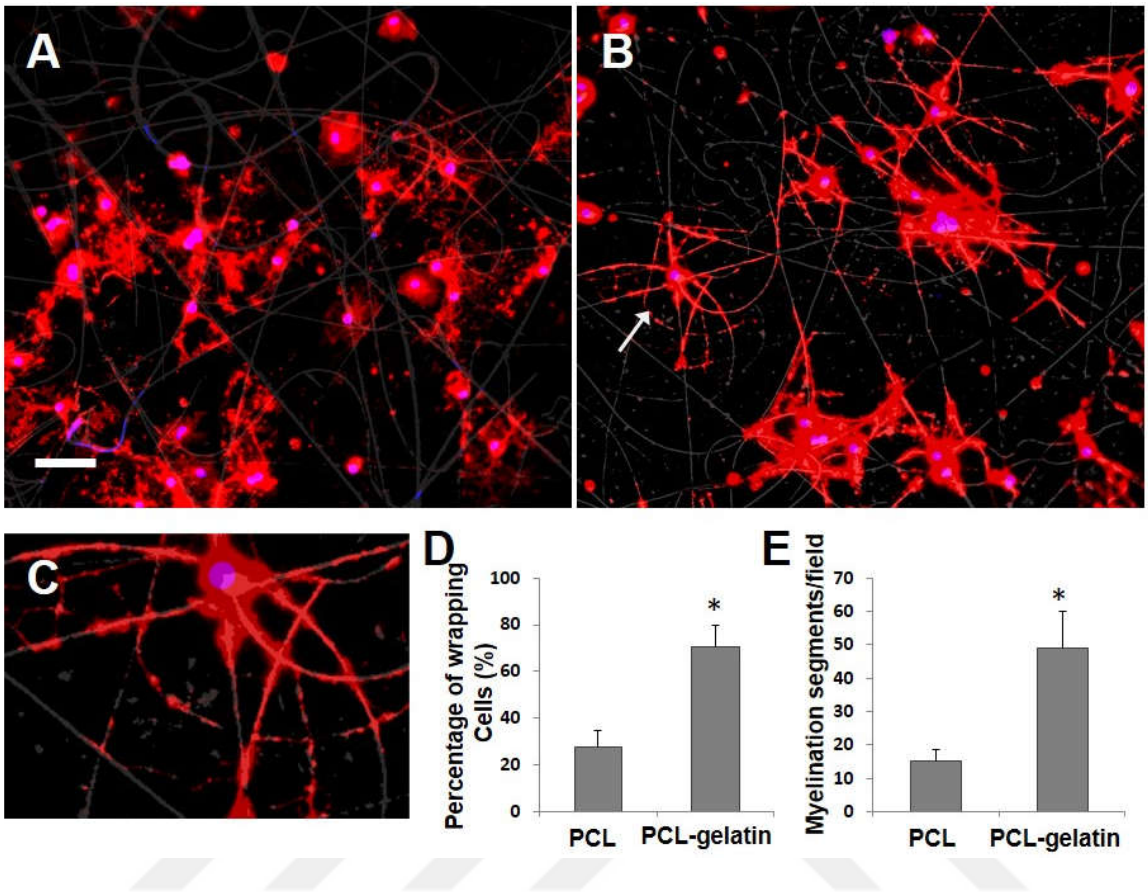


Figure 5.6: Differentiated OPCs ensheath nanofibers. (A) Differentiated OPCs ensheath PCL fibers. (B) Differentiated OPCs ensheath PCL-gelatin fibers. Scale bar: 100 μm. (C) Magnified image of myelinated PCL-gelatin nanofibers, as indicated by arrow in (B). Cells were labeled with anti-MBP antibody. (D) Analysis of percentage of cells wrapping nanofibers (* indicates significant difference compared with differentiated OPCs myelinate PCL nanofibers, $p < 0.01$). (E) Analysis of percentage of myelinated nanofiber segments (* indicates significant difference compared with myelinated segments of PCL nanofibers, $p < 0.01$). Experiment was performed and data collected by Dr. Yongchao and Dr.Yao.

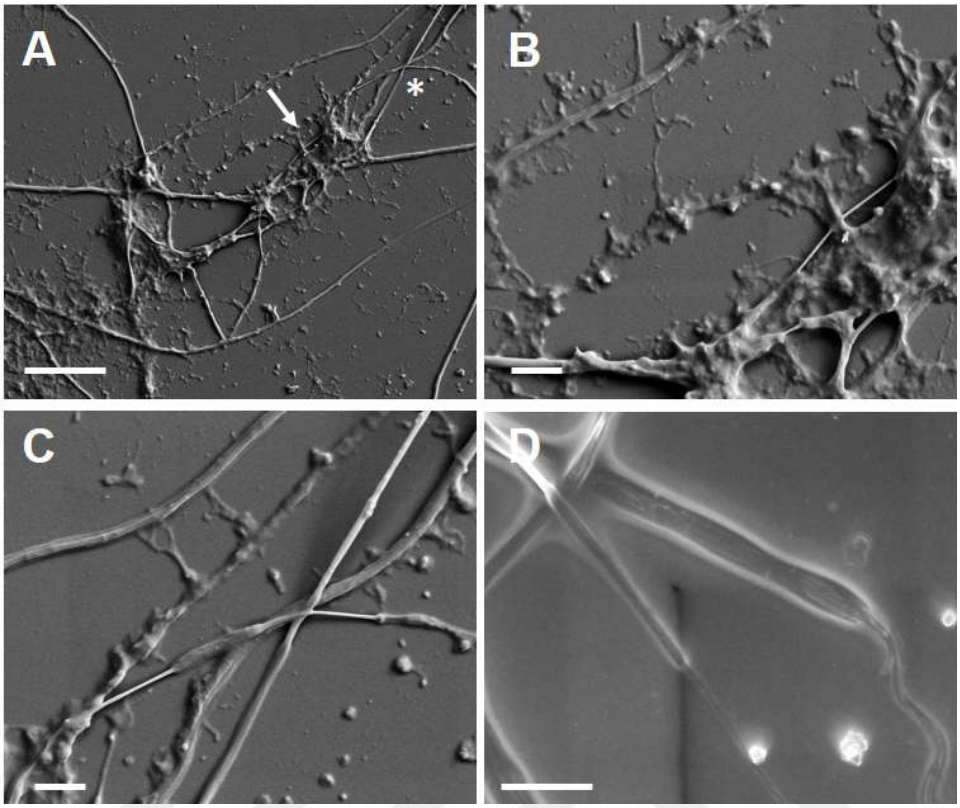


Figure 5.7: SEM images showing differentiated OPC-ensheathed PCL-gelatin nanofibers. (A) Differentiated OPCs extend multiple processes. Scale bar: 10 µm. (B) Magnified image showing myelinated and unmyelinated fiber segments, as indicated by arrow in (A). Scale bar: 2 µm. (C) Magnified image showing myelinated and unmyelinated fiber segments, as indicated by asterisk in (A). Scale bar: 2 µm. (D) Magnified images show end of myelinated fiber segments. Scale bar: 2 µm. Experiment was performed and data collected by Dr. Yongchao and Dr.Yao.

5.5 Discussion

In this study, PCL and PCL-gelatin electrospun fibers were fabricated. The addition of gelatin in the fibers was affirmed by EDS testing. To manufacture fibers of a PCL and gelatin co-polymer, PCL and gelatin were dissolved in acetonitrile and acetic acid. Acetic acid was used here to dissolve the gelatin. It was found that producing fibers this way is not toxic to the OPCs. The growth OPCs on the electrospun fibers were marked with OPC-particular antibodies (anti-A2B5 and anti-PDGFα), and the OPCs were changed into oligodendrocytes on the fibers. SEM images were used to determine fiber diameters. Similar diameters of PCL and PCL-gelatin

electrospun fibers were fabricated in order to perform a cell growth and myelination study. PCL and PCL-gelatin electrospun fibers did not demonstrate much difference in the cell viability of OPCs.

PCL is a biocompatible and biodegradable material used for several applications including tissue engineering. PCL fibers have a hydrophobic property, which is confirmed by this study. However, past studies have suggested that the surface is unfavorable for cell growth [24]. On the other hand, the addition of gelatin increases the hydrophilicity in PCL-gelatin electrospun fibers. As it can be seen from Figure 5.2 in the contact angle study, it is confirmed that the addition of gelatin decreases the contact angle. The cell viability of OPCs did not exhibit much difference between PCL and PCL-gelatin electrospun fibers, which suggests that the hydrophilicity property of the nanofibers does not influence the growth and differentiation of OPCs. Differentiated OPC-wrapped electrospun fibers after 8 days of cell culture in the myelination medium were also investigated. This study is different from previous studies [22, 23], in that the differentiated OPCs wrapped the fibers without a coating of poly-D,L-ornithine (Sigma-Aldrich, St. Louis, MO). Furthermore, PCL-gelatin fibers had a higher number of myelination segments and number of cells that wrapped the fibers compared to the PCL fiber itself. Outcomes suggest that the incorporation of biological molecules to the artificial polymer fibers can increase myelination formation by OPCs.

Numerous polymers are available for research purposes, one of which is polystyrene, which is biocompatible and usually used to treat tissue cultures for cell attachment and growth. Previous studies have demonstrated myelination structuring on polystyrene fibers by cultured OPCs [21, 22]. However, polystyrene biodegradation is very slow. On the other hand, PCL has been approved by the Food and Drug Administration (FDA) in applications used in the human

body as implantable material. PCL has likewise demonstrated important potential in the application of neural reproduction. Furthermore, the biological application of PCL might be improved by adding biomacromolecules in PCL to create implantable scaffolds with the co-polymer. In this study, PCL-gelatin electrospun fibers were produced, and their capacity to support OPCs growth and differentiation was observed. Also researched was the myelination formation of oligodendrocytes on these fibers as a without-neuron model. To study myelination on the fibers, PCL and PCL-gelatin electrospun fibers were produced with average diameters of 0.73 μm and 0.8 μm, respectively. The differentiated OPC-wrapped electrospun nanofibers were investigated. The rate of cells that formed myelin sections around the fibers was around 70%. A previous study demonstrated that the differentiated OPCs myelinated the electrospun polystyrene nanofibers, and around 60% MBP positive cells wrapped the polystyrene nanofibers (0.4–0.8μm) [22]. The rate of cells making myelin segments around the nanofibers was about 30% in this study. It is recommended that the composition and coating of fibers can affect the efficiency of OPC differentiation and fiber wrapping. Electrospun fibers may serve a simple model to examine the myelination of different molecules in axonal regeneration.

5.6 Conclusion

Nanofibers utilizing a PCL and gelatin co-polymer were produced. The proportion of PCL and gelatin parts in the fibers was affirmed by EDS testing. It was demonstrated that gelatin in the PCL-gelatin co-polymer for electrospinning diminished the fiber contact angle, and as a result, hydrophilicity of the electrospun fibers increased. Additionally, it was demonstrated that both PCL and PCL-gelatin electrospun fibers can support OPC growth and differentiation. The OPCs kept up their phenotype and viability on both PCL and PCL-gelatin fibers and could separate into oligodendrocytes when well cultured with an OL medium. The differentiated OPCs

associated with the electrospun fibers and structured myelin along the fibers. PCL-gelatin fibers had more differentiated OPCs formed in the myelinated area than PCL fibers alone. This study may open up new possibilities for repairing repair harmed spinal cords and different nerves.

Acknowledgements

This work was supported by National Center for Research Resources (P20 RR016475) and the National Institute of General Medical Sciences (P20 GM103418) from the National Institutes of Health.

5.7 References

[1] Spilker, M. H., Yannas, I. V., Kostyk, S. K., Norregaard, T. V., Hsu, H. P., and Spector, M. (2001). The effects of tubulation on healing and scar formation after transection of the adult rat spinal cord. *Restorative Neurology and Neuroscience*,*18*(1), 23-38.

[2] King, V. R., Alovskaya, A., Wei, D. Y., Brown, R. A., and Priestley, J. V. (2010). The use of injectable forms of fibrin and fibronectin to support axonal ingrowth after spinal cord injury. *Biomaterials*, *31*(15), 4447-4456.

[3] Li, X., Yang, Z., Zhang, A., Wang, T., and Chen, W. (2009). Repair of thoracic spinal cord injury by chitosan tube implantation in adult rats. *Biomaterials*,*30*(6), 1121-1132.

[4] Almad, A., Sahinkaya, F. R., and McTigue, D. M. (2011). Oligodendrocyte fate after spinal cord injury. *Neurotherapeutics*, *8*(2), 262-273.

[5] Wang, S., Sdrulla, A. D., diSibio, G., Bush, G., Nofziger, D., Hicks, C., Weinmaster, G., and Barres, B. A. (1998). Notch receptor activation inhibits oligodendrocyte differentiation. *Neuron*, *21*(1), 63-75.

[6] Olson, H. E., Rooney, G. E., Gross, L., Nesbitt, J. J., Galvin, K. E., Knight, A., Chen, B., Yaszemski, M. J., and Windebank, A. J. (2009). Neural stem cell–and Schwann cell–loaded biodegradable polymer scaffolds support axonal regeneration in the transected spinal cord. *Tissue Engineering Part A*, *15*(7), 1797-1805.

[7] Teng, Y. D., Choi, H., Onario, R. C., Zhu, S., Desilets, F. C., Lan, S., Woodard, E. J., Snyder, E. Y., Eichler, M. E., and Friedlander, R. M. (2004). Minocycline inhibits contusion-triggered mitochondrial cytochrome c release and mitigates functional deficits after spinal cord injury. *Proceedings of the National Academy of Sciences of the United States of America*, *101*(9), 3071-3076.

[8] Nomura, H., Zahir, T., Kim, H., Katayama, Y., Kulbatski, I., Morshead, C. M., Shoichet, M. S., and Tator, C. H. (2008). Extramedullary chitosan channels promote survival of transplanted neural stem and progenitor cells and create a tissue bridge after complete spinal cord transection. *Tissue Engineering Part A*, *14*(5), 649-665.

[9] Wang, J. M., Zeng, Y. S., Wu, J. L., Li, Y., and Teng, Y. D. (2011). Cograft of neural stem cells and schwann cells overexpressing TrkC and neurotrophin-3 respectively after rat spinal cord transection. *Biomaterials*, *32*(30), 7454-7468.

[10] Yao, L., O'Brien, N., Windebank, A., and Pandit, A. (2009). Orienting neurite growth in electrospun fibrous neural conduits. *Journal of Biomedical Materials Research Part B: Applied Biomaterials*, *90*(2), 483-491.

[11] Zander, N. E., Orlicki, J. A., Rawlett, A. M., and Beebe, T. P. (2010). Surface-modified nanofibrous biomaterial bridge for the enhancement and control of neurite outgrowth. *Biointerphases*, *5*(4), 149-158.

[12] Prabhakaran, M. P., Venugopal, J. R., Chyan, T. T., Hai, L. B., Chan, C. K., Lim, A. Y., and Ramakrishna, S. (2008). Electrospun biocomposite nanofibrous scaffolds for neural tissue engineering. *Tissue Engineering Part A*, *14*(11), 1787-1797.

[13] Zamani, F., Amani-Tehran, M., Latifi, M., Shokrgozar, M. A., and Zaminy, A. (2014). Promotion of spinal cord axon regeneration by 3D nanofibrous core–sheath scaffolds. *Journal of Biomedical Materials Research Part A*, *102*(2), 506-513.

[14] Wang, W., Itoh, S., Konno, K., Kikkawa, T., Ichinose, S., Sakai, K., Ohkuma, T., and Watabe, K. (2009). Effects of Schwann cell alignment along the oriented electrospun chitosan nanofibers on nerve regeneration. *Journal of Biomedical Materials Research Part A*, *91*(4), 994-1005.

[15] Neal, R. A., Tholpady, S. S., Foley, P. L., Swami, N., Ogle, R. C., and Botchwey, E. A. (2012). Alignment and composition of laminin–polycaprolactone nanofiber blends enhance peripheral nerve regeneration. *Journal of Biomedical Materials Research Part A*, *100*(2), 406-423.

[16] Yu, W., Zhao, W., Zhu, C., Zhang, X., Ye, D., Zhang, W., Zhou, Y., Jiang, X., and Zhang, Z. (2011). Sciatic nerve regeneration in rats by a promising electrospun collagen/poly (ε-caprolactone) nerve conduit with tailored degradation rate. *BMC Neuroscience*, *12*(1), 68.

[17] Alvarez-Perez, M. A., Guarino, V., Cirillo, V., and Ambrosio, L. (2010). Influence of gelatin cues in PCL electrospun membranes on nerve outgrowth. *Biomacromolecules*, *11*(9), 2238-2246.

[18] Chan, J. R., Watkins, T. A., Cosgaya, J. M., Zhang, C., Chen, L., Reichardt, L. F., Shooter, E. M., and Barres, B. A. (2004). NGF controls axonal receptivity to myelination by Schwann cells or oligodendrocytes. *Neuron*, *43*(2), 183-191.

[19] Wang, H., Tewari, A., Einheber, S., Salzer, J. L., and Melendez-Vasquez, C. V. (2008). Myosin II has distinct functions in PNS and CNS myelin sheath formation. *The Journal of Cell Biology*, *182*(6), 1171-1184.

[20] O'Meara, R. W., Ryan, S. D., Colognato, H., and Kothary, R. (2011). Derivation of enriched oligodendrocyte cultures and oligodendrocyte/neuron myelinating co-cultures from post-natal murine tissues. *Journal of Visualized Experiments*, 54.

[21] Lee, S., Chong, S. C., Tuck, S. J., Corey, J. M., and Chan, J. R. (2013). A rapid and reproducible assay for modeling myelination by oligodendrocytes using engineered nanofibers. *Nature protocols*, *8*(4), 771-782.

[22] Lee, S., Leach, M. K., Redmond, S. A., Chong, S. C., Mellon, S. H., Tuck, S. J., Feng, Z. Q., Corey, J. M., and Chan, J. R. (2012). A culture system to study oligodendrocyte myelination processes using engineered nanofibers. *Nature Methods*, *9*(9), 917-922.

[23] Chen, Y., Balasubramaniyan, V., Peng, J., Hurlock, E. C., Tallquist, M., Li, J., and Lu, Q. R. (2007). Isolation and culture of rat and mouse oligodendrocyte precursor cells. *Nature protocols*, *2*(5), 1044-1051.

[24] Zhu, Y., Gao, C., and Shen, J. (2002). Surface modification of polycaprolactone with poly (methacrylic acid) and gelatin covalent immobilization for promoting its cytocompatibility. *Biomaterials*, *23*(24), 4889-4895.

CHAPTER 6

GENERAL CONCLUSIONS

For this study, polycaprolactone was used with different inclusions, such as gelatin, gentamicin, and plasmid DNA. PCL with different additions was discussed in four chapters (Chapter 2 to 5) in this study. The synthesis and evaluation of electrospun PCL-plasmid DNA nanofibers for biomedical applications are concerned with the fabrication of electrospun nanofibers with plasmid DNA for biomedical applications. PCL incorporated with plasmid DNA was electrospun, and nanofibers were examined to determine whether PCL would be able to carry the plasmid DNA. PCL was chosen because it is biodegradable, biocompatible, and approved by the Food and Drug Administration for applications as implantable material for use in the human body. Plasmid DNA was extracted from *E. coli*. Also, PCL nanofibers have no cytotoxicity. Results show that PCL can deliver plasmid DNA to tissues, wounds, or wherever it is applicable. From this study, PCL proves that it can be used as a biomaterial for wound dressing, tissue engineering, and scaffolding.

The effects of gentamicin-loaded PCL nanofibers against the growth of gram-positive and gram-negative bacteria is concerned with bacterial problems. In this study, both gram-positive and gram-negative bacteria were examined, and PCL nanofibers with inclusions of gentamicin in different concentrations (0, 2.5%, 5%, and 10wt%) were investigated. One, two, and four nanofiber layers were used to observe the effect on the inhibition zone. This investigation used gram-negative and gram-positive bacteria, such as *E. coli*, *Salmonella*, and *S. Epidermidis*. Scanning electron microscope images show that PCL fibers range of 50–200 nm with various bead sizes. Bacterial test results showed that gentamicin molecules in the PCL nanofiber were released gradually and prevented bacterial growth at different inhibition zones.

Chapter 2 provides detailed information about how to develop the antibacterial properties of new drug delivery systems for many biomedical fields such as scaffolding, wound healing, and tissue engineering.

The effects of gentamicin-loaded PCL nanofibers on cell viability and the release rate of plasmid DNA is concerned with cell viability and plasmid DNA release rate. PCL nanofibers were incorporated with gentamicin and plasmid DNA in this research. PCL nanofiber-gentamicin concentrations were 0, 2.5%, 5%, and 10 wt%. Also, different cell types—neuroblast (B104) and fibroblast (L929) cells—were discussed. L929 cells exhibited much higher cell viability with the addition of gentamicin. However, B104 cells did not show much affect on cell viability, which may be because of the cell type and strong interactions between the PCL, plasmid DNA, and gentamicin, as well as the low surface area and volume size.

Nanofibers supported oligodendrocyte precursor cell growth and function as a neuron-free model for the myelination study, which is concerned with the repair of injured spinal cords and different nerves. In this study, PCL was incorporated with gelatin and electrospun in various conditions. SEM images showed that submicron size fibers were formed. It was observed that PCL-gelatin electrospun fibers showed more myelinated segments formed by oligodendrocytes than PCL fibers alone. This study may open up new potential studies for the repair of harmed spinal cord and different nerves. Since this research mainly focused on creating biomaterial using the electrospinning method, historical background on the electrospinning process was provided.

Overall from this study, PCL confirmed once again that this experiment is not toxic. The study showed that cell viability was more than 70%. SEM images proved that PCL composed with gentamicin-plasmid DNA gelatin is in the nano size range of 50 nm–800 nm. It was proven that PCL nanofibers can be used in DNA, gene, drug delivery, wound dressing, and tissue

engineering. Chapter 2 proved that PCL showed great response to carrying plasmid DNA. The release study was held for a week but could clearly go much longer. Chapter 3 discussed the antibacterial electrospun mat used with gram-positive and gram-negative bacteria. As shown in this chapter, the PCL nanofiber composed with gentamicin showed inhibition zone areas for different types of bacteria. Chapter 4 focused on cell viability and a release study with B104 and L929 cell types. L929 fibroblast cells showed higher cell viability with PCL composed with gentamicin and plasmid DNA, rather than PCL alone. PCL with the addition of gentamicin and plasmid DNA did not show much affect on the B104 neuroblast cells. The plasmid DNA release study did not show much change with PCL with the inclusion of gentamicin. Chapter 5 discussed the addition of gelatin to the PCL nanofiber in different weight percentages.

CHAPTER 7

FUTURE WORK

Future experiments could be performed to gain further confidence in this drug delivery and cell culturing system. An in vivo study could be conducted. Different types of polymers could be used and compared to the plasmid DNA release as a function of time. PCL could be used with different antibiotics and different bacteria to observe the inhibition zone areas and also observe which antibiotics work for both gram-positive and gram-negative bacteria. PCL nanofibers with different types of antibiotics could be used with different cell types to study cell viability as well as the plasmid DNA release rate. Also, instead of PCL nanofibers, different types of polymers could be used to observe the overall change in release rate and cell viability. A myelination study with gelatin collagen could be undertaken to see if this could be used instead of PCL with gelatin copolymer nanofibers. The polymer type could be changed and a copolymer as a gelatin or collagen could be used to observe whether there is a greater difference in the myelination study. Finally, some nanoparticles can be added into electrospun nanofibers to study the myelination effects of nanoscale inclusions.